NASA/CR-97- 206465

IN-61-CR
OCIT
125917

FINAL REPORT

ON

THE STUDY OF THE RELATIONSHIP

BETWEEN

PROBABILISTIC DESIGN
AND
AXIOMATIC DESIGN METHODOLOGY

NASA Grant No. NAG3-1479

Submitted By

Dr. Chinyere Onwubiko, P.E.
Principal Investigator
Dr. Landon Onyebueke
Research Associate

TENNESSEE STATE UNIVERSITY
DEPARTMENT OF MECHANICAL ENGINEERING

December 12, 1996

Vol. 2

FINAL REPORT

ON

THE STUDY OF THE RELATIONSHIP

BETWEEN

PROBABILISTIC DESIGN
AND
AXIOMATIC DESIGN METHODOLOGY

NASA Grant No. NAG3-1479

Submitted By

Dr. Chinyere Onwubiko, P.E.
Principal Investigator
Dr. Landon Onyebueke
Research Associate

TENNESSEE STATE UNIVERSITY
DEPARTMENT OF MECHANICAL ENGINEERING

December 12, 1996

Vol. 2

Appendix C

Copies of Masters Theses

1. Design of worm gears using probabilistic design methodology with NESSUS computer code.
2. Comparative study of the use of AGMA geometry factors and PDM in the design of compact spur gear set.

DESIGN OF WORM GEARS USING PROBABILISTIC DESIGN METHODOLOGY WITH NESSUS AS THE COMPUTER CODE

A Project

Submitted to the College

of

Engineering and Technology

in

Partial Fulfillment of the Requirements

for the degree of

Master of Engineering

with option in

Mechanical Engineering

Muthuswamy Ethirajan

August 1996

ACKNOWLEDGEMENTS

I wish to express my deepest appreciation to Dr. Chinyere Onwubiko and Dr. Landon Onyebueke, for their understanding and support throughout this project. I would not be at this stage of my graduate career without the support and encouragement from them. I am also thankful to the committee member, Dr. Amir Shirkhodaie for his time and patience.

I also like to thank NASA Lewis Research Center for providing support for this research under NASA grant NAG3-1479.

M.E

TABLE OF CONTENTS

Page

ABSTRACT..... iii

DEDICATION..... iv

ACKNOWLEDGMENT..... v

LIST OF FIGURES..... viii

LIST OF TABLES..... x

CHAPTER

I INTRODUCTION..... 1

1.1 Need for Probabilistic design..... 1

1.2 Rloe of Probabilistic Methodology... 2

1.3 Organization of thesis..... 3

II PROBABILISTIC DESIGN METHODOLOGY..... 5

2.1 Function fo Probability in Engineering..... 5

2.2 Terms involved with Probabilistic Analysis..... 6

2.3 Uncertainty associated with design.. 9

2.4 Designing under uncertainty..... 10

2.5 Design Stages of PDM..... 13

2.6 Probability Sensitivity factors..... 24

III APPLICATION OF PROBABILISTIC DESIGN METHODOLOGY..... 29

3.1 Failure modes of Worm Gear..... 29
3.1.1 Bending Stress..... 29
3.1.2 Thermal Capacity..... 30
3.1.3 Contact Stress..... 32
3.1.4 Wear..... 32
3.2 Deterministic Method..... 33
3.3 Algorithm for Probabilistic Design Methodology..... 36
3.4 Application of the Algorithm in the Design of worm Gear..... 38
3.5 Explanation of Results..... 44
IV FAULT-TREE ANALYSIS..... 83
4.1 System Reliability..... 83
4.2 Adaptive Importance Sampling Method. 85
4.3 Monte-Carlo Method..... 87
V FINITE ELEMENT METHOD..... 92
5.1 Basic Concept..... 92
5.2 General Description of Finite Element Method..... 92
VI CONCLUSION..... 101
6.1 Recommendations..... 102
APPENDIXES..... 104
REFERENCES..... 107
BIOGRAPHICAL SKETCH..... 111

LIST OF FIGURES

Figure		Page
2-1	Fatigue life of S-t Aluminum	11
2-2	Design stages of PDM	14
2-3	Modules of NESSUS	18
2-4	Illustration of most probable point	20
2-5	Illustration of Sensitivity Factor	28
3-1	Flow Chart for PDM	39
3-2	Bending Stress Sensitivity Analysis Trial-4	42
3-3	Contact Stress Sensitivity Analysis Trial-4	42
3-4	Thermal Capacity Sensitivity Analysis Trial-4	42
3-5	Wear Sensitivity Analysis Trial-4	42
3-6	Bending Stress Sensitivity Analysis Trial-1	48
3-7	Thermal Capacity Sensitivity Analysis Trial-1	50
3-8	Contact Stress Sensitivity Analysis Trial-1	52
3-9	Wear Sensitivity Analysis Trial-1	54
3-10	Bending Stress Sensitivity Analysis Trial-2	56
3-11	Thermal Capacity Sensitivity Analysis Trial-2	58
3-12	Contact Stress Sensitivity Analysis Trial-2	60
3-13	Wear Sensitivity Analysis Trial-2	62
3-14	Bending Stress Sensitivity Analysis Trial-3	64
3-15	Thermal Capacity Sensitivity Analysis Trial-3	66

3-16 Contact Stress Sensitivity Analysis Trial-3..... 68

3-17 Wear Sensitivity Analysis Trial-3..... 70

3-18 Bending Stress Sensitivity Analysis Trial-5..... 76

3-19 Thermal Capacity Sensitivity Analysis Trial-5..... 78

3-20 Contact Stress Sensitivity Analysis Trial-5..... 80

3-21 Wear Sensitivity Analysis Trial-5..... 82

4-1 Representation of Fault-Tree Analysis..... 86

4-2 Relationship between probability of failure and weight..... 90

4-3 Relationship between coefficient of variation and probability of failure..... 91

5-1 Displacement Obtained from Deterministic Design... 97

5-2 Stress Obtained from Deterministic Design..... 98

5-3 Displacement Obtained from Probabilistic Design... 99

5-4 Stress Obtained from Probabilistic Design..... 100

LIST OF TABLES

Table		Page
3-1	Deterministic Design Values of Design Parameters..	34
3-2	Probability of failure of the failure modes.....	41
3-3	Final Probabilistic Design Values.....	42
3-4	System Probability of failure and Reliability.....	44
3-5	Bending Stress Failure mode data Trial-1.....	47
3-6	Thermal Capacity Failure mode data Trial-1.....	49
3-7	Contact Stress Failure mode data Trial-1.....	51
3-8	Wear Failure mode data Trial-1.....	53
3-9	Bending Stress Failure mode data Trial-2.....	55
3-10	Thermal Capacity Failure mode data Trial-2.....	57
3-11	Contact Stress Failure mode data Trial-2.....	59
3-12	Wear Failure mode data Trial-2.....	61
3-13	Bending Stress Failure mode data Trial-3.....	63
3-14	Thermal Capacity Failure mode data Trial-3.....	65
3-15	Contact Stress Failure mode data Trial-3.....	67
3-16	Wear Failure mode data Trial-3.....	69
3-17	Bending Stress Failure mode data Trial-4.....	71
3-18	Thermal Capacity Failure mode data Trial-4.....	72
3-19	Contact Stress Failure mode data Trial-4.....	73
3-20	Wear Failure mode data Trial-4.....	74

3-21 Bending Stress Failure mode data Trial-5..... 75

3-22 Thermal Capacity Failure mode data Trial-5..... 77

3-23 Contact Stress Failure mode data Trial-5..... 79

3-24 Wear Failure mode data Trial-5..... 81

CHAPTER I

INTRODUCTION

1.1 Need for Probabilistic Design

The structural design, or the design of machine elements, has been traditionally based on deterministic design methodology. The deterministic method considers all design parameters to be known with certainty. This methodology is, therefore, inadequate to design complex structures that are subjected to a variety of complex, severe loading conditions. A nonlinear behavior that is dependent on stress, stress rate, temperature, number of load cycles, and time is observed on all components subjected to complex conditions. These complex conditions introduce uncertainties; hence, the actual factor of safety margin remains unknown. In the deterministic methodology, the contingency of failure is discounted; hence, there is a use of a high factor of safety. It may be most useful in situations where the design structures are simple.

The probabilistic method is concerned with the probability of non-failure performance of structures or machine elements. It is much more useful in situations where the design is characterized by complex geometry, possibility

of catastrophic failure, or sensitive loads and material properties.

1.2 Role of Probabilistic Methodology

The probabilistic design methodology (PDM) produces designs that are robust and allows the quantification of the level of reliability in the design. Probabilistic methods enable us to model the uncertainties and random variabilities and to include them consistently in our computations. Using probabilistic models, the sensitivity of the failure risk to different uncertainties (randomness and modelling uncertainties) in design parameters is rigorously analyzed. It is becoming substantially evident that the PDM is beginning to attract more attention. The evidence includes the growing number of reliability-oriented specialty conferences, short courses, sponsored research, and technical papers [1-5]. Some of the reasons for the increasing acceptance of PDM are [6]

1) The deterministic method can provide some basic information to complex design problems, but it provides no information with regard to the reliability of the design.

2) Probabilistic computations are becoming simpler and less expensive because of new software being developed.

3) The PDM and the information it provides are becoming more widely understood and better appreciated.

Probabilistic design approach has been successfully applied to various loading conditions encountered during space flight. This methodology has successfully been applied to both large scale and small scale problems such as buckling, transient dynamics, random vibration and harmonic excitation. Shaio and Chamois [7] applied this approach to determine structural reliability and to assess the associated risk due to various uncertainties in design variables. Using this approach Shantaram et al [8] studied the effect of combined mechanical and thermal loads on space strusses. Most of these works relied on the tool NESSUS, developed under NASA's probabilistic structural analysis program.

In this project, the PDM has been applied to the design of a worm gear, to illustrate its applicability to the design of machine elements. In the design analysis, four failure modes are considered: bending stress, thermal capacity, contact stress, and wear. Several trial runs were made using NESSUS; each trial was aimed at improving the design. The most sensitive parameter in the design is identified using sensitivity analysis.

1.3 Organization of thesis

The basic concepts and the statistical parameters applied in probabilistic design methodology are discussed in Chapter

2. In Chapter 3, the application of probabilistic design methodology in the design of worm gears is given. In Chapter 4, the system reliability using PDM is addressed. The finite element analysis of the stress distribution and the displacement of the gear teeth due to the applied load are examined in chapter 5. The conclusion of the project and suggestions for future research are presented in chapter 6. The diagram of the worm gear is shown in Appendix-A. Appendixes B and C contains the step-by-step procedure for running Nessus, for individual failure mode and system failure.

CHAPTER II

PROBABILISTIC DESIGN METHODOLOGY

2.1 Function of Probability in Engineering

In engineering designs, decisions are often required irrespective of the state of completeness or quality of information and thus are made under conditions of uncertainty. In other words, the consequence of a given decision cannot be determined with complete confidence. Additionally information must often be inferred from similar circumstances or derived through modelling. Many problems in engineering involve natural processes and phenomena that are inherently random; the states of such phenomena are naturally indeterminate and thus cannot be described definitely. For these reasons, decisions required in the process of engineering planning and design invariably must be made and are made under conditions of uncertainty.

The effects of such uncertainties in design and planning are important, to be sure; however, the quantification of such uncertainty and proper evaluation of its effects on the performance and design of an engineering system, should include concepts and methods of probability. Further more, under conditions of uncertainty, the design and planning of

engineering systems involve risks, and the formulation of related decisions requires them to be risk free. The problems of uncertainty in design can be overcome by applying the methods of probability. Thus, the role of probability is quite pervasive in engineering. It ranges from the description of information to the development of bases for design and decision making.

2.2 Terms involved with Probabilistic Analysis

Many phenomena or processes of concern to engineers contain randomness; that is, the actual outcomes to some degree are unpredictable. Such phenomena are characterized by experimental observations that are different from one experiment to another, even if performed under identical conditions. In other words, there is usually a range of measured or observed values, and within this range, certain values may occur more frequently than others. Clearly, if recorded data are of a variable exhibit scatter or dispersion, the value of the variable cannot be predicted with certainty [9]. Such a variable is known as a **random variable**, and its value or range of values can be predicted only with an associated probability. When two or more random variables are involved, the characteristics of one variable may depend on the other.

Since there is a range of possible values of random variables, we would be interested in some central value, such as the average. In particular, because the different values of the random variable are associated with different probabilities, the weighted average is taken into consideration. This weighted average is known as the **sample mean** value of the random variable. Therefore, if X is a discrete random variable, then the mean value μ_x is obtained as follows:

$$\mu_x = \frac{\Sigma X}{n} \qquad (2\text{-}1)$$

where,

μ_x is the mean

X is the random variable.

n is the number of observations.

Besides the sample mean, the next most important quantity of a random variable is its measure of dispersion or variability; that is, the quantity that gives a measure of how widely the values of the variate are spread around its mean value. This deviation can be above or below its central value. If the deviations are taken with respect to its mean value, then a suitable average measure of dispersion is called the

variance and is computed using the following relation:

$$Var(X) = \frac{\Sigma(X - \mu_x)^2}{n - 1} \qquad (2\text{-}2)$$

where,

Var(X) is the variance of the random variable X.

Dimensionally, a more convenient measure of dispersion is the square root of the variance, or the **standard deviation**:

$$\sigma_x = \sqrt{Var(X)} \qquad (2\text{-}3)$$

where,

σ_x is the standard deviation of the random variable X.

It is difficult to say whether the dispersion is large or small, on the basis of the variance or standard deviation. For this purpose, the measure of dispersion relative to the central value is more useful. In other words, whether the dispersion is large or small is meaningful only in relation to the central value. For this reason, **coefficient of variation** (COV) is often preferred; COV is a convenient non-dimensional measure of dispersion or variability. The coefficient of variation is related to the mean and standard deviation is as follows:

$$COV = \frac{\sigma_x}{\mu_x} \qquad (2\text{-}4)$$

where,

σ_x= Standard deviation of the variable X.

μ_x= Mean value of the variable X.

The application of probability is not limited to the description of experimental data, or the evaluation of the statistics, such as the mean and standard deviation. In fact, the more significant role of probability concepts is in the utilization of this information in the formulation of proper bases for the design.

2.3 Uncertainty associated with design

Engineering uncertainty is not limited to the variability observed in the basic variables. First, the estimated values of a given variable (such as the mean), based on observational data, will not be error-free. Second, the mathematical or simulation models. For example, formulas, equations, algorithms, and laboratory models, that are often used in engineering analysis and design are idealized representations of reality. Consequently, predictions and calculations made on the basis of these models may be inaccurate (to some unknown degree) and thus also contain uncertainty. Human error can

result from errors made by engineers and technicians during the design or operations phases. It can be reduced by improving the quality- of-control program, but it cannot be avoided entirely. In general, human error is very difficult to define. In this study, human error will be treated as modelling error [10]. In some cases, the uncertainties associated with such predictions or model errors may be much more significant than those associated with the inherent variabilities.

All uncertainties, whether they are associated with inherent variability or with prediction error, may be assessed in statistical terms and the evaluation of their significance on the design can be accomplished by the concepts and the methods of probability.

2.4 Designing under uncertainty

If there are uncertainties in the design, the next step is, to ask how should designs be formulated or decisions affecting a design be resolved? Presumably, we may assume the worst conditions and develop conservative design on this basis. From the system performance and safety point of view, this approach may be suitable. However, the resulting design would be too costly as a result of over-conservatism. On the other hand, an inexpensive design may not ensure the desired

level of performance and safety. Therefore, the decisions should be made considering cost and safety of the design. The most desirable solution is one that is optimal, in the sense of minimum cost and maximum benefits. If the available information and the models to be evaluated contain uncertainties, the analysis should include the effects of such uncertainties [9].

Let us consider a simple example of design of structures and machines. In structural or machine components that are subjected to cyclic loads, the fatigue life of the component is also random, even at constant amplitude stress cycle, as shown in Figure 2-1. For this reason, the useful life of the component is to some degree unpredictable. A design will depend on the life and reliability. For a given design, the shorter the required service life, the higher the reliability against possible breakdowns within the specified service life. Fatigue life is also a function of the applied stress level. Generally, the higher the stress, the shorter the fatigue life.

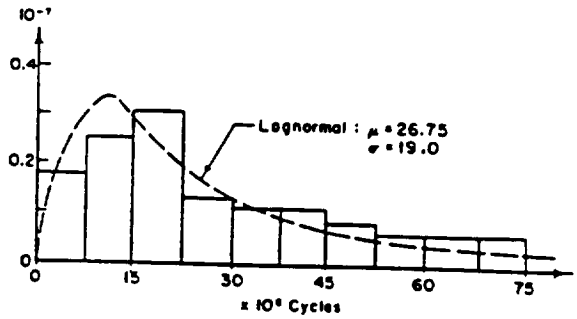


Figure 2-1: Fatigue life of 75 S-t Aluminum [6]

If a desired life is specified, the components could be designed to be massive so that the maximum stresses will be low; thus, the design can have a longer life. This approach will be expensive in terms of material cost. In contrast, if the parts are under-designed, high stresses may be induced, resulting in shorter life and frequent replacements.

The optimal life may be determined on the basis of minimizing the total expected cost, which would include the initial cost and the expected cost of replacement (a function of reliability or probability of less failure). The total expected cost as a function of probability is given as follows [11]:

$$C_t = C_i + P_f C_m \qquad (2\text{-}5)$$

where,

C_t= Total expected cost.

C_m= Maintenance cost.

C_i= Initial cost.

P_f= Probability of failure of the design.

Once the desired probability of failure of the design is decided, the components may then be proportioned accordingly.

Thus, probabilistic design is concerned with the probability of failure or preferably reliability. This methodology is most useful when uncertainties in material

properties and loading conditions are considered. To apply probabilistic methodologies, all uncertainties are modelled as random variables, with selected distribution types, means, and standard deviations [12]. The primitive (random) variables that affect the structural behavior have to be identified.

2.5 Design Stages of PDM

Every design project demands some sequential stages of reflection before one can arrive at the final design goal. This is also the case with PDM. The various design stages of PDM are as follows:

1. Defining the Problem.
2. Generating design parameters.
3. Relating the defined problem to the design parameters.
4. Assembling data and applying probability concepts.
5. Using probabilistic analysis.
6. Interpreting results.

The design stages of PDM are shown in Figure 2-2.

1. Defining the Problem.

The first step which a designer takes in solving a design problem is to find out the main objective of the design. After finding out the objective, the next step is to define in a precise manner the functional requirements of the system or component to be designed. These functional requirements should

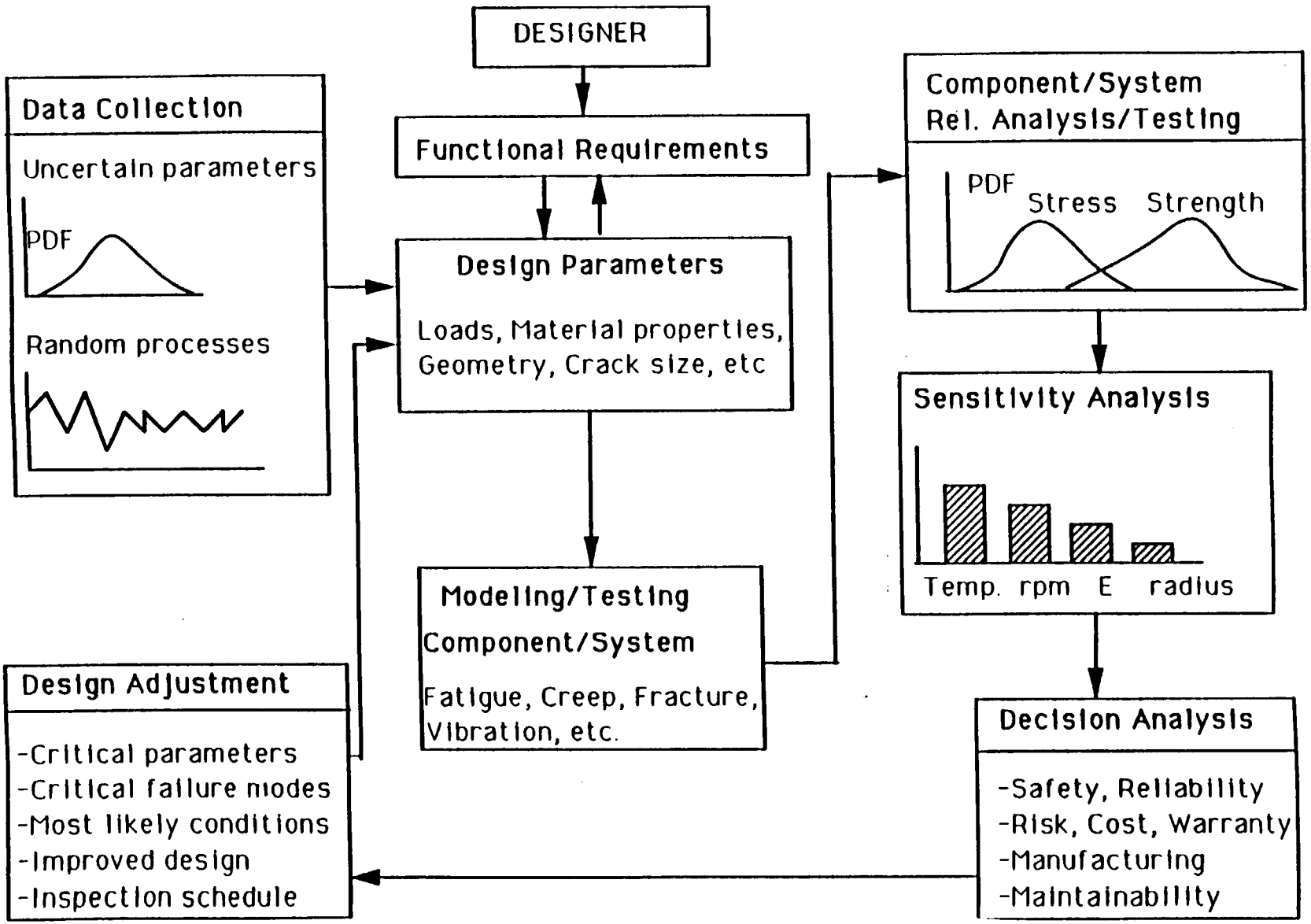


Figure 2-2: Design Stages of Probabilistic Design Methodology. [6]

be able to completely characterize the design objective by defining it in terms of specific needs. With a clear understanding of what one is searching for, the designer then goes to the next stage.

2. Generating design parameters.

In order to solve the defined problem, acceptable design parameters that will meet the defined functional requirements must be generated. To generate the design parameters, one utilizes an appropriate design model. The various parameters, such as load, material properties, geometry, crack size, etc, are taken into consideration. The design parameters to be selected depend on the objective of the design [13].

3. Relating the defined problem to the design parameters.

After defining the design parameters the designer then relates the functional requirements in the functional domain to the design parameters in the physical domain, to be sure that the objective is satisfied. If the relation is satisfactory, the designer proceeds to the next stage; if not, the relation is redefined so that the objective is satisfied.

4. Assembling data and applying probability concepts.

This stage requires assembling the essential data that

are available on the problem with regard to the design parameters. If some of the data are unavailable, then it becomes necessary to perform a computational simulation analysis to generate the missing details. Once the data have been assembled, the next stage is to analyze the assembled data. NESSUS is the computer tool that is used to perform the analysis. NESSUS has three modules: NESSUS/PRE, NESSUS/FEM, and NESSUS/FPI.

NESSUS/PRE is a preprocessor which prepares the statistical data needed for the probabilistic design analysis. It allows the user to describe the uncertainties in the structural design parameters. The uncertainties in these parameters are specified by defining the mean value, the standard deviation, and the distribution type, together with an appropriate form of correlation. Correlated random variables are then decomposed into a set of uncorrelated vectors by a modal analysis.

NESSUS/FEM is a general purpose finite element code, which is used to perform structural analysis and evaluation of sensitivity due to variation in different uncorrelated random variables. The failure surface, defined in terms of random variables required for probabilistic analysis in NESSUS/FPI, is obtained from NESSUS/PRE. NESSUS/FEM incorporates an efficient perturbation algorithm to compute

the sensitivity of random variables [13].

NESSUS/FPI is an advanced reliability module, which extracts the database generated by NESSUS/FEM to develop a response model in terms of random variables. In this module, the probabilistic structural response is calculated from the performance model [14]. The probability of exceeding a given response value is estimated by a reliability method. Inside the NESSUS/FPI module is a sensitivity analysis program, which determines the most critical design parameters in the design.

The input data for NESSUS/PRE require fundamental knowledge of statistics or probability theorems. The expected details will include determining the mean, standard deviation, median, coefficient of variation, variance, etc., associated with each random variable. The designer also determines the probability distribution function that best describes each random variable. The different modules of NESSUS are shown in Figure 2-3.

5. Using probabilistic analysis

It is at this stage of the design that the designer defines a **limit state function.** The limit state function defines the boundary between the safe and failure region. In the limit state function approach for structural reliability analysis, a limit state function $g(\mathbf{X})$ is first defined. The g-

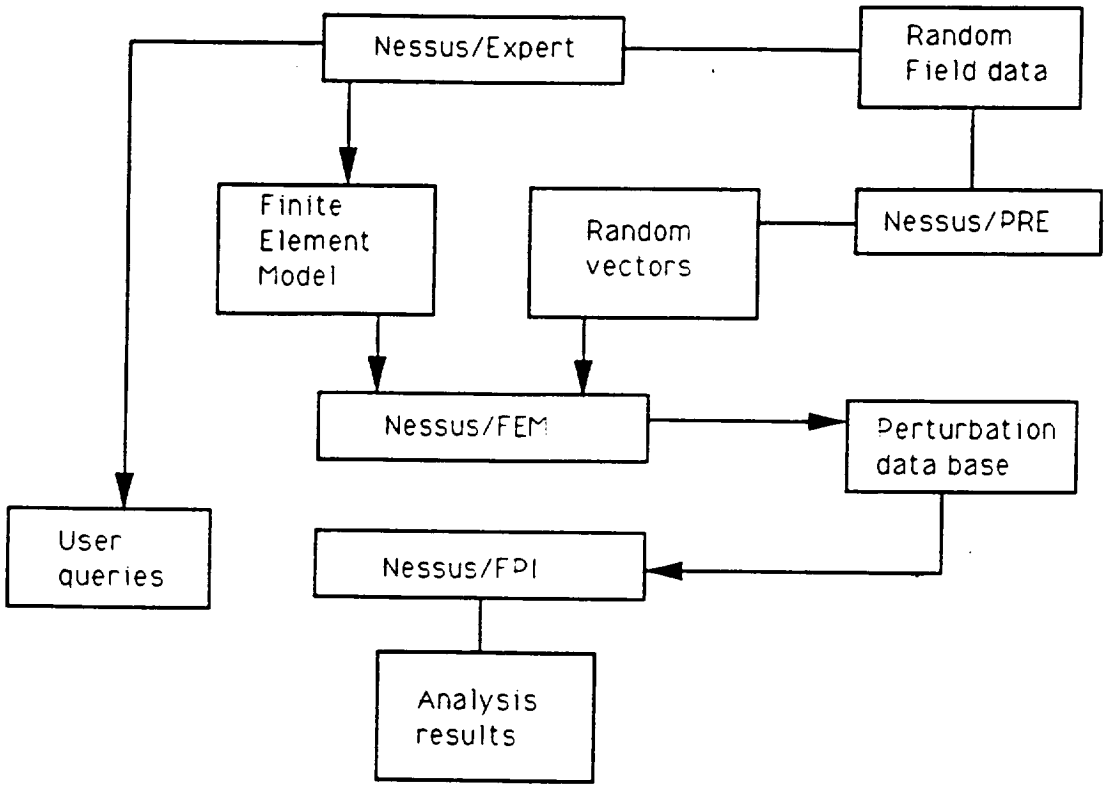


Figure 2-3: Modules of NESSUS

function is a function of a vector of basic random variables, $\underline{X}=(X_1,X_2,X_3,....X_n)$ with $g(\underline{X}) = 0$ being the limit state surface that separates the design space into two regions, namely, the failure $g(\leq 0)$ and the safe $g(>0)$ regions [15]. Geometrically, the limit state equation, $g(X)=0$, is an n-dimensional surface that may be called the "failure surface". One side of the failure surface is the safe state, $g(X)>0$,

whereas the other side of the failure surface is the failure state, $g(X)<0$.

The probability of failure in the failure domain, Ω, is given by [16]

$$P_f = \int_\Omega \ldots \int f_x(X)\ dx \qquad (2\text{-}6)$$

where $f_x(X)$ is the joint probability density function of X, and Ω is the failure region. The solution of this multiple integral is, in general, extremely complicated. Alternatively, a Monte Carlo solution provides a convenient but usually time consuming approximation.

From the Figure 2-4, as the limit state surface $g(X)=0$ moves closer to the origin, the safe region, $g(X)>0$, decreases accordingly. Therefore, the position of the failure surface relative to the origin of the reduced variates, should determine the safety or reliability of the system. The position of the failure surface may be represented by the minimum distance from the surface $g(X)=0$ to the origin. The point on the surface with minimum distance to the origin is the Most Probable Point (MPP). This is usually determined by fitting a local tangent to g(X) and moving this tangent until MPP is estimated [17]. The limit state function method uses the Most Probable Point (MPP) search approach. The Most Probable Point is the key approximation point for the FPI analysis; therefore, the identification of MPP is an important task. In general, the identification of the MPP can be

formulated as a standard optimization problem and solved by proper optimization methods [18].

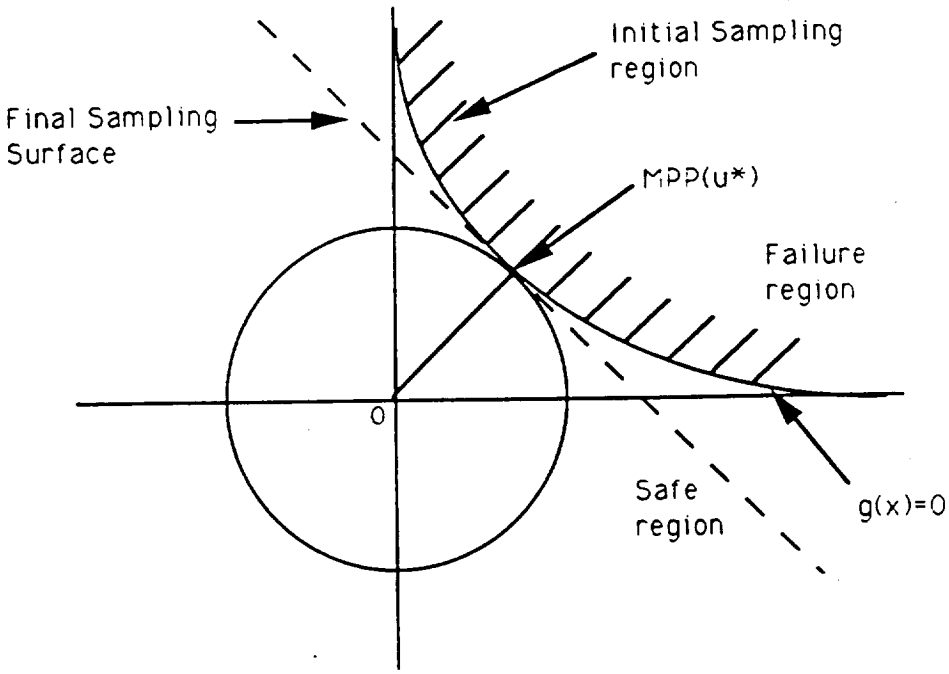


Figure 2-4 Illustration of Most probable point.

In the NESSUS code, MPP is defined in a transformed space called u-space, where the u's are independent to facilitate the probability computations. By transforming g(x) to g(u), the most probable point, u*, on the limit state, g(**X**)=0, is the point which defines the minimum distance from the origin to the limit state surface. This point is most probable (in the u-space) because it has maximum joint probability density

on the limit state surface [19]. The required minimum distance is determined as follows. The distance from a point $u^*=(u_1^*, u_2^*, \ldots, u_n^*)$ on the failure surface $g(u)=0$ to the origin is

$$D = \sqrt{u_1^{*2} + u_2^{*2} + \ldots\ldots\ldots + u_n^{*2}} \qquad (2\text{-}7)$$

where D is the minimum distance from the point on the limit state surface to the origin.

The FPI code assumes only one MPP. In general, however, the possibility exists that there may exist multiple local and global Most Probable Points. A two MPP problem can occur, for example, if the g-function is quadratic and the search algorithm results in an oscillating (non-convergent) search. The required number of iterations for finding MPP is usually less than ten.

Several approaches are available to search for the MPP. The search procedure depends on the forms of the g-function. One efficient method is the Advanced Mean Value method. This method blends the conventional mean value method with the advanced structural reliability analysis method. This method provides efficient cumulative density function analysis as well as the reliability analysis. The step wise AMV method can be summarized as follows [20]

1. Obtain the g(X) function based on perturbations about

the mean values.

2. Compute the cumulative density function of the performance function at selected points using the fast probability integration method.

3. Select a number of cumulative density function values that cover a sufficiently wide probability range.

4. For each cumulative density function value, identify the most probable point.

Another approach that is considered efficient as well is the Adaptive Importance Sampling Method. This method focusses on minimizing the sampling domain in the search space after the MPP is identified. The Adaptive Importance Sampling method is generally used for system reliability analysis.

The analytical process involved in the limit state approach can be illustrated by a basic structural reliability example, where one load effect S, restricted by one resistance R, is considered.

If one considers a case when R and S are independent, the limit state equation can be expressed as,

$$g = R - S \tag{2-8}$$

and the probability of failure can be expressed as,

$$P_f = P(R-S\leq 0) = \iint f_R(r) f_S(s) dr\, ds \tag{2-9}$$

For any random variable the cumulative density function $F(x)$, is given by

$$F_x(x) = P(X \leq x) = \int f_x(y)\,dy \qquad (2\text{-}10)$$

provided that $x \geq y$

Therefore P_f is expressed as

$$P_f = P(R-S \leq 0) = \int F_R(x)\, f_S(x)\,dx \qquad (2\text{-}11)$$

Assuming a special case of normal random variables, for some distributions of R and S, it is possible to integrate the equation (2-11) analytically and determine the probability of failure. If S and R have mean μ_R and μ_S and variances σ_R^2 and σ_S^2 respectively, the g-function has a mean μ_g and variance σ_g^2, given by

$$\mu_g = \mu_R - \mu_S \qquad (2\text{-}12)$$

$$\sigma_g^2 = \sigma_R^2 + \sigma_S^2 \qquad (2\text{-}13)$$

Hence, the probability of failure is given as,

$$P_f = P(R-S \leq 0) = P(g \leq 0) = \Phi\left[\frac{0-\mu_g}{\sigma_g}\right] \qquad (2\text{-}14)$$

Which reduces to,

$$\Phi\left[-\frac{(\mu_R-\mu_S)}{\sqrt{(\sigma_S^2+\sigma_R^2)}}\right] = \Phi(-\beta) \qquad (2\text{-}15)$$

where β is defined as the safety index and is given by,

$$\beta = \frac{\mu_g}{\sigma_g} \qquad (2\text{-}16)$$

Thus the probability of failure is given as

$$P_f = \phi(-\beta) \qquad (2\text{-}17)$$

which can be written as:

$$P_f = 1 - \phi(\beta) \qquad (2\text{-}18)$$

The reliability of the system is given by

$$P_r = 1 - P_f \qquad (2\text{-}19)$$

where P_r is the reliability of the system.

6. Interpreting results:

This is the last stage in the methodology. When the designer approaches this stage, he interprets the results obtained with reference to the initial objective. If the results do not satisfy the functional requirements in the stage 1, the designer may make necessary adjustments in order to achieve the set objective.

2.6 Probability Sensitivity Factors

In engineering performance analysis, many sensitivity measures can be defined. It is important for the designer to know the effect of each random variable in the analysis. The sensitivity information is quantified by sensitivity factors.

Sensitivity factors indicate which random variables are crucial and require special attention. In order to perform a sensitivity analysis of the effect of each of the random variables, one uses the generic material property degradation model, known as the Multifactor Integration Equations, given by Shah et al [21]. A specific form of this model is given as

$$M_p = M_{po}\left(\frac{T_f - T}{T_f - T_o}\right)^n\left(\frac{S_f - \sigma}{S_f - \sigma_o}\right)^p\left(\frac{LogN_{mf} - LogN_m}{logN_{mf} - logN_{mo}}\right)^q \qquad (2\text{-}20)$$

where,

M_p = Degraded material property

M_{po} = Reference material property

T = Temperature

T_f = Final temperature

T_o = Reference Temperature

S_f = Strength

σ = Stress

σ_o = Reference Stress

N_m = Mechanical cycles

N_{mf} = Final Mechanical cycles

N_{mo}= Reference mechanical cycles

The exponents n, p, and q are determined from available experimental data or can be estimated from the

anticipated material behavior due to the particular primitive random variables. Each term inside the bracket in the equation (2-20) is called an effect. Any number of effects can be included in the equation. In general, the generic form of equation (2-20) is

$$\frac{M_p}{M_{po}} = \prod_{i=1}^{N} \left[\frac{V_f - V}{V_f - V_o}\right]_i^{a} \qquad (2\text{-}21)$$

where V denotes an effect and the subscripts o and f represent conditions at reference and final stages. The variable in the above equation can be random and have any probability distribution.

The commonly used sensitivity in deterministic analysis is the performance sensitivity, $\partial Z/\partial X_i$, which measures the change in the performance due to the change in a design parameter. This concept can be extended to the probabilistic analysis in which a more direct sensitivity measure is the reliability sensitivity, which measures the change in the probability/reliability relative to the distribution parameters, such as the mean and the standard deviation. Although not automated in the code, this analysis can be performed by varying the parameters [22].

Another, perhaps more important, kind of probability or reliability sensitivity analysis is the determination of the relative importance of the random variables. This analysis can

be done, for example, by repeated probabilistic analysis in which one random variable at a time is treated as a deterministic variable. The results of the analyses, for example, are a number of cumulative density function curves or reliabilities. Based on the results, the relative importance of the random variables can be analyzed. The standard FPI output includes a first order sensitivity factor which provides approximate relative importance of the random variables. The probability sensitivity factors are defined as follows.

At the most probable point, $U^* = (u_1^*, u_2^*, \ldots u_n^*)$, the first order probability estimate is $\Phi(-\beta)$ where

$$\beta = u_1^{*2}+u_2^{*2}+.. u_n^{*2} \qquad (2\text{-}22)$$

The sensitivity factor α is defined as:

$$\alpha_i = u_1^*/\beta \qquad (2\text{-}23)$$

which is the direction cosine of the OP vector (from the origin to the minimum distance point) as shown in Figure 2-5. Thus,

$$\alpha_1^2 +\alpha_2^2 +.....\alpha_n^2 =1 \qquad (2\text{-}24)$$

which implies each α_i^2 is a measure of the contribution to the probability (since the probability is related to β). Higher α indicates higher contribution and vice versa.

Based on a geometrical analysis in the u- space, it can be shown that [10]

$$\text{mod}\,\alpha_i \propto [\frac{\partial g}{\partial X_i}]\sigma_i \qquad (2\text{-}25)$$

where σ_i is the normal standard deviation. It can be concluded that α depends on both the performance sensitivity and the uncertainty. In general, the sensitivity factors depend on the g-function as well as the probability distribution.

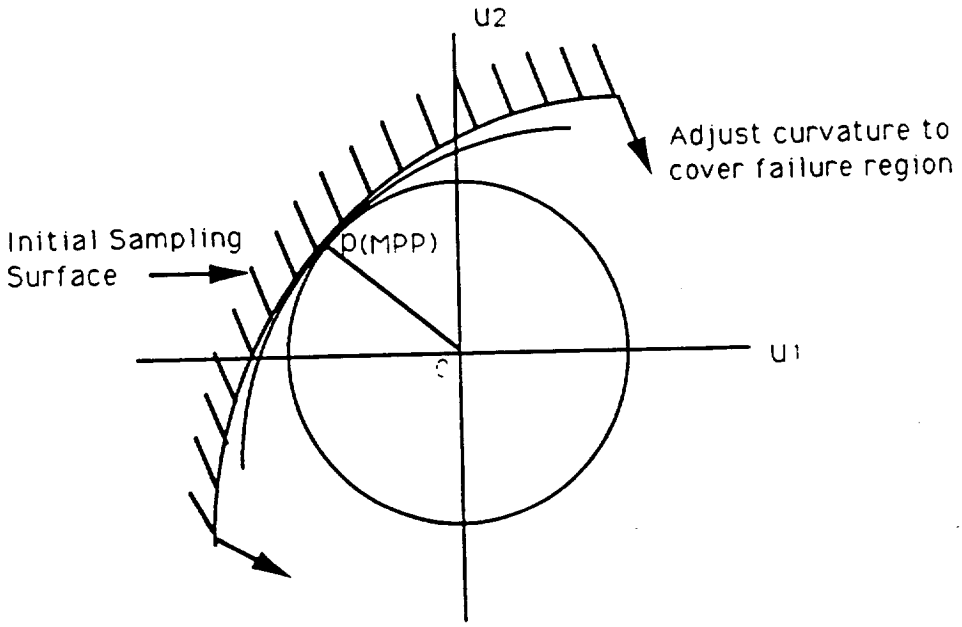


Figure 2-5: Illustration of Sensitivity Factor.

CHAPTER III

APPLICATION OF PROBABILISTIC METHODOLOGY IN DESIGN

The probabilistic design methodology described previously was applied to design worm gears, to illustrate its application in machine design . The worm gear Figure with the terminology is shown in Appendix-A. In the analysis of the design, four different failure modes of the worm gears were considered: bending stress, thermal capacity, contact stress and failure due to wear. An overview of these failure modes is given as follows.

3.1 Failure modes of Worm Gear

3.1.1 Bending stress: When worm gear sets are used intermittently or at slow gear speeds, the bending strength of the gear tooth may become a principal design factor [23]. The teeth of worm gears are thick and short at the two edges of the face and thin at the central plane, and this makes it difficult to determine the bending stress. The equation for the bending stress given by Buckingham is as follows:

$$\sigma_b = \frac{F_d \cdot P}{b \cdot Y} \qquad (3\text{-}1)$$

where,

σ_b = Bending stress, psi

F_d = Dynamic load, lb

P = Axial pitch, in

b = Face width of the gear, in

Y = Form factor of the gear.

3.1.2 Thermal capacity of worm gear set: One of the major problems associated with worm gear sets is the question of how much heat is developed during operation and whether the gear case is capable of dissipating this heat. In fact, most worm gear units have their horsepower capacity limited by the heat dissipation ability of the casting. The transfer of heat is accomplished by both radiation and convection [24]. In arriving at an equation to determine how much heat can be dissipated, such factors as housing area, temperature change between lubricant and ambient air, and a combined heat transfer coefficient must be considered. The usual heat transfer equation can be written as

$$H = C_r * A_c * \Delta t \qquad (3\text{-}2)$$

where,

H = The energy dissipated through the housing, ft-lb/min

C_r = Combined heat transfer Coefficient, ft-lb/min in^2 F

A_c = Area of housing exposed to ambient air, in^2

Δt = Temperature difference between oil and ambient air, F

The heat energy that must be dissipated from the casing can be determined by considering the frictional or lost horse-power. The heat energy which must be dissipated is given by

$$H_d = HP*(1-e) \qquad (3-3)$$

where ,

H_d = The heat energy developed, ft-lb/min.

HP = Horse power input.

e = Efficiency.

The efficiency is computed using the relation

$$e = \frac{\cos\phi_n - f\tan\lambda_w}{\cos\phi_n + f\cot\lambda_w} \qquad (3-4)$$

where,

Φ_n= Pressure Angle

λ_w= Lead Angle.

f, coefficient of friction is computed using the following equation

$$f = 0.32/V_s^{0.36} \qquad (3-5)$$

where,

V_s is the Sliding velocity in ft/min.

Clearly the heat energy developed, H_d, must be equal to or less than the heat energy dissipation capacity H.

3.1.3 Contact stress: The contact stress is developed due to the contact between two members. To design for a safe contact stress, the working contact stress must be less than the endurance strength of the gear material. The contact stress for the worm gears is given as follows:

$$\sigma_c = \frac{2 \cdot F_d}{\pi \cdot C_l \cdot D} \qquad (3\text{-}6)$$

D is given by

$$D = \sqrt{\frac{2F_d \dfrac{1-\mu^2}{E}}{\pi \cdot C_l \left(\dfrac{1}{d_g} + \dfrac{1}{d_w}\right)}} \qquad (3\text{-}7)$$

where,

σ_c = Contact stress developed, psi

F_d = Dynamic load, lb

C_l = Contact Length, in

μ = Poisson ratio

E = Youngs modulus of the material, lb/in^2

d_w = Diameter of the worm, in

d_g = Diameter of the gear, in

3.1.4 Wear: An approximate equation suggested by

Buckingham is usually used to determine the allowable wear load. The limiting wear load is given by

$$F_w = D_g * b * K \qquad (3\text{-}8)$$

where,

F_w = Limiting wear load, lb

D_g = Pitch diameter of the gear, in

b = Face width, in

K= A constant dependent on the material used, lb/in^2

The functional requirement in the design is to reduce the probability of failure or increase the reliability of the system. In order to achieve this, each failure mode is considered separately, and the corresponding probability of failure is computed. After finding the individual probability of failure, the combined effect of the failure modes is computed. But before going actually into PDM, the problem solved by the deterministic method is given to show the contrast between the two methodologies.

3.2 Deterministic method

Problem Statement: Design a worm gear set to deliver 15 hp from a shaft rotating at 1500 rpm to another rotating at 75 rpm. Assume that normal pressure angle is to be 20 degrees. The lead angle should not exceed 25 degrees. Allow 6 degree per thread of worm. The worm could have 4 or less teeth [25].

The design parameters and the deterministic design values are shown in Table 3-1

Table 3-1: Deterministic Design Values

Design Parmater	* Value
S_b (psi)	12000
F_d (lb)	1731
P (in)	3.23
b (in)	2.0
Y	0.392
C_r (ft-lb/min in. °F)	0.43
A_c (in^2)	2766.6
D_t (°F)	350
HP (hp)	16.7
e	0.92
S_c (psi)	40000
C_l (in)	5.004
M_u	0.4
E (psi)	0.18E+08
D_w (in)	4.0
D_g (in)	19.1
K (lb/in^2)	80

*** Mean Values taken from [25]**

where,

S_b = Bending stress, psi

S_c = Contact stress, psi

M_u = Poisson ratio

Summary of Results [25]:

Bending

$\sigma_{b(max)}$= 12000 psi (845.4 kg/cm^2)

σ_b = 7131.54 psi (502.41 kg/cm^2)

F.S = 1.682

Thermal

H = 119,000 ft-lb/min (30050.505 kg-cm/sec)

H_d = 378521.18 ft-lb/min (13095.95 kg-cm/sec)

F.S = 2.29

Contact

$\sigma_{c(max)}$= 40000 psi (2818 kg/cm^2)

σ_c = 37924.3 psi (2671 kg/cm^2)

F.S = 1.05

Wear

Fw = 3056 lb (1389.09 kg)

Fd = 2500 lb (1136.36 kg)

F.S = 1.344

3.3 Algorithm for Probabilistic Design Methodology.

Step 1. Determine the objective and functional requirement of the design.

Step 2. Identify the design parameters involved.

Step 3. Obtain the statistical parameters such as mean, standard deviation and the distribution type of the design parameters.

Step 4. **If** (the mean is known) **then** (**Go to** step 5)

else

Do a computer simulation to calculate the mean or get the mean from a deterministic design without factor of safety.

end if

Step 5. **If** (the standard deviation is known) **then** (**Go to** step 6).

else

Calculate the standard deviation by probability method or assume acceptable standard deviation.

end if

Step 6. **If** (the distribution type is known) **then** (**Go to** step 7)

else

Determinte the distribution from probability paper or assume the distribution type.

end if

Step 7. Identify the major failure modes present in the design.

Step 8. Formulate the limit state functions of the failure modes.

Step 9. **Do** probabilistic analysis with available software.

Step 10. Obtain the most critical parameters from the sensitivity analysis.

Step 11. Obtain the safety index and probability of failure calculated from the analysis.

Step 12. **If** (the safety index is low or if the probability of failure is high)

then (the values of the critical parameters are adjusted). **Go to** step 9 to repeat the process till acceptable probability of failure is obtained

else

Get the probability of failure and design values.

end if

Step 13. **If** (the number of failure modes is more than one)

then (**Go to** step 14)

else

Go to step 17

end if

Step 14. System reliability is to be done. Fault -Tree analysis is performed to compute system reliability.

Step 15. **Do** the system reliability analysis with the available software.

Step 16. Get the reliability of the system, probability of failure.

Step 17. **Stop** the analysis

The flow chart representation of the algorithm is shown in figure 3-1.

3.4 Application of the algorithm in the Design of Worm Gear.

Step 1. The objective is to design a worm gear set and the functional requirement is to increase the reliability of an existing worm gear design.

Step 2. The design parameters are shown in Table 3-1

Step 3. The mean values of the design parameters are taken from an existing design [25]

Step 4. The standard deviation of the design parameters were not known. The standard deviation was assumed.

Step 5. The distribution type was not known, hence the distribution type was assumed.

Step 6. The major failure modes in worm gear design are bending stress, thermal capacity, contact stress, and failure due to wear.

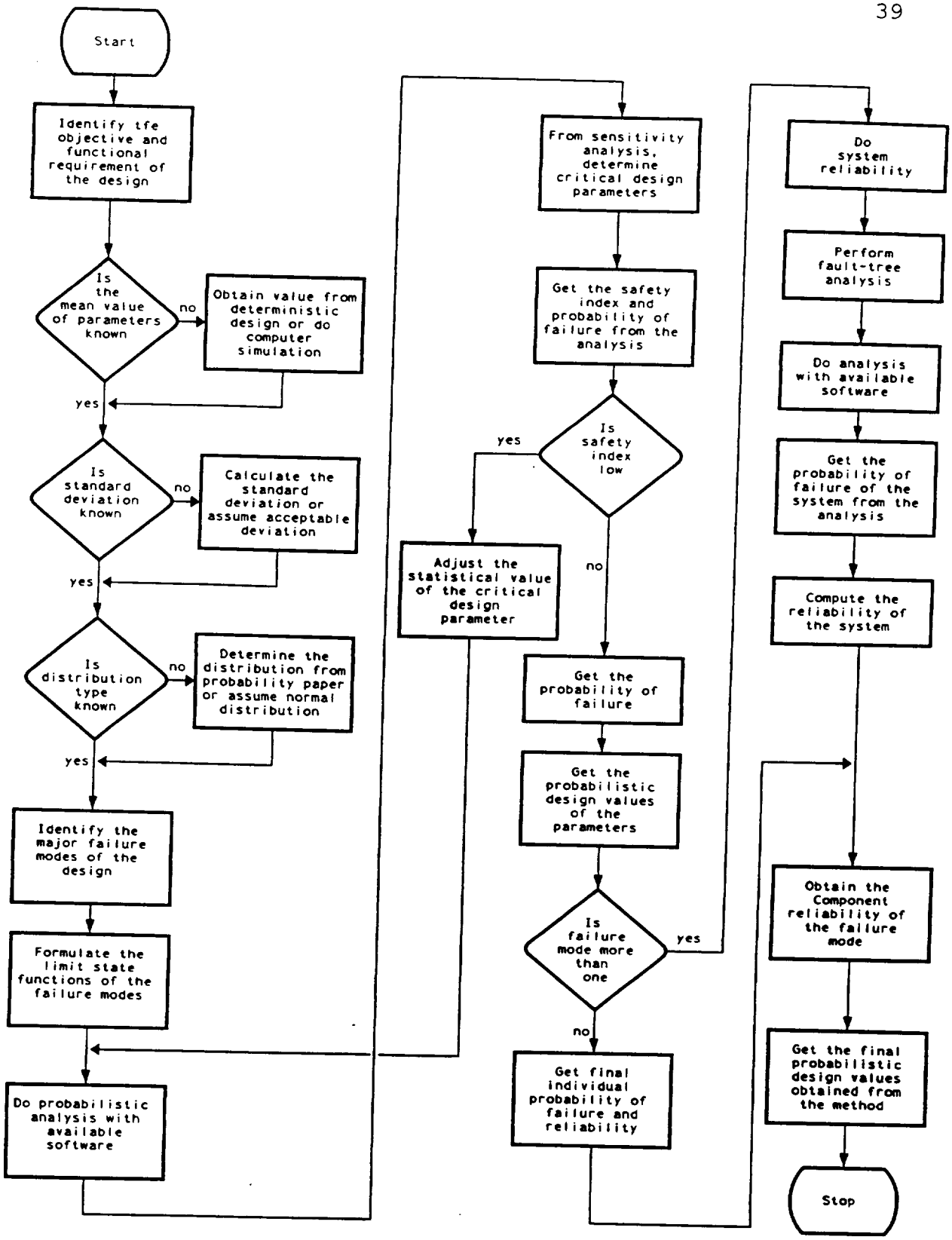


Figure 3-1: Flow chart for PDM

Step 7. The limit state functions for the four failure modes of worm gear design are:

Bending Stress

$$g_1 = S_b - \frac{F_d \cdot P}{b \cdot Y} = 0 \qquad (3\text{-}9)$$

Thermal Stress

$$g_2 = C_r \cdot A_c \cdot D_t - HP\ (1\text{-}e) = 0 \qquad (3\text{-}10)$$

Contact Stress

$$g_3 = S_c - \frac{2 \cdot F_d}{\pi \cdot C_l \cdot D} = 0 \qquad (3\text{-}11)$$

where D is defined by equation (3-7).

Wear

$$g_4 = D_g \cdot b \cdot K - F_d = 0 \qquad (3\text{-}12)$$

Step 8. The probabilistic analysis was done using Nessus. The step-by-step procedure for running Nessus is given in Appendix-B

Step 9. The critical design parameters were found from the sensitivity analysis. From figures 3-2 through 3-5, it can be seen that the critical parameters are, b, face width, c_1, contact length, e,thermal efficiency

Step 10. The probability of failure for the four failure modes obtained after the first trial are shown in Table 3-2.

Step 11. The probability of failure was high after the first trial. The design values of the critical parameters were adjusted and four trial runs were made with each trial aimed at improving the design.

Step 12. The probability of failure of the failure modes after the fourth trial are shown in Table 3-2.

Table 3-2: Probability of failure of the failure modes.

FAILURE MODE	PROBABILITY OF FAILURE	
	Initial	Final
Bending Stress	0.1311524E-02	0.55279E-05
Thermal Capacity	0.1508843	0.704601E-01
Contact Stress	0.2206627	0.813815E-01
Wear	0.117788	0.111040E-03

Step 13. The final probabilistic design values obtained after the fourth trial are shown in the Table 3-3.

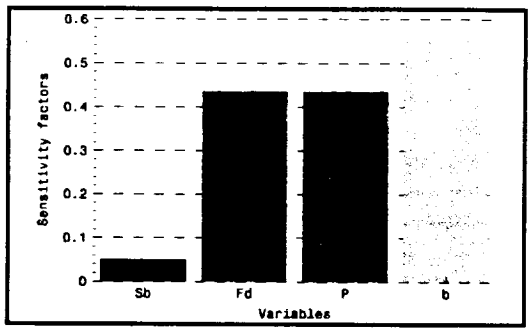


Fig 3-2: Sensitivity analysis of variables in bending failure mode (Pf = 0.55279E-05)

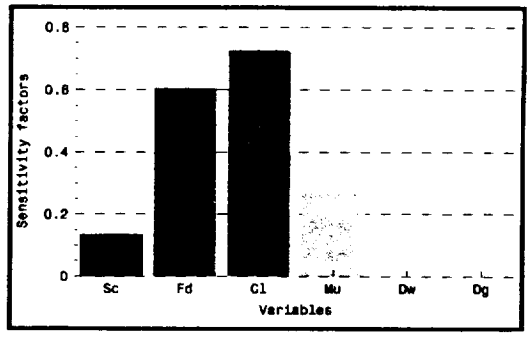


Fig 3-3: Sensitivity analysis of variables in contact failure mode (Pf = 0.813815E-01)

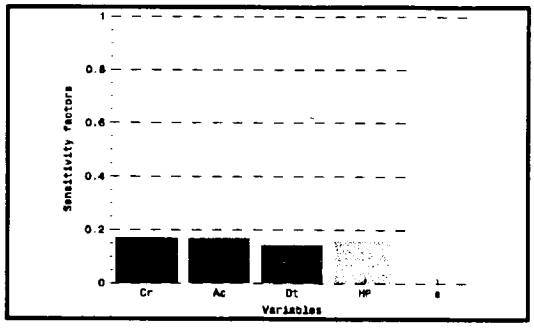


Fig 3-4: Sensitivity analysis of variables in thermal failure mode (Pf = 0.704604E-01)

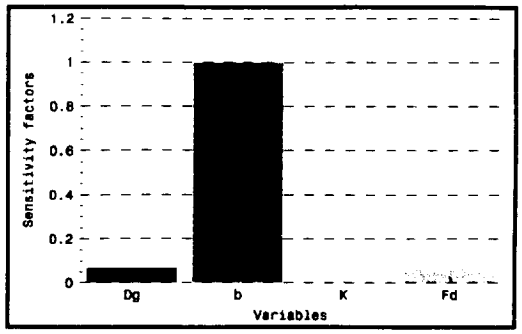


Fig 3-5: Sensitivity analysis of variables in wear failure mode (Pf = 0.11104E-03)

Table 3-3 : Final Probabilistic Design Values for Worm Gear Design

Design Parameter	Probabilistic Design Value	Standard Deviation	Distribution Type
S_b (psi)	12000	1200	NORMAL
F_d (lb)	1731	173.1	NORMAL
P (in)	3.23	0.323	NORMAL
b (in) *	2.6	0.26	NORMAL
C_r (ft-lb/ min in °F)	0.43	0.043	NORMAL

Table Continued:

Y	0.392	0	
A_c (in^2)	2766.6	276.6	NORMAL
D_t (°F)	350	35	NORMAL
HP (ft-lb/min)	229000	229	NORMAL
e *	0.97	0.097	NORMAL
S_c (psi)	40000	400	NORMAL
C_l (in) *	5.504	0.5504	NORMAL
M_u	0.4	0.04	NORMAL
E (psi)	0.18E+08	0	
D_w (in)	4	0.4	NORMAL
D_g (in)	19.1	1.91	NORMAL
K (lb/in^2)	80	8	NORMAL

*** Critical Design Parameter**

Step 14. The number of failure modes is more than one. So system reliability is done.

Step 15. The design values obtained in step 13 are used to do system reliability.

Step 16. Fault-Tree analysis is used to compute the system reliability. The methods used are

1. Adaptive Importance Sampling Method
2. Monte-Carlo Method.

Step 17. The analysis is done using Nessus software. The step-by-step procedure for running Nessus to compute system reliability is shown in Appendix-C

Step 18. The probability of failure of the system and the reliability computed are shown in Table 3-4.

Table 3-4: System Probability of failure and Reliability

Method	Probability of failure	Reliability
Adaptive Importance Sampling method	0.666591E-01	0.933341
Monte- Carlo Method	0.66657E-01	0.933343

3.5 Explanation of results.

The analysis yields a probability of failure for the defined limit state function. From the sensitivity analysis of the bending stress, it can be interpreted that the face width, b is the most sensitive parameter, shown in Figure 3-6. The value of the face width is increased from 2.0 to 2.2, and the analysis is done for the second trial. Four trials were made during the analysis. The Figures 3-6, 3-10, 3-14, and 3-2 show the sensitivity analysis and the probability of failure.

The results of the sensitivity analysis of the thermal

capacity of the gear set are shown in Figures 3-7, 3-11, 3-15, and 3-4. Figure 3-7 indicates that power efficiency is the most sensitive parameter. The value of the efficiency is as shown in equation (3-4) is increased to reduce the probability of failure. The efficiency can be increased by reducing the churning loss of oil in the gear casing. Four trial runs are made, and the corresponding values are shown in Tables 3-6, 3-10, 3-14 and 3-18.

In contact stress, the contact length, C_1 is found to be the most sensitive parameter. The value of the contact length is increased and the second trial is made. Four trials are made in a similar way. The sensitivity analysis and the probability of failure are shown in Figures 3-8, 3-12, 3-16, and 3-3. The values of the design parameters are shown in Tables 3-7, 3-11, 3-15, and 3-19.

In wear failure mode the most sensitive parameter was found to be K, a constant dependent on the material. Since this parameter is a constant, which depends on the material, the next sensitive parameter face width, b, is taken into consideration. The value of the face width is increased from 2.0 to 2.2. The second trial is made with the new values, and the corresponding sensitivity analysis and the probability of failure are noted down. Four trial runs were made, and the sensitivity analysis is shown in Figures 3-9, 3-13, 3-17, and

3-5. The values of the variables are shown in Tables 3-8,3-12, 3-16, and 3-20.

The values of the most sensitive design parameter in the design are reduced slightly to study the effect on the probability of failure. The reduced values of the four failure modes are shown in Tables 3-21, 3-22, 3-23, and 3-24. The sensitivity analysis and the probability of failure for these values are shown in Figures 3-18, 3-19, 3-20, and 3-21. It is found from the present analysis that as the value of the most sensitive design parameter is reduced, the probability of failure increases, which is undesirable.

The data which was put into the NESSUS for the four failure modes are shown in Tables 3-5, 3-6, 3-7, and 3-8. The sensitivity analysis of this trial is shown in Figures 3-6, 3-7, 3-8, and 3-9. From the results of the present design analysis, it can be concluded that the system fails mainly by contact stress.

3-5. The values of the variables are shown in Tables 3-8,3-12, 3-16, and 3-20.

The values of the most sensitive design parameter in the design are reduced slightly to study the effect on the probability of failure. The reduced values of the four failure modes are shown in Tables 3-21, 3-22, 3-23, and 3-24. The sensitivity analysis and the probability of failure for these values are shown in Figures 3-18, 3-19, 3-20, and 3-21. It is found from the present analysis that as the value of the most sensitive design parameter is reduced, the probability of failure increases, which is undesirable.

The data which was put into the NESSUS for the four failure modes are shown in Tables 3-5, 3-6, 3-7, and 3-8. The sensitivity analysis of this trial is shown in Figures 3-6, 3-7, 3-8, and 3-9. From the results of the present design analysis, it can be concluded that the system fails mainly by contact stress.

TABLE 3 - 5 : BENDING STRESS FAILURE MODE DATA

INPUT TABLE

TRIAL -1

Design paramters	Mean	Standard Deviation	Distribution type
S_b (psi)	12000	1200	NORMAL
F_d (lb)	1731	173.1	NORMAL
P (in)	3.23	0.323	NORMAL
b (in)	2.0	0.2	NORMAL
Y	0.392	0	

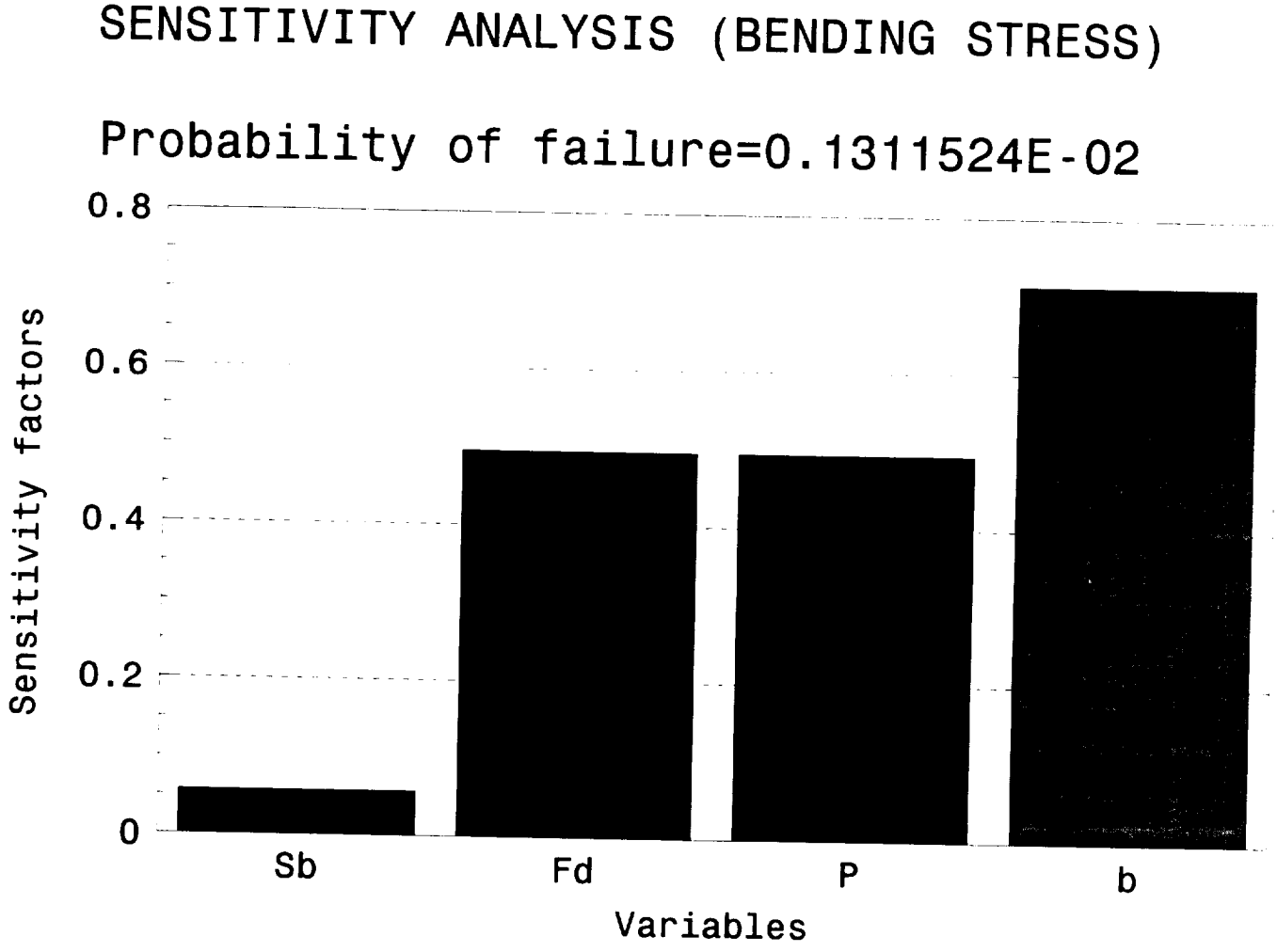


Figure 3-6: Bending Stress Analysis Trial -1

TABLE 3 - 6 : THERMAL CAPACITY FAILURE MODE DATA

INPUT TABLE

TRIAL -1

Design paramters	Mean	Standard Deviation	Distribution type
C_r (ft-lb/min in °F)	0.43	0.043	NORMAL
A_c (in^2)	2766.6	276.6	NORMAL
D_t (°F)	350	35	NORMAL
HP (ft-lb/min)	0.229E+06	0.229E+03	NORMAL
e	0.92	0.092	NORMAL

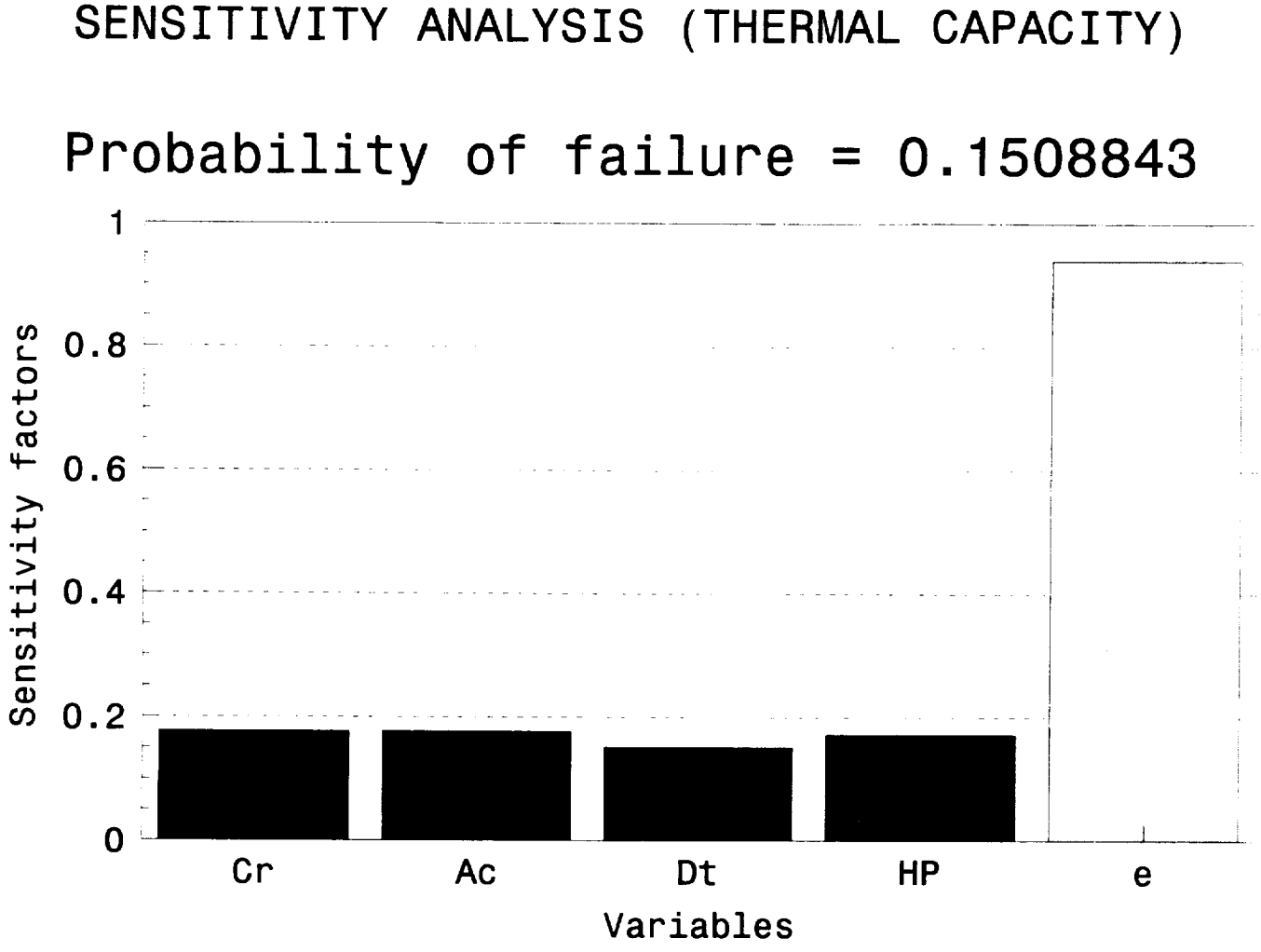


Figure 3-7: Thermal Capacity Analysis Trial -1

TABLE 3-7 : CONTACT STRESS FAILURE MODE DATA

INPUT TABLE

TRIAL -1

Design Parameters	Mean	Standard Deviation	Distribution Type
S_c (psi)	40000	400	NORMAL
F_d (lb)	1731	173.1	NORMAL
C_l (in)	5.004	0.5004	NORMAL
M_u	0.4	0.04	NORMAL
E (psi)	18E+06	0	
D_w (in)	4.0	0.4	NORMAL
D_g (in)	19.1	1.91	NORMAL

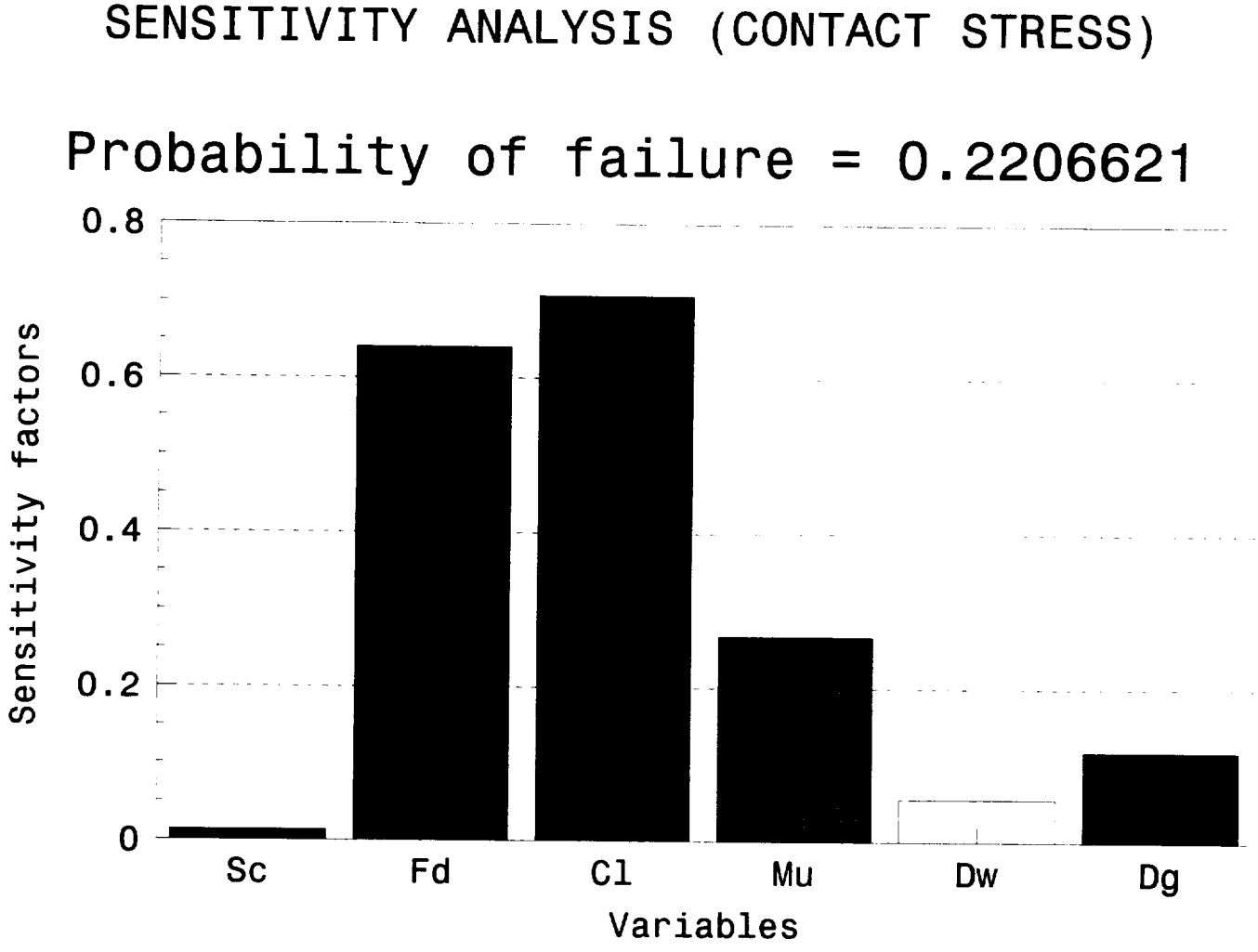


Figure 3-8: Contact Stress Analysis Trial-1

TABLE 3 - 8 : WEAR FAILURE MODE DATA

INPUT TABLE

TRIAL -1

Design paramters	Mean	Standard Deviation	Distribution type
D_g (in)	19.1	1.91	NORMAL
b (in)	2.0	0.2	NORMAL
K (lb/in^2)	80	8	NORMAL
F_d (lb)	1731	173.1	NORMAL

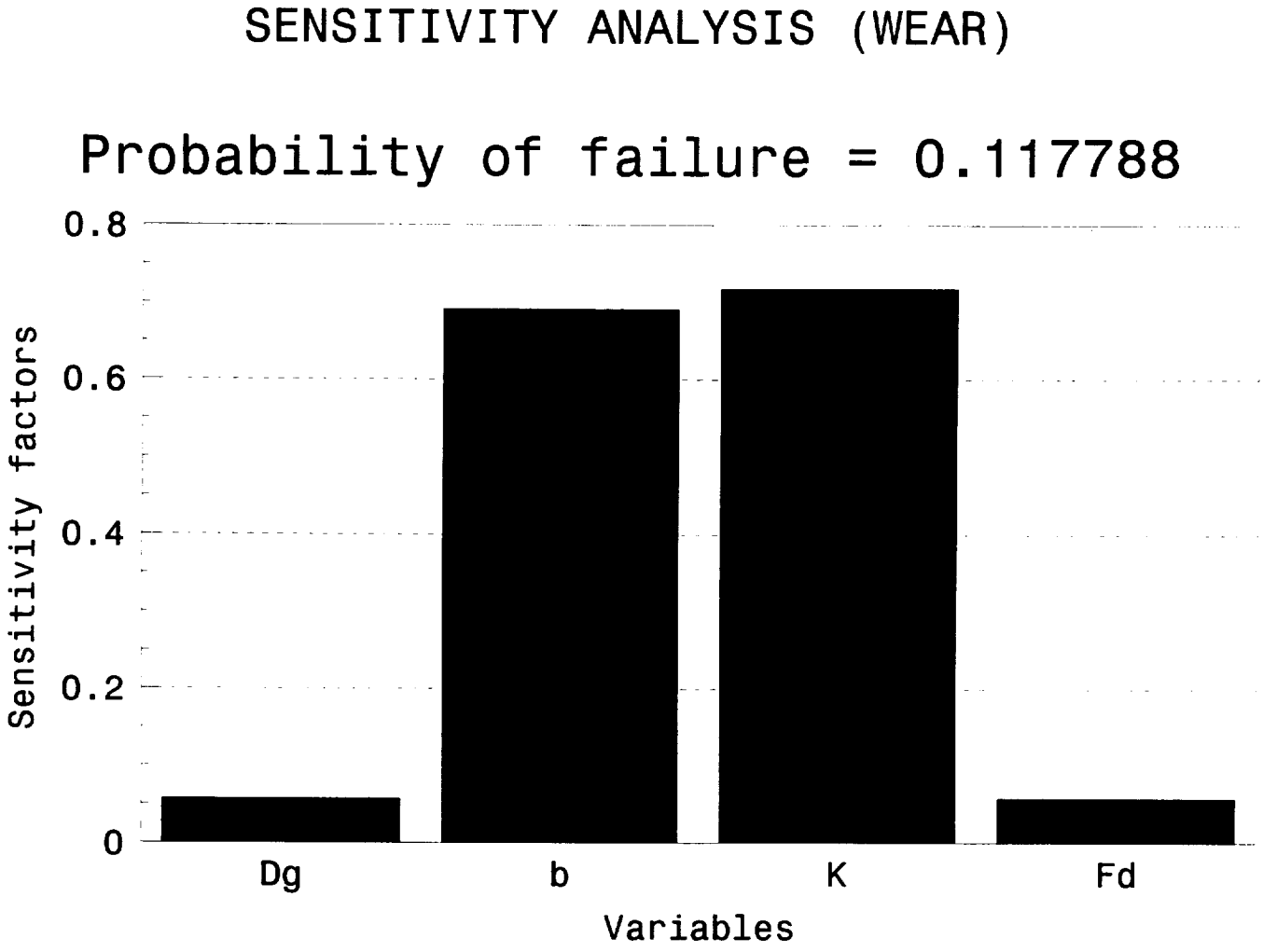


Figure 3-9: Wear Analysis Trial -1

TABLE 3 - 9 : BENDING STRESS FAILURE MODE DATA

INPUT TABLE

TRIAL -2

Design paramters	Mean	Standard Deviation	Distribution type
S_b (psi)	12000	1200	NORMAL
F_d (lb)	1731	173.1	NORMAL
P (in)	3.23	0.323	NORMAL
b (in)	2.2	0.22	NORMAL
Y	0.392	0	

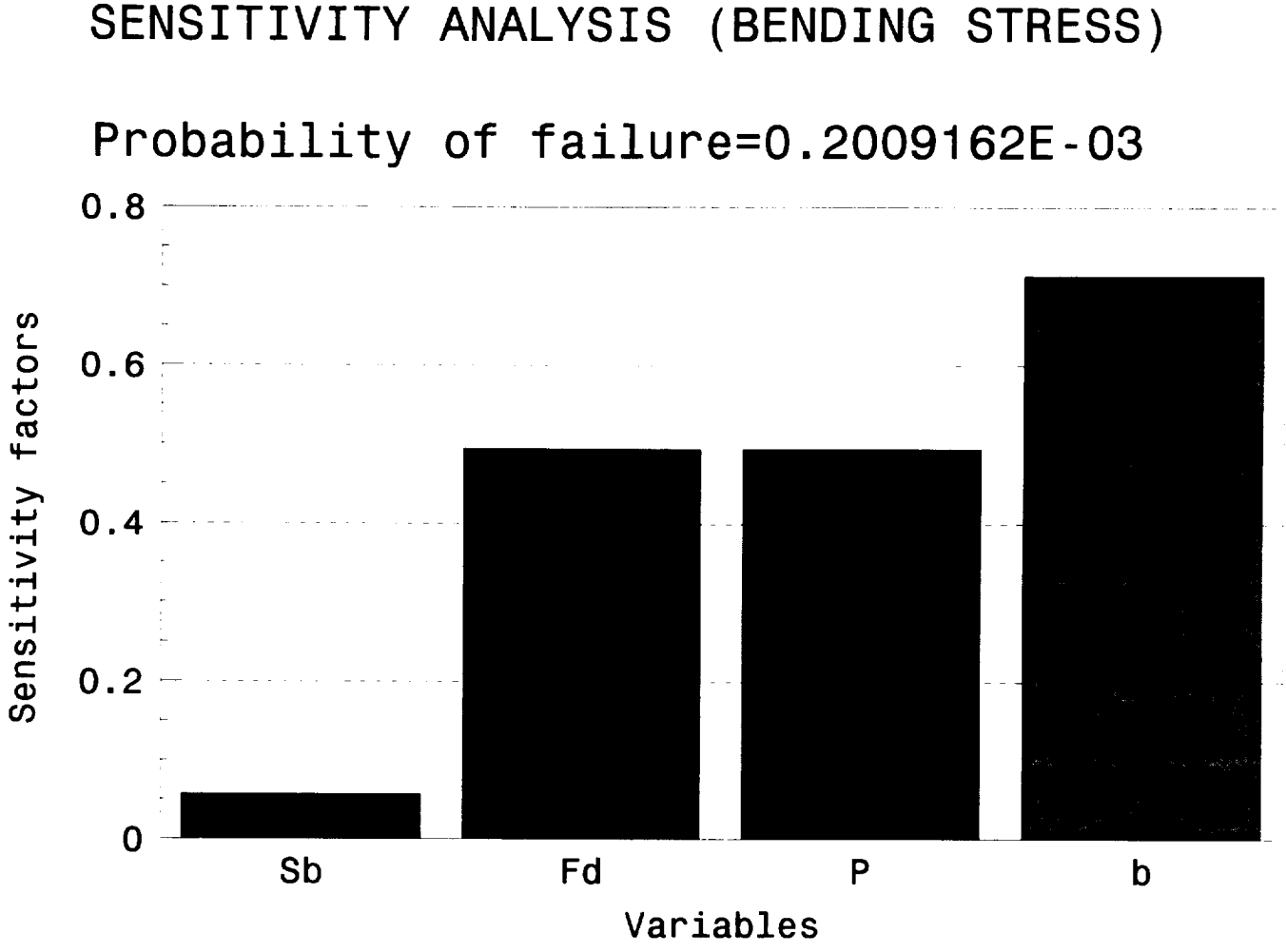


Figure 3-10: Bending Stress Analysis Trial -2

TABLE 3 - 10 : THERMAL CAPACITY FAILURE MODE DATA

INPUT TABLE

TRIAL -2

Design paramters	Mean	Standard Deviation	Distribution type
C_r (ft-lb/min in °F)	0.43	0.043	NORMAL
A_c (in^2)	2766.6	276.6	NORMAL
D_t (°F)	350	35	NORMAL
HP (ft-lb/min)	0.229E+06	0.229E+03	NORMAL
e	0.95	0.095	NORMAL

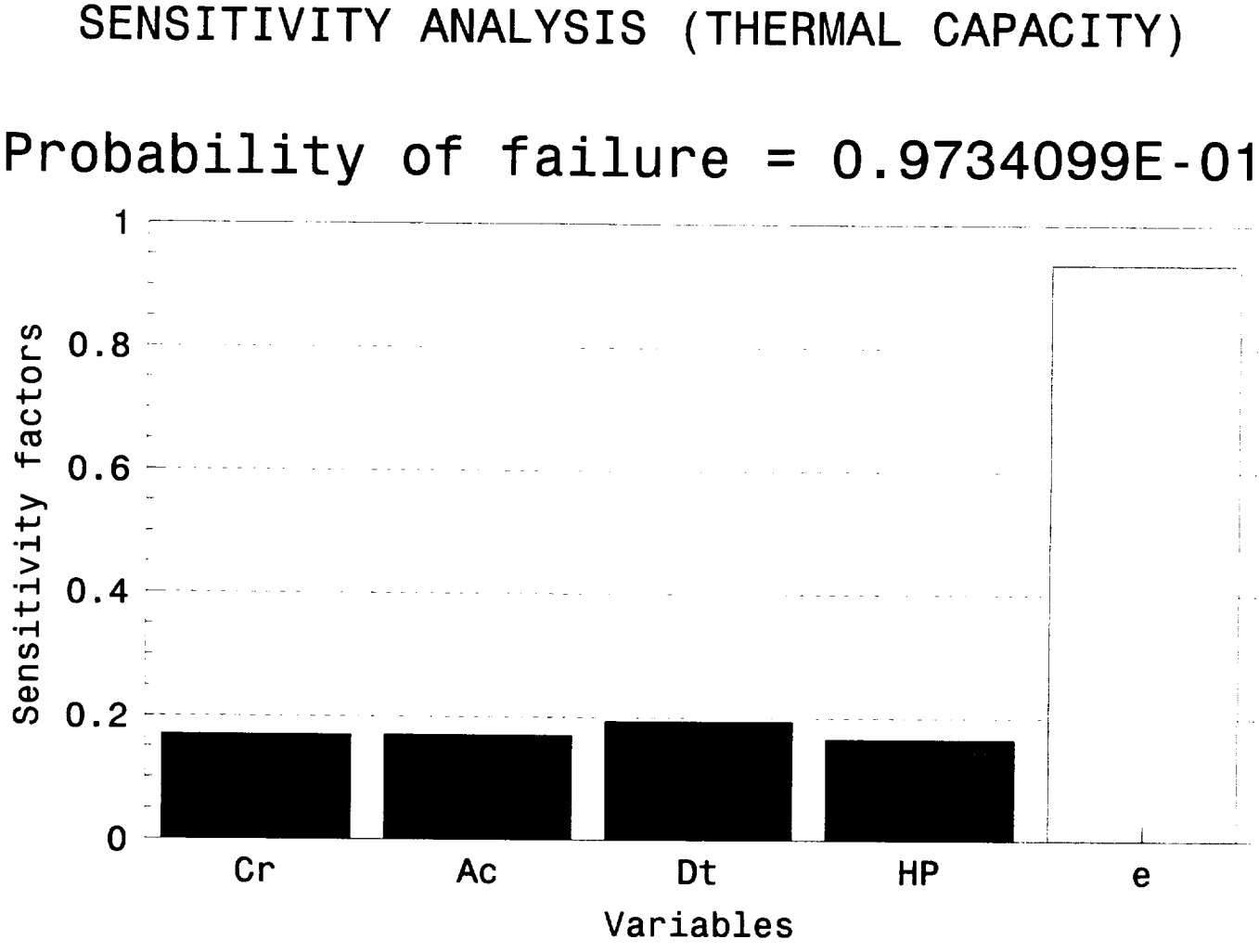


Figure 3-11:Thermal Capacity Analysis Trial-2

TABLE 3-11 : CONTACT STRESS FAILURE MODE DATA

INPUT TABLE

TRIAL -2

Design Parameters	Mean	Standard Deviation	Distribution Type
S_c (psi)	40000	400	NORMAL
F_d (lb)	1731	173.1	NORMAL
C_l (in)	5.204	0.5204	NORMAL
M_u	0.4	0.04	NORMAL
E (psi)	18E+06	0	
D_w (in)	4.0	0.4	NORMAL
D_g (in)	19.1	1.91	NORMAL

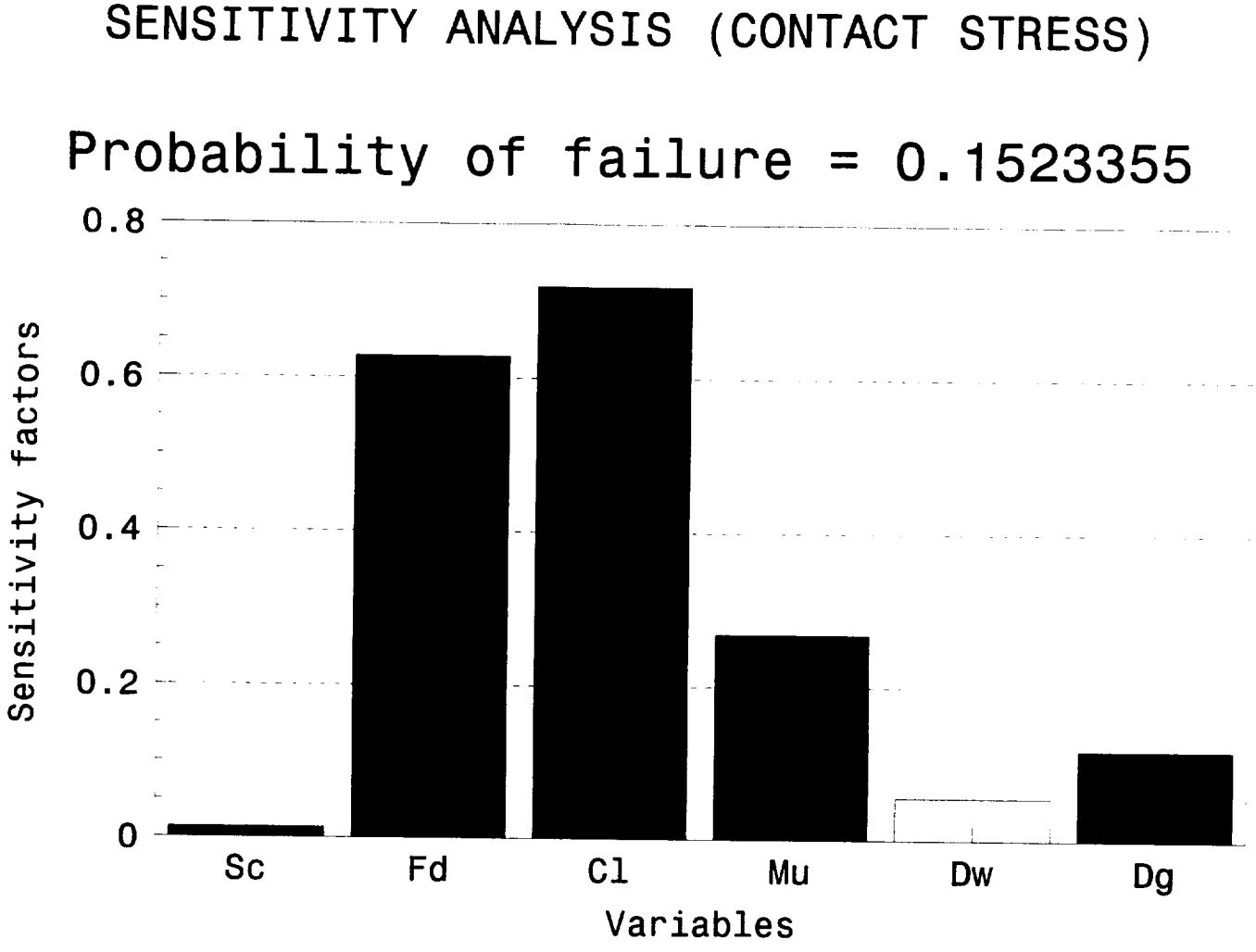


Figure 3-12: Contact Stress Analysis Trial-2

TABLE 3 - 12 : WEAR FAILURE MODE DATA

INPUT TABLE

TRIAL -2

Design paramters	Mean	Standard Deviation	Distribution type
D_g (in)	19.1	1.91	NORMAL
b (in)	2.2	0.22	NORMAL
K (lb/in^2)	80	8	NORMAL
F_d (lb)	1731	173.1	NORMAL

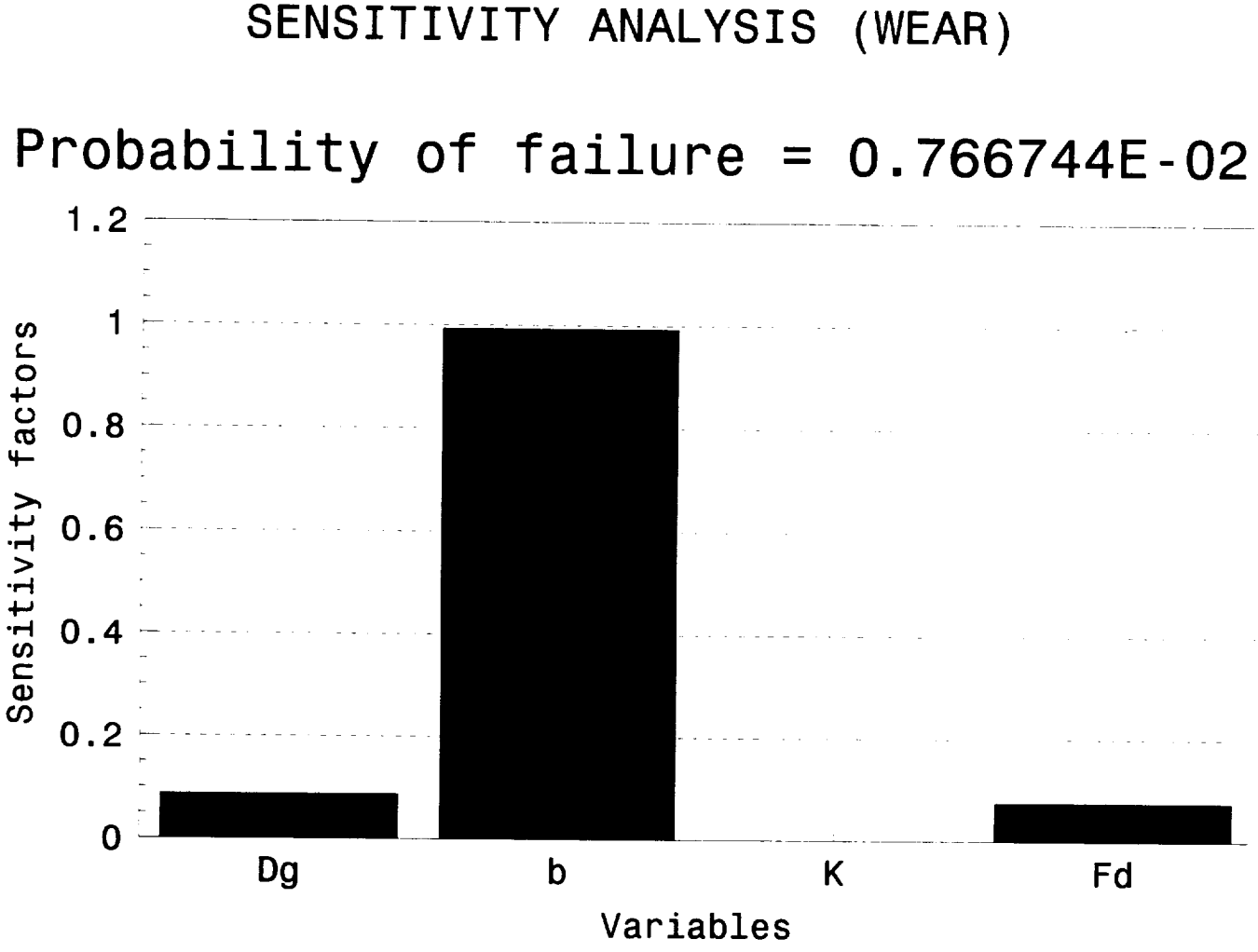


Figure 3-13: Wear Analysis Trial -2

TABLE 3 - 13 : BENDING STRESS FAILURE MODE DATA

INPUT TABLE

TRIAL -3

Design paramters	Mean	Standard Deviation	Distribution type
S_b (psi)	12000	1200	NORMAL
F_d (lb)	1731	173.1	NORMAL
P (in)	3.23	0.323	NORMAL
b (in)	2.4	0.24	NORMAL
Y	0.392	0	

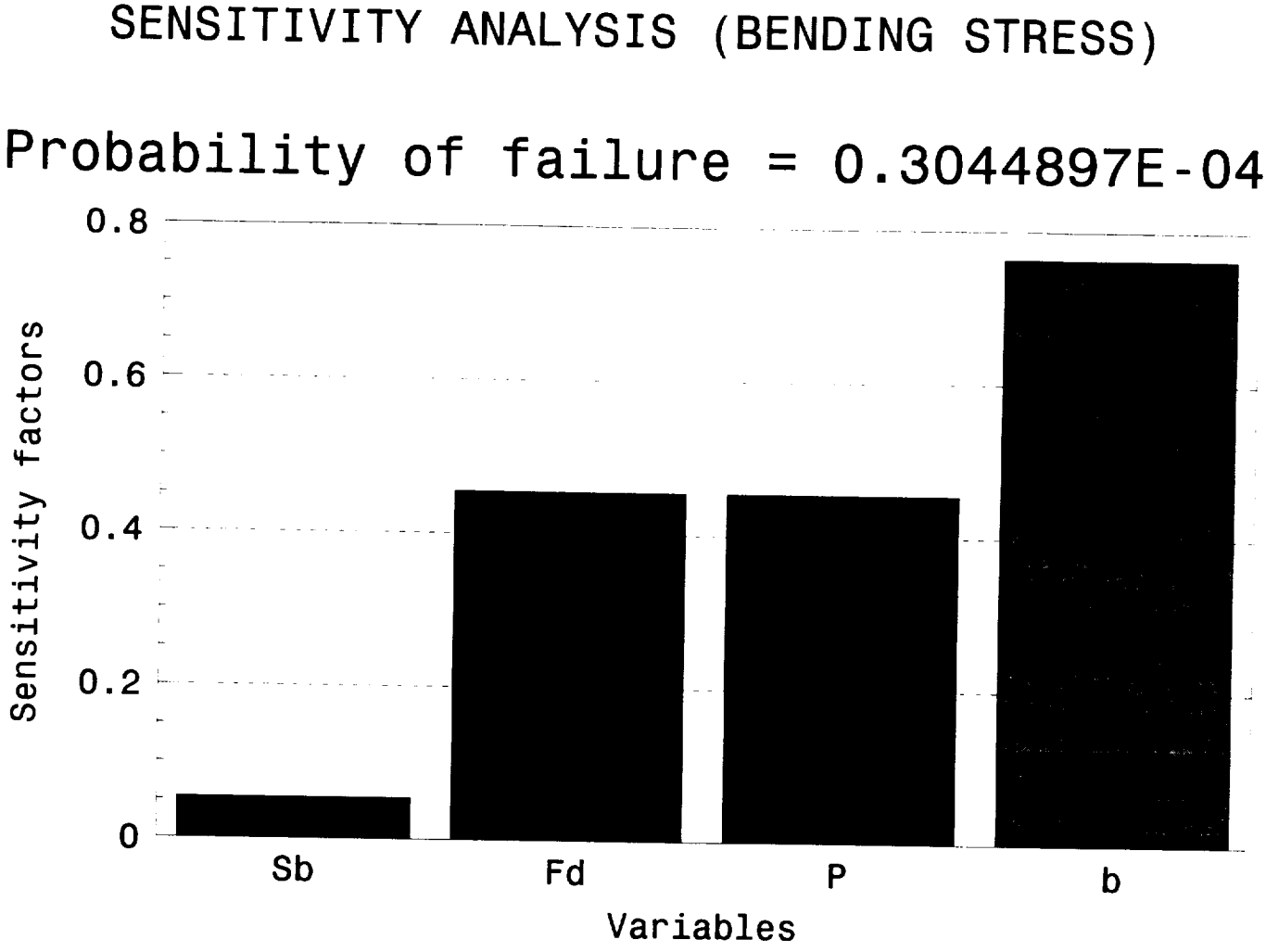


Figure 3-14: Bending Stress Analysis Trial-3

TABLE 3 - 14 : THERMAL CAPACITY FAILURE MODE DATA INPUT TABLE

TRIAL -3

Design paramters	Mean	Standard Deviation	Distribution type
C_r (ft-lb/min in °F)	0.43	0.043	NORMAL
A_c (in^2)	2766.6	276.6	NORMAL
D_t (°F)	350	35	NORMAL
HP (ft-lb/min)	0.229E+06	0.229E+03	NORMAL
e	0.96	0.096	NORMAL

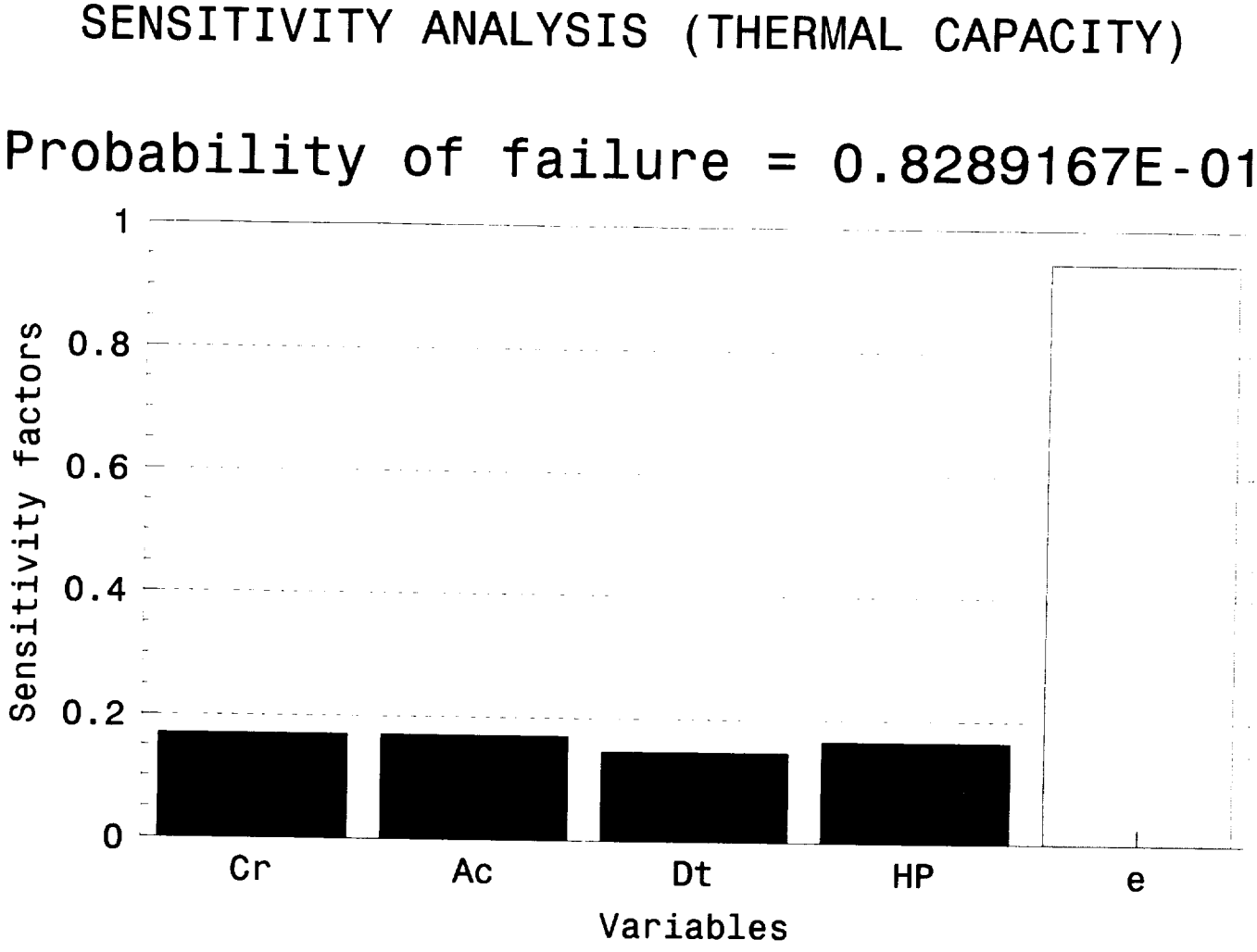


Figure 3-15: Thermal Capacity Analysis Trial -3

TABLE 3-15 : CONTACT STRESS FAILURE MODE DATA

INPUT TABLE

TRIAL -3

Design Parameters	Mean	Standard Deviation	Distribution Type
S_c (psi)	40000	400	NORMAL
F_d (lb)	1731	173.1	NORMAL
C_l (in)	5.404	0.5404	NORMAL
M_u	0.4	0.04	NORMAL
E (psi)	18E+06	0	
D_w (in)	4.0	0.4	NORMAL
D_g (in)	19.1	1.91	NORMAL

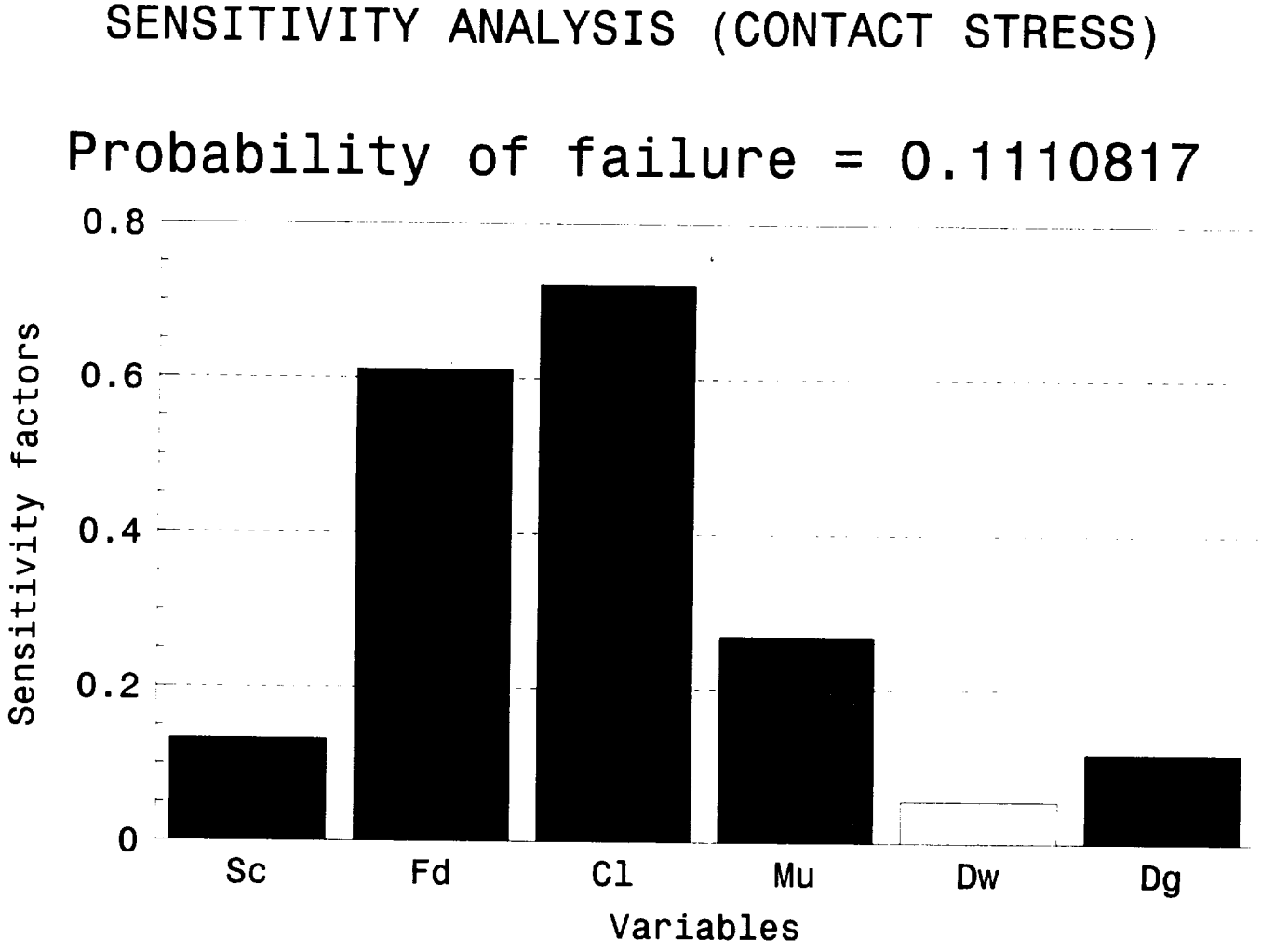


Figure 3-16: Contact Stress Analysis Trial -3

TABLE 3 -16 : WEAR FAILURE MODE DATA

INPUT TABLE

TRIAL -3

Design paramters	Mean	Standard Deviation	Distribution type
D_g (in)	19.1	1.91	NORMAL
b (in)	2.4	0.24	NORMAL
K (lb/in^2)	80	8	NORMAL
F_d (lb)	1731	173.1	NORMAL

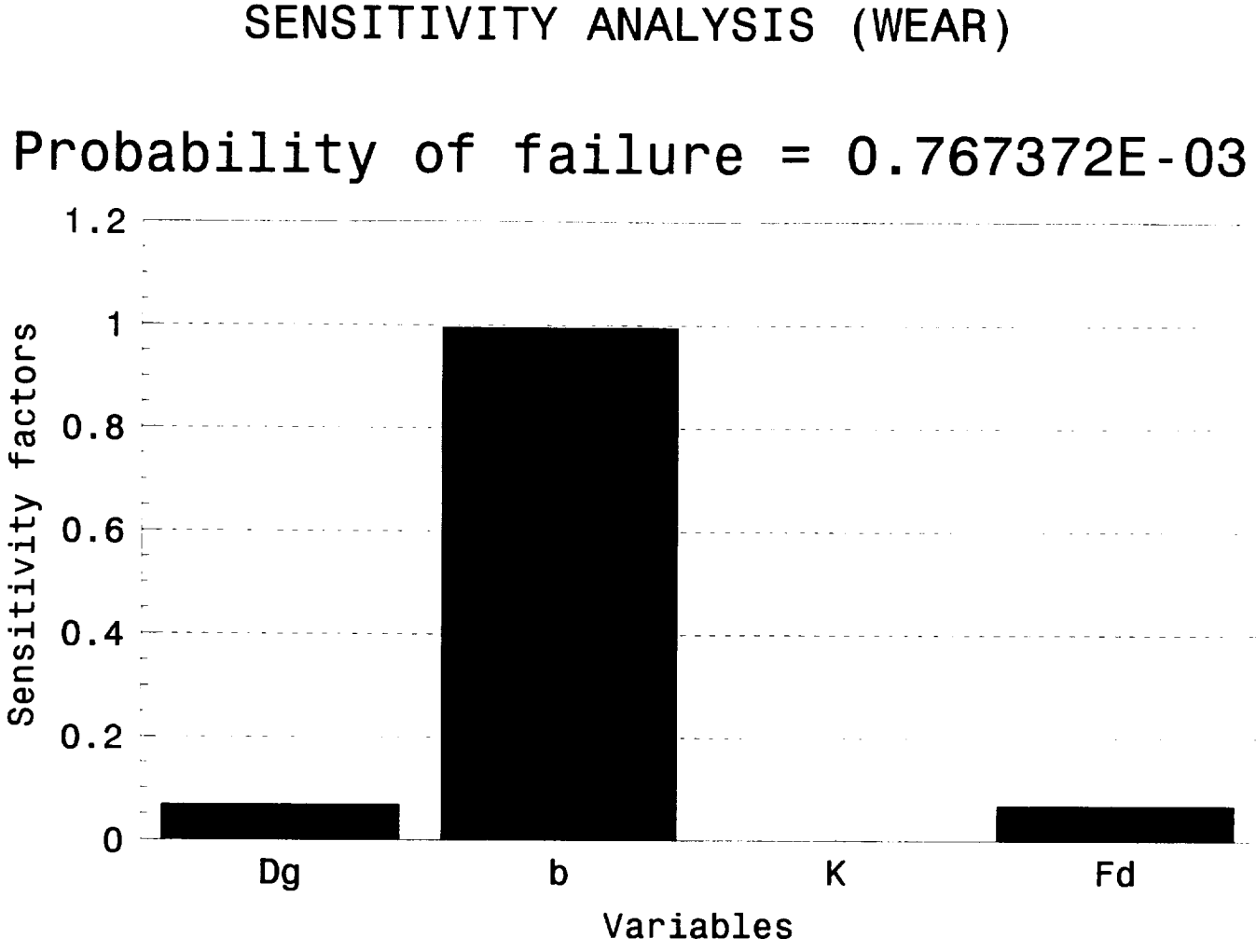


Figure 3-17: Wear Analysis Trial -3

TABLE 3 - 17 : BENDING STRESS FAILURE MODE DATA

INPUT TABLE

TRIAL -4

Design paramters	Mean	Standard Deviation	Distribution type
S_b (psi)	12000	1200	NORMAL
F_d (lb)	1731	173.1	NORMAL
P (in)	3.23	0.323	NORMAL
b (in)	2.6	0.26	NORMAL
Y	0.392	0	

TABLE 3 - 18 : THERMAL CAPACITY FAILURE MODE DATA

INPUT TABLE

TRIAL -4

Design paramters	Mean	Standard Deviation	Distribution type
C_r (ft-lb/min in °F)	0.43	0.043	NORMAL
A_c (in^2)	2766.6	276.6	NORMAL
D_t (°F)	350	35	NORMAL
HP (ft-lb/min)	0.229E+06	0.229E+03	NORMAL
e	0.97	0.097	NORMAL

TABLE 3-19 : CONTACT STRESS FAILURE MODE DATA

INPUT TABLE

TRIAL -4

Design Parameters	Mean	Standard Deviation	Distribution Type
S_c (psi)	40000	400	NORMAL
F_d (lb)	1731	173.1	NORMAL
C_l (in)	5.504	0.5504	NORMAL
M_u	0.4	0.04	NORMAL
E (psi)	18E+06	0	
D_w (in)	4.0	0.4	NORMAL
D_g (in)	19.1	1.91	NORMAL

TABLE 3 - 20 : WEAR FAILURE MODE DATA

INPUT TABLE

TRIAL -4

Design paramters	Mean	Standard Deviation	Distribution type
D_g (in)	19.1	1.91	NORMAL
b (in)	2.6	0.26	NORMAL
K (lb/in^2)	80	8	NORMAL
F_d (lb)	1731	173.1	NORMAL

TABLE 3 - 21 : BENDING STRESS FAILURE MODE DATA

INPUT TABLE

TRIAL -5

Design paramters	Mean	Standard Deviation	Distribution type
S_b (psi)	12000	1200	NORMAL
F_d (lb)	1731	173.1	NORMAL
P (in)	3.23	0.323	NORMAL
b (in)	1.8	0.18	NORMAL
Y	0.392	0	

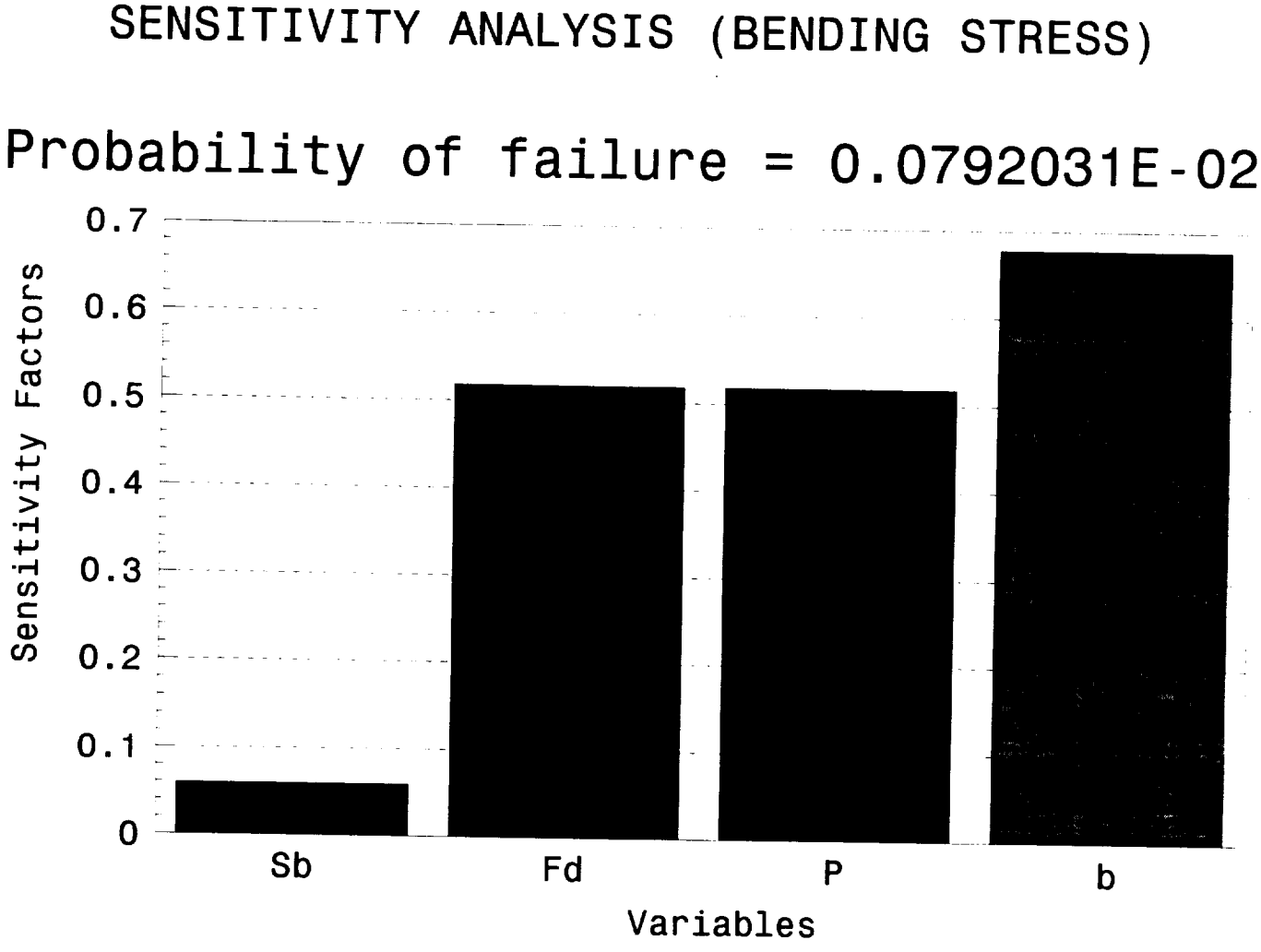


Figure 3-18: Bending Stress Analysis Trial-5

TABLE 3 - 22 : THERMAL CAPACITY FAILURE MODE DATA INPUT TABLE

TRIAL -5

Design paramters	Mean	Standard Deviation	Distribution type
C_r (ft-lb/min in °F)	0.43	0.043	NORMAL
A_c (in^2)	2766.6	276.6	NORMAL
D_t (°F)	350	35	NORMAL
HP (ft-lb/min)	0.229E+06	0.229E+03	NORMAL
e	0.90	0.090	NORMAL

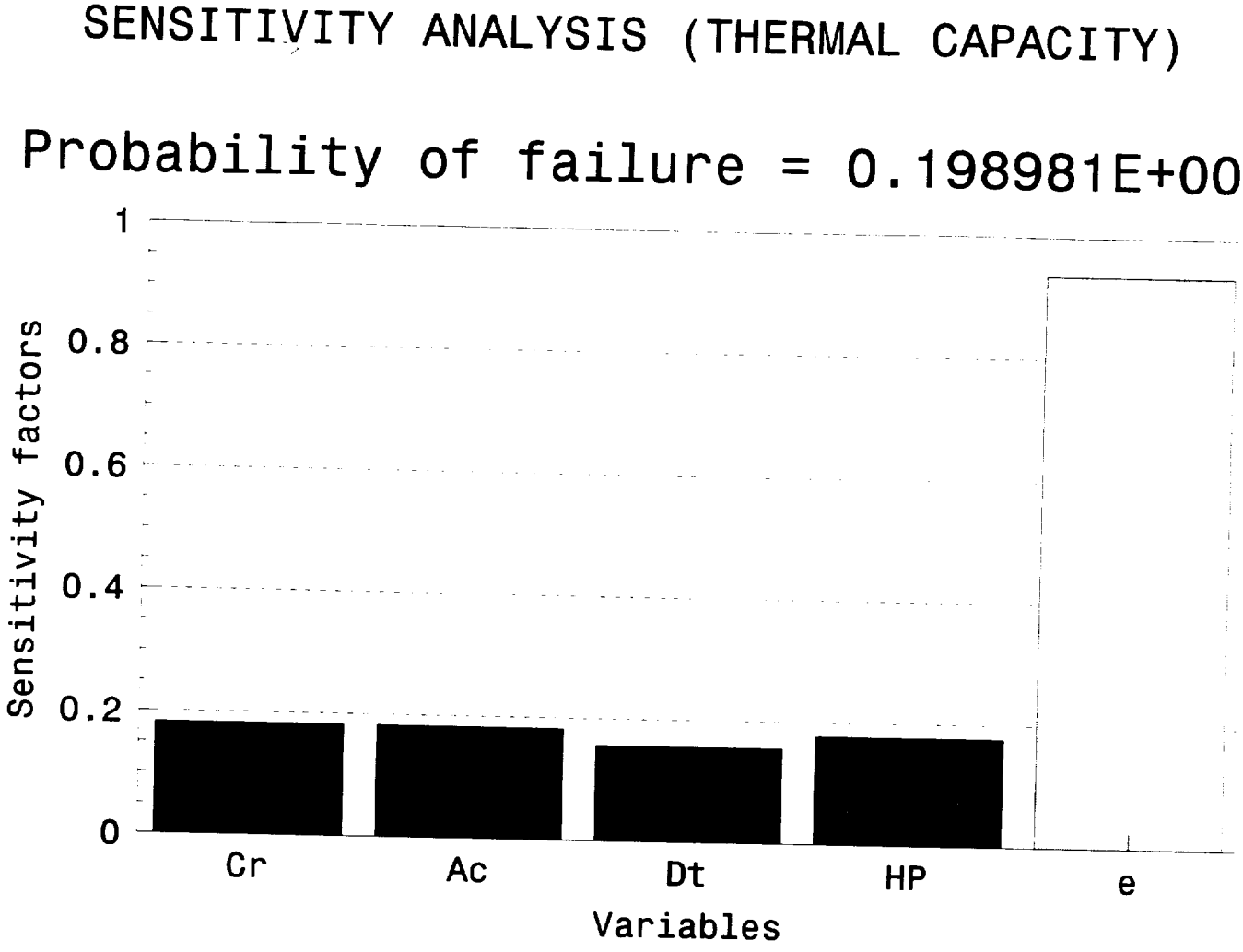


Figure 3-19: Thermal Capacity Analysis Trial -5

TABLE 3-23 : CONTACT STRESS FAILURE MODE DATA

INPUT TABLE

TRIAL -5

Design Parameters	Mean	Standard Deviation	Distribution Type
S_c (psi)	40000	400	NORMAL
F_d (lb)	1731	173.1	NORMAL
C_l (in)	4.804	0.4804	NORMAL
M_u	0.4	0.04	NORMAL
E (psi)	18E+06	0	
D_w (in)	4.0	0.4	NORMAL
D_g (in)	19.1	1.91	NORMAL

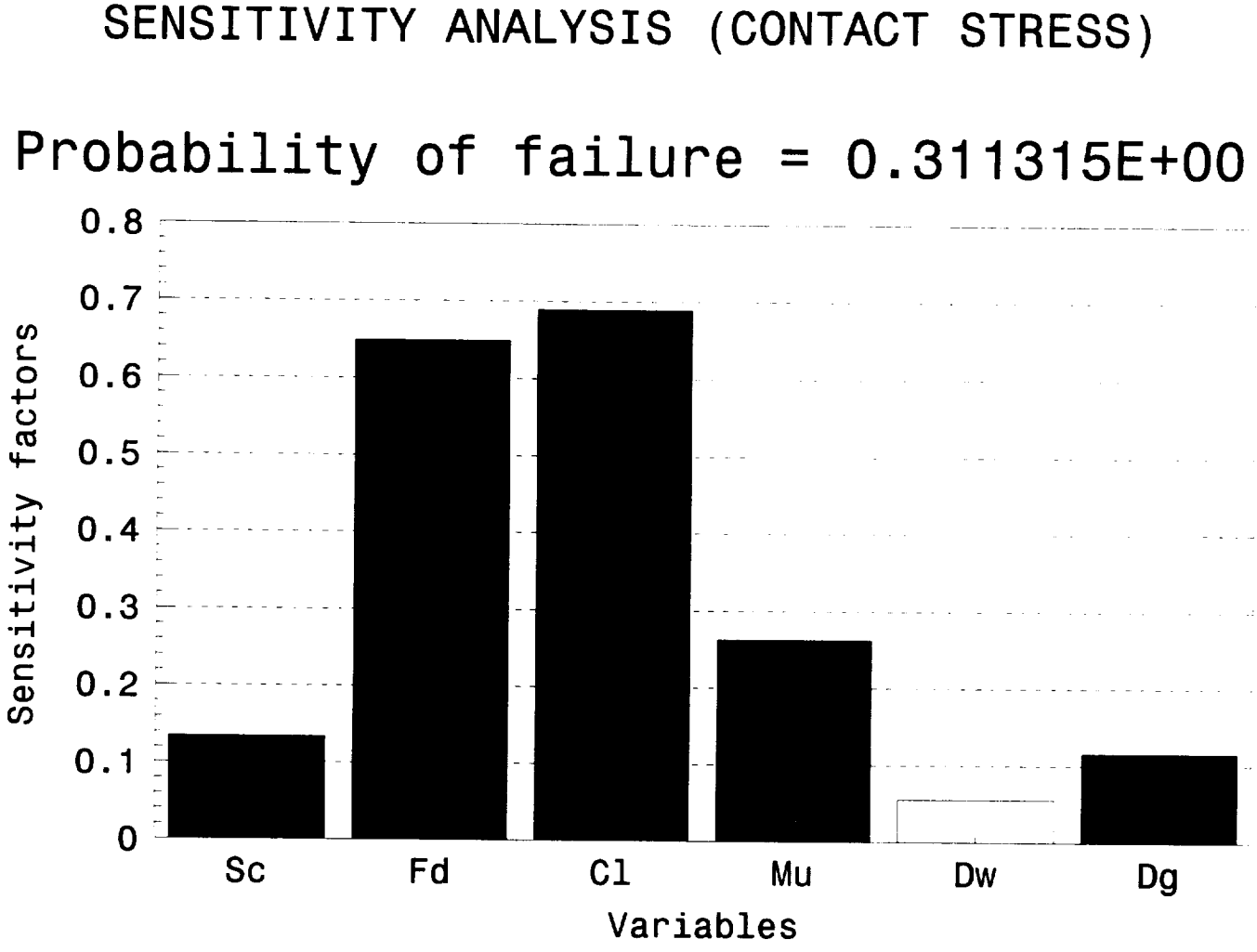


Figure 3-20: Contact Stress Analysis Trial -5

TABLE 3 - 24 : WEAR FAILURE MODE DATA

INPUT TABLE

TRIAL -5

Design paramters	Mean	Standard Deviation	Distribution type
D_g (in)	19.1	1.91	NORMAL
b (in)	1.8	0.18	NORMAL
K (lb/in^2)	80	8	NORMAL
F_d (lb)	1731	173.1	NORMAL

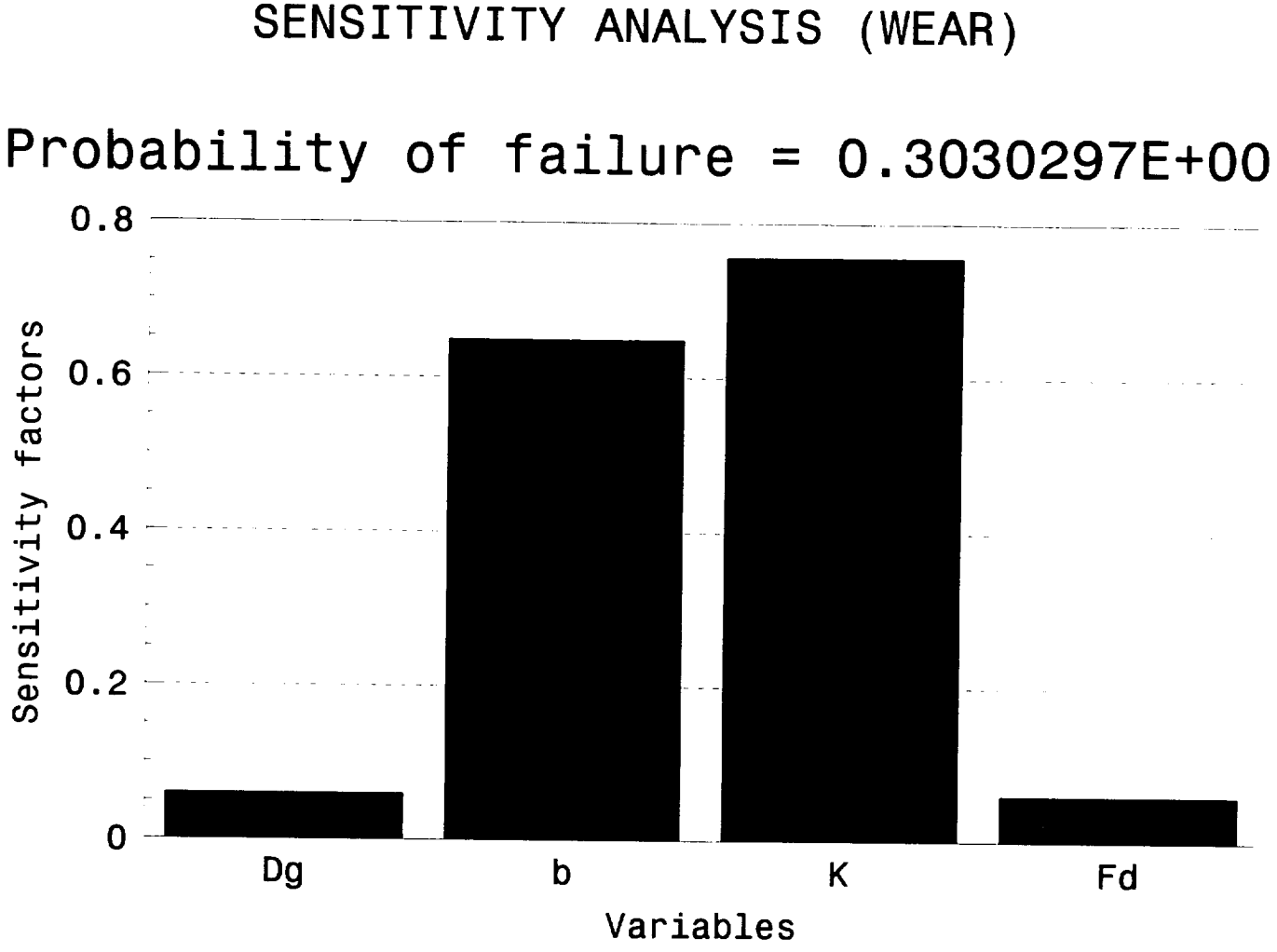


Figure 3-21: Wear Analysis Trial -5

CHAPTER IV

FAULT-TREE ANALYSIS

4.1 System Reliability

In calculating system reliability, it is important to include the probabilistic dependencies between multiple component failures or between different failure modes. Failure to do so could result in significant errors. Fault Tree Analysis is a commonly used tool in risk assessment. A fault tree is a mathematical construction of assumed component failure modes (bottom events) linked in series or parallel and leading to a top event, which denotes the total system failure. A fault tree diagram essentially decomposes the main failure event (top event) into unions and intersections of subevents or combination of subevents. The decomposition continues until the probabilities of the subevents can be evaluated as single mode failure probabilities. The probabilistic fault-tree analysis is based on the limit state definition of the bottom events. Thus, one requirement for system risk assessment is to compute failure function of each bottom event. Each bottom event is defined by a close form

equation.

A fault tree has three major characteristics: bottom events, combination gates, and the connectivity between the bottom events and the case. The system risk assessment is limited to OR and AND gates. The OR gate implies that the output fault event is the union of subevents [26]. The AND gate signifies that the output fault event is the intersection of the subevents. The different steps involved in the application of the fault-tree analysis method can be summarized as follows [26]:

1. Development of a fault tree to represent the structural system.

2. Construction of an approximate performance function for each bottom event.

3. Determination of a dominant sampling sequence for all bottom events.

4. Calculation of the system reliability using an Adaptive Importance Sampling method.

To illustrate the fault tree analysis, consider a simple example consisting of two failure modes: yielding and excessive displacement. Two failure functions can be expressed as

$$g_1 = R \text{ (Yield strength)} - S \text{ (Stress)} \qquad (4\text{-}1)$$

g_2 = D (Allowable displacement) - d (displacement) (4-2)

Failure occurs if [g_1<0] or [g_2<0]. Using standard probability notations, the system probability of failure is [27]:

$$P_f = P[(g_1 < 0) \cup (g_2 < 0)] \quad (4\text{-}3)$$

In general,

$$P_f = P[g_1<0]+P[g_2<0]-P[(g_1<0)\cap(g_2<0)] = P_1+P_2-P_{12} \quad (4\text{-}4)$$

In general P_{12} ranges from 0 to the smaller value of P_1 and P_2. Therefore, P_f ranges from [P_1 +P_2] to P_2(assuming P_2 >P_1). Hence, by assuming independent events, the error ranges from $-P_1P_2$ to $P_1(1-P_2)$.

In application to the worm gear, one OR gate is considered with four bottom events. The four bottom events represent the four failure modes of the worm gear. The representation of fault tree with four failure modes is shown in Figure 4-1.

The Fault-tree analysis is carried out by two methods:

1. Adaptive importance sampling method.

2. Standard Monte Carlo sampling method.

4.2 Adaptive Importance sampling method

Adaptive Importance Sampling is different from traditional importance sampling methods because of its ability to automatically adjust and thereby minimize the sampling

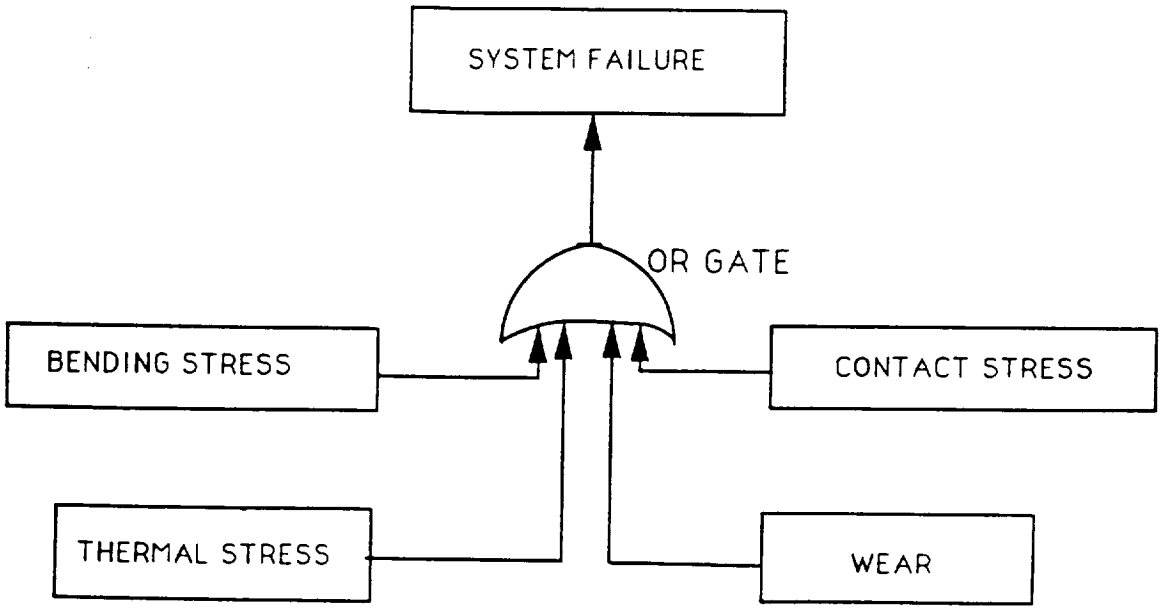


FIGURE 4-1: Representation of Fault Tree Analysis

space [28]. Because of this attribute, adaptive importance sampling method is a highly efficient and accurate alternative for probabilistic analysis.

Two options are available for selecting the sampling boundaries. The first-order adaptive sampling method uses hyperplanes, and the second-order adaptive sampling method uses parabolic surfaces. Both surfaces are constructed in the u-space and use the most probable point to define the beginning sample space. In general, sampling space can be adjusted by increasing or decreasing the curvatures of the parabolic surface until there are no more failure points in the final sampling space [29]. In the first order based

method, only the distance to the hyperplane is changed. In the second-order based method, the curvature of the sampling boundary is updated first; then, the final surface is shifted toward the origin.

4.3 Monte Carlo Sampling method

Monte Carlo sampling method is a way of generating information for a simulation when events occur in a random way. It uses unrestricted random sampling (it selects items from a population in such a way that each item in the population has an equal probability of being selected) in a computer simulation in which the results are run off repeatedly to develop statistically reliable answers. A sample from a Monte Carlo simulation is similar to a sample of experimental observations. Therefore the results of Monte Carlo simulations may be treated statistically. Monte Carlo methods are useful because they can handle very complex models, are guaranteed to work, and are exact in the limit as the number of samples become large. The disadvantage is that a very large number of simulations may be necessary [30]. The probability of failure obtained by the above two methods are as follows:

1. Probability of failure by **Sampling method = 0.6665916E-01**
2. Probability of failure by **Monte Carlo method = 0.66657E-01**

The weight, W, of the gear can be determined as a function of the probability of failure. The weight is computed by the equation

$$W = \gamma V \tag{4-5}$$

where,

γ = Specific weight of phosphor bronze , lb/in^3

V = Volume of the gear, in^3

The volume of the gear is calculated from the equation

$$V = (\pi/4) d_g^2 b \tag{4-6}$$

where,

d_g = Diameter of the gear, in.

b = Face width of the gear, in.

As the face width value changes, the weight of the gear changes; hence, the probability of failure changes. The weight is plotted versus the probability of failure and is shown in Figure 4-2.

Figure 4-3 shows the coefficient of variation plotted against the probability of failure. The coefficient of variation is related to the mean and standard deviation by the equation

$$C.O.V = \frac{\sigma}{\mu} \qquad (4\text{-}7)$$

where,

σ = Standard deviation

μ = Mean value of the design parameter

The mean value of the face width is kept constant at 2.6 in and the c.o.v is varied from 0.01 to 0.1. It is learned from the Figure 4-3 that, as the uncertainty increases, the probability of failure increases. A deviation of 0.182 in is suggested to the manufacturer from the mean value. The final value for the face width using probabilistic design methodology is 2.6 in with a deviation of +0.182 in or -0.182 in.

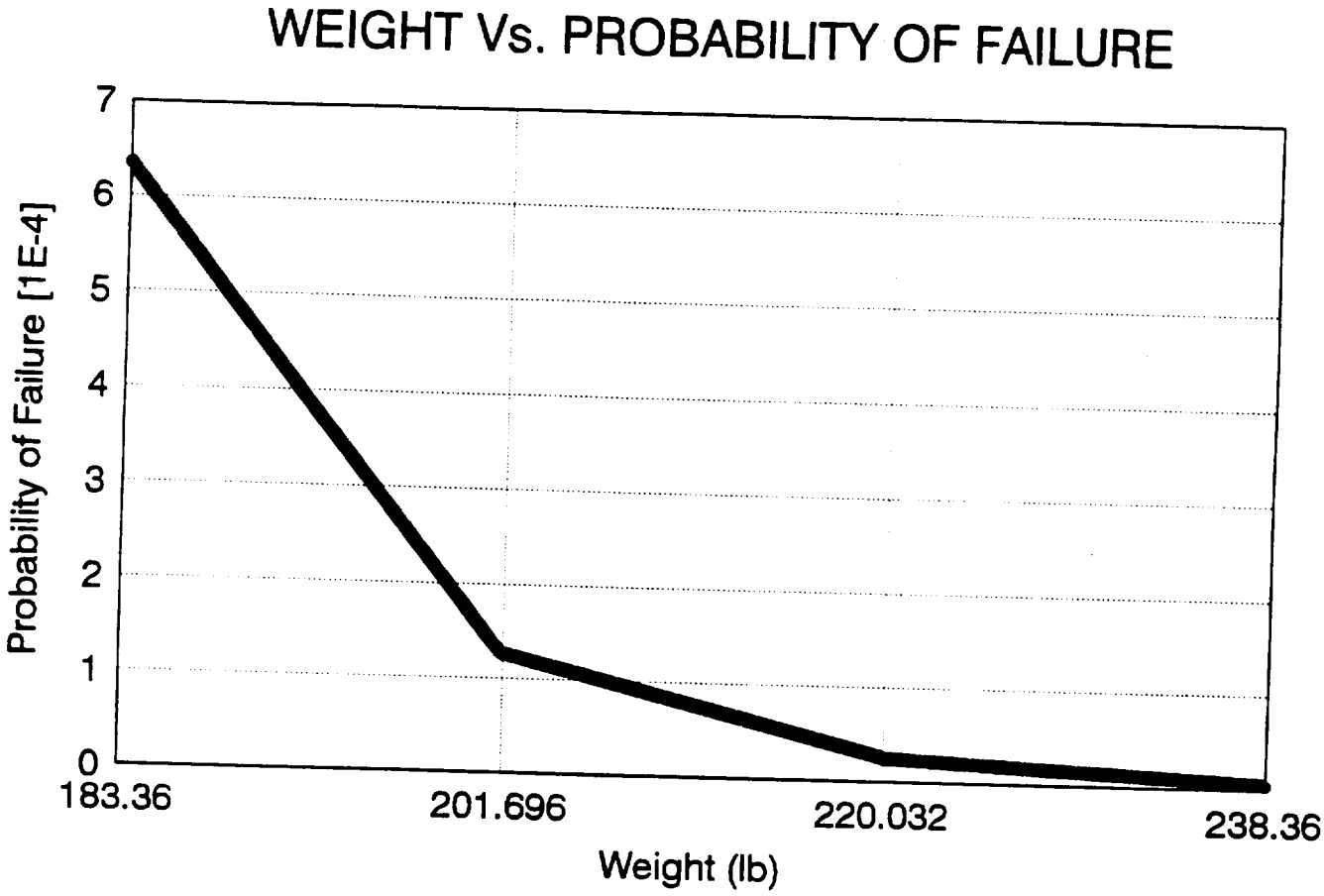


Figure 4-2: Relationship Between Weight and Probability of Failure

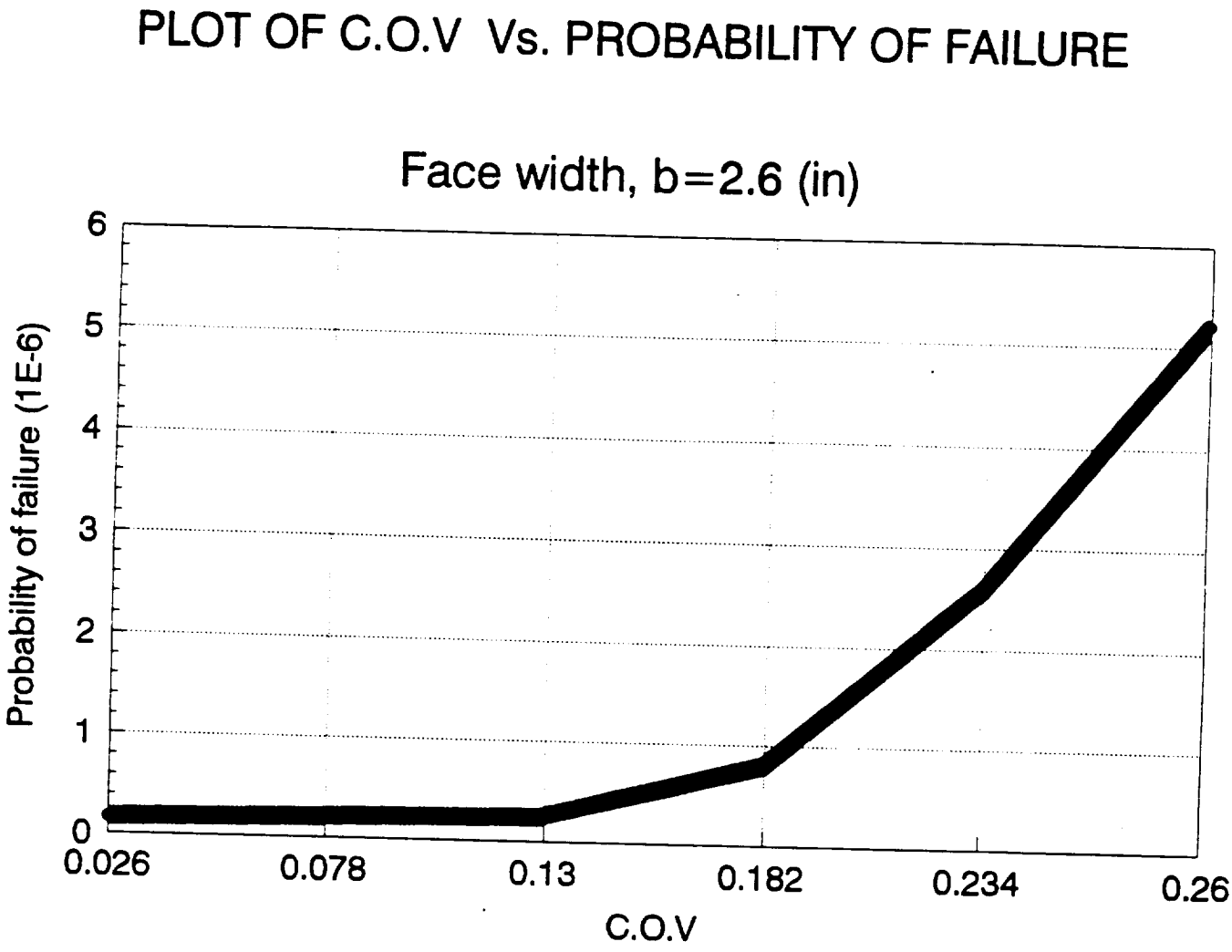


Figure 4-3: Relationship Coefficient of Variation and Probability of Failure

CHAPTER V

FINITE ELEMENT METHOD

5.1 Basic concept

The basic idea in the finite element method is to find the solution of a complicated problem by replacing it with a simpler one. Since the actual problem is replaced by a simpler one in finding the solution, we will be able to find only an approximate solution rather than the exact solution. The existing mathematical tools will not be sufficient to find the exact solution of most of the practical problems. Thus, in the absence of any other convenient method to find even the solution of a given problem, we have to prefer the finite element method. Moreover, in the finite element method, it will often be possible to improve or refine the approximate solution by spending more computational effort. In the finite element method, the solution region is considered as built up of many small, interconnected subregions called finite elements.

5.2 General description of the Finite Element Method

In the finite element method, the actual continuum or

body of matter like solid, liquid or gas is represented as an assemblage of subdivisions called finite elements. These elements are considered to be interconnected at special joints which are called nodes or nodal points. The nodes usually lie on the element boundaries where adjacent elements are considered to be connected. Since the actual variation of the field variable (like displacement, stress, temperature, pressure or velocity) inside the continuum is not known, we assume that the variation of the field variable inside a finite element can be approximated by a simple function. These approximating functions (also called interpolation models) are defined in terms of the values of the field variables at the nodes. When field equations (like equilibrium equations) for the whole continuum are written, the new unknowns will be the nodal values of the field variable. By solving the field equations, which are generally in the form of matrix equations, the nodal values of the field variable will be known. Once these are known, the approximating functions define the field variable throughout the assemblage of elements. The solution of general continuum problem by the finite element method always follows an orderly step by step process.

The step-by-step procedure can be stated as follows.

Step 1: Discretization of the structure

The first step in the finite element method is to divide the structure or solution region into subdivisions or elements. Hence, the structure that is being analyzed has to be modelled with suitable finite elements. The number, type, size and arrangement of the elements have to be decided.

Step 2: Selection of a proper interpolation or displacement model

Since the displacement solution of a complex structure under any specified load conditions cannot be predicted exactly, we assume some suitable solution within an element to approximate the unknown solution. The assumed solution must be simple from a computational point of view, but it should satisfy certain convergence requirements. In general, the solution or interpolation model is taken in the form of a polynomial.

Step 3: Derivation of element stiffness matrices and load vectors

From the assumed displacement model, the stiffness matrix $[K^{(e)}]$ and the load vector $P^{(e)}$ of the element "e" are to be derived by using either equilibrium conditions or a suitable variational principle

Step 4: Assemblage of element equations to obtain the overall equilibrium equations.

Since the structure is composed of several finite elements, the individual element stiffness matrices and load vectors are to be assembled in a suitable manner and the overall equilibrium equations have to be formulated as

$$[K]'\Phi' = P' \tag{5-1}$$

Where [K]' is called the assembled stiffness matrix, Φ' is the vector of nodal displacements, and P' is the vector of nodal forces for the complete structure.

Step 5: Solution for the unknown nodal displacements.

The overall equilibrium equations have to be modified to account for the boundary conditions of the problem. After the incorporation of the boundary conditions, the equilibrium equations can be expressed as

$$[K]\Phi = P \tag{5-2}$$

For linear problems, the vector Φ can be solved very easily. But for nonlinear problems, the solution has to be obtained in a sequence of steps, each step involving the modification of the stiffness matrix [K] and/or the load vector P.

Step 6: Computation of element strains and stresses.

From the known nodal displacements Φ, if required, the element strain and stresses can be computed by using the

necessary equations of solid or structural mechanics.

The above mentioned six steps were applied in the finite element analysis of the tooth of the worm gear to analyze the stress distribution and displacement. The analysis was done for both probabilistic and deterministic method. The analysis was carried out using finite element software, **COSMOS/M**. The analysis was first carried out using the deterministic design. The displacement and the stress distribution due to the transmitted load for the deterministic design are shown in Figures 5-1 and 5-2. The maximum stress and the displacement obtained using the deterministic design values are 1.4E+05 psi and 0.001170 in.

The finite element analysis was next carried out using the probabilistic design. The displacement, and the stress distribution due to the transmitted load for the probabilistic design are shown in Figures 5-3 and 5-4. The maximum stress, and the displacement obtained using the probabilistic design are 8.34E+04 psi and 0.000848 in.

The reason for the reduced stress in the probabilistic design values is due to the increase in the face width.

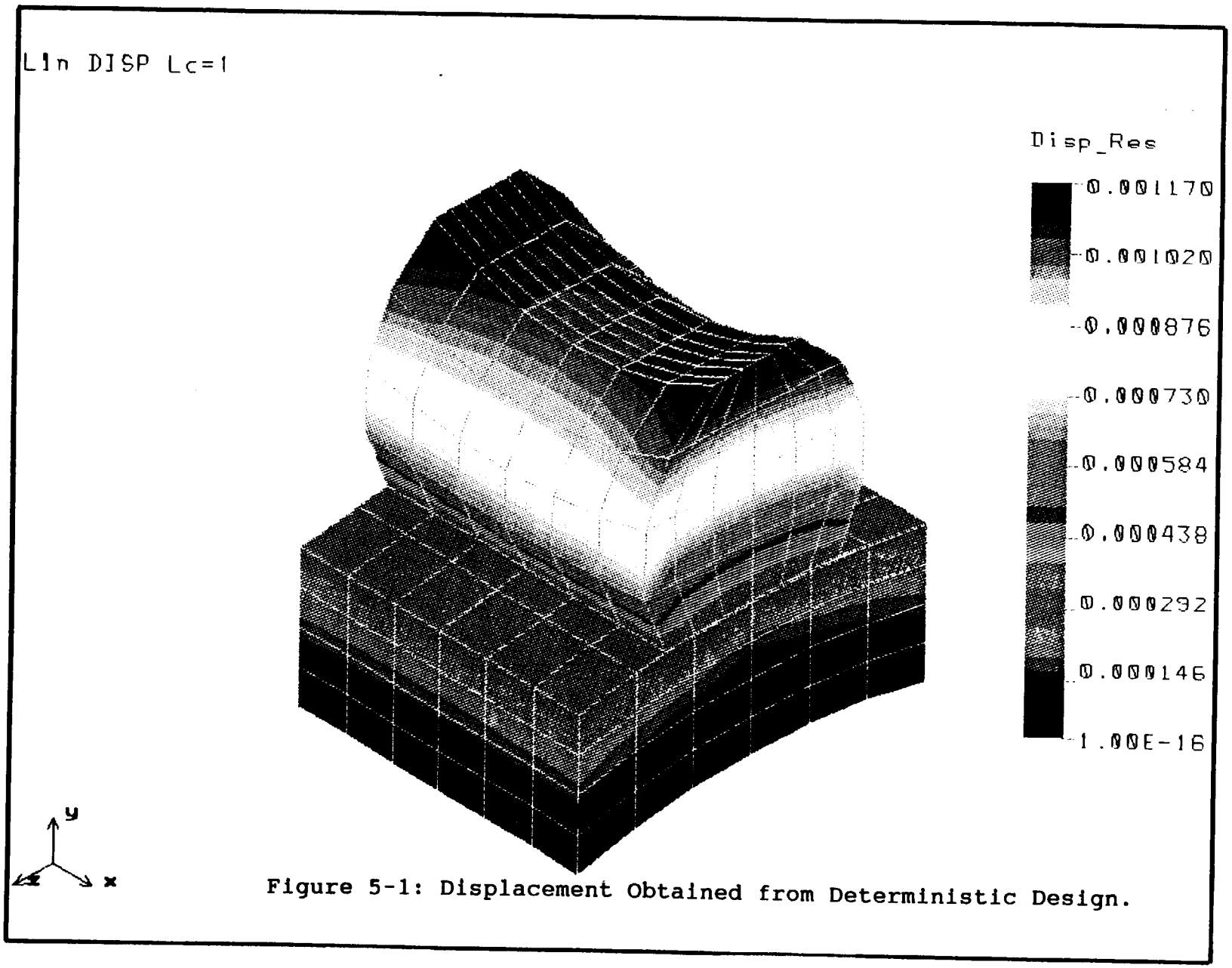


Figure 5-1: Displacement Obtained from Deterministic Design.

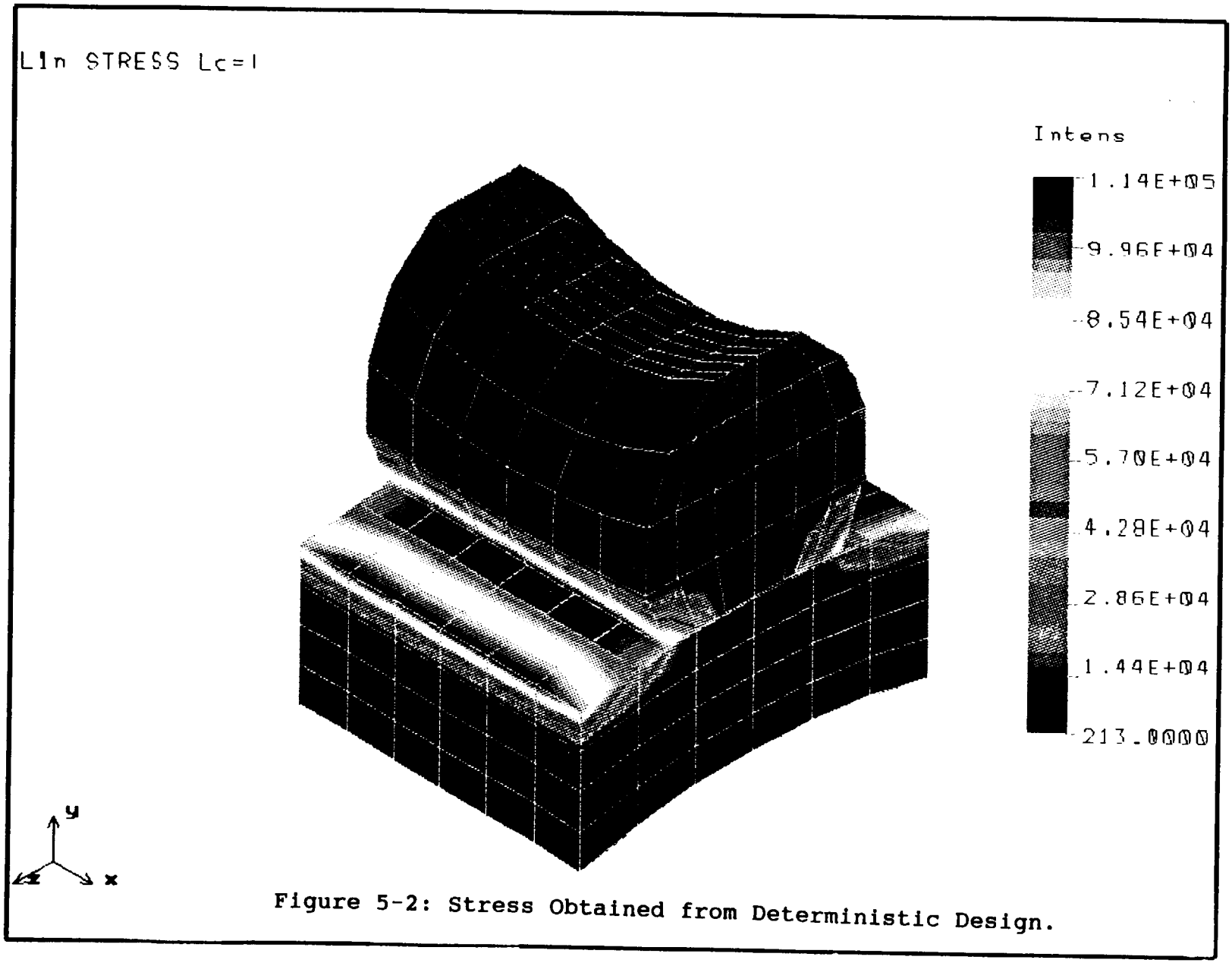


Figure 5-2: Stress Obtained from Deterministic Design.

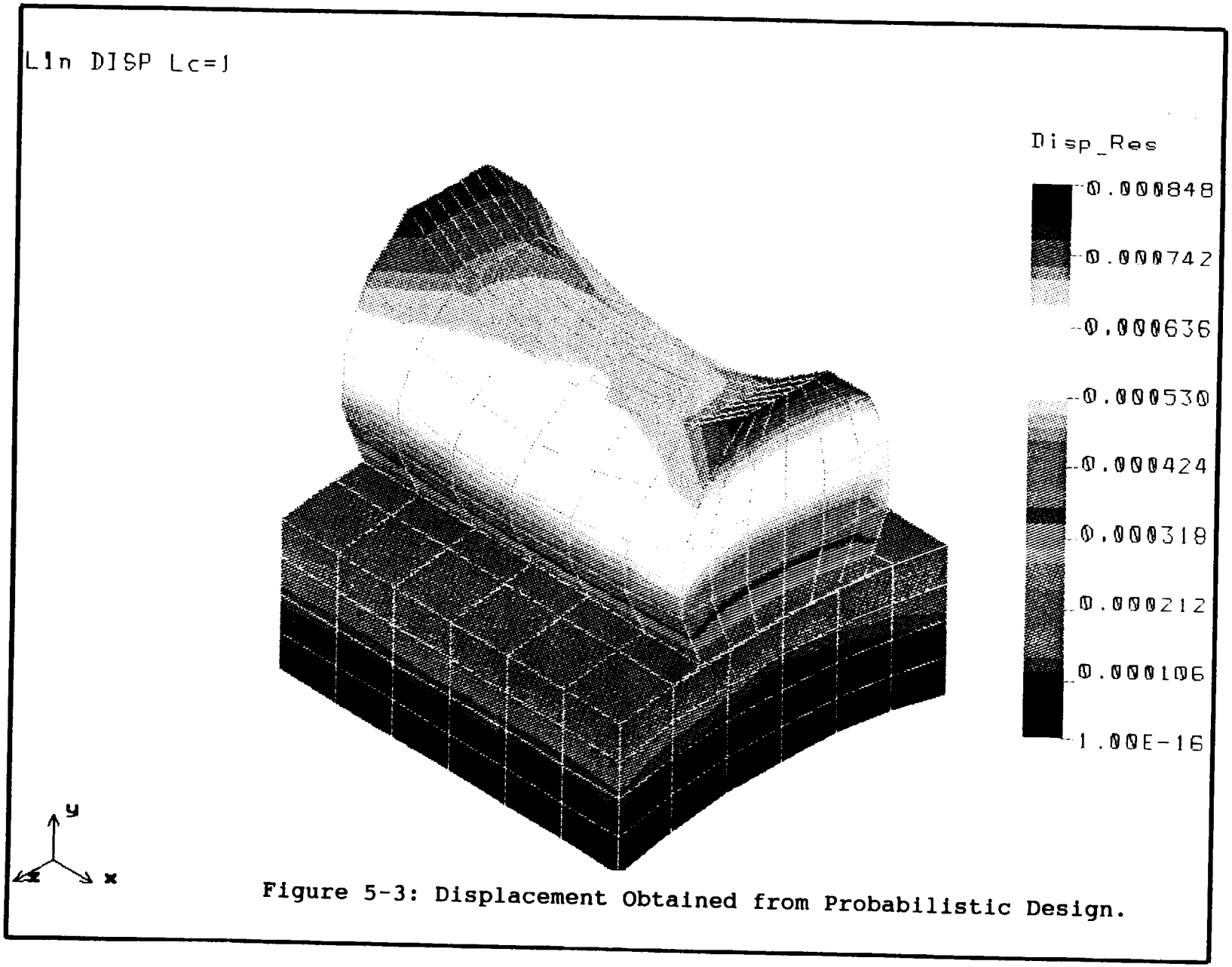


Figure 5-3: Displacement Obtained from Probabilistic Design.

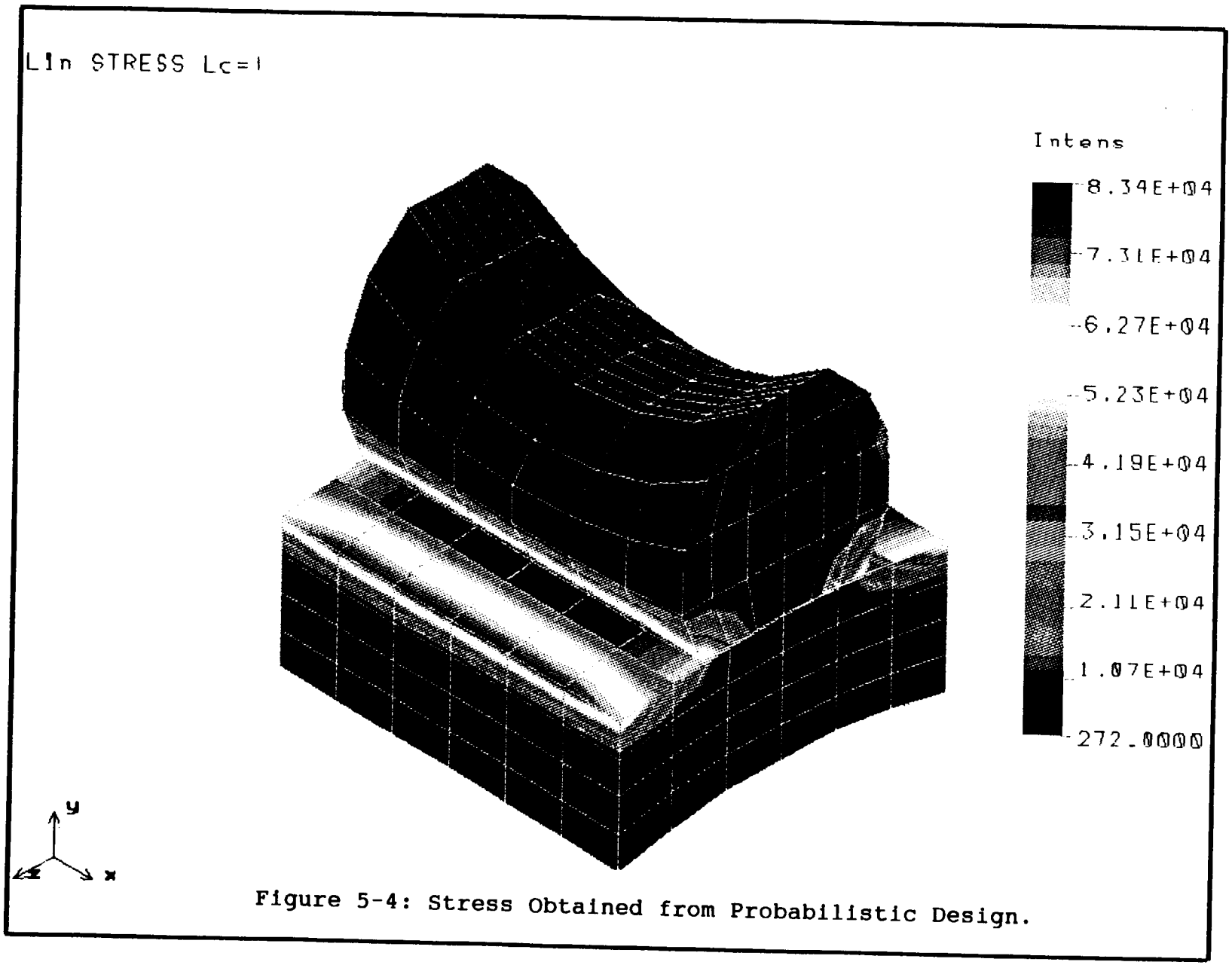


Figure 5-4: Stress Obtained from Probabilistic Design.

CHAPTER VI

CONCLUSION

In this project an existing worm gear design was taken and was analyzed for the failure modes using probabilistic design methodology. The purpose of this project is to identify the sensitive design parameters and to increase the reliability of the worm gear design. The initial probability of failure of the system was found to be around 30 percent. By using the probabilistic design methodology and the sensitivity factors, the sensitivity of each design parameter was found out and correspondingly the probability of failure was reduced by altering the values of the design parameters. The sensitivity analysis which is used in the probabilistic design is more helpful in knowing which design parameter is crucial and sensitive in the design. The probability of failure of the design after altering the design values was computed to be 6.6 percent. The critical design parameters of the worm gear design were found to be the face width, contact length, and the thermal efficiency.

Probabilistic design procedures promise to improve

the quality of engineering systems for the following reasons:

1) Probabilistic design incorporates given statistical data explicitly into the design algorithms. Conventional design discards such data.

2) It is more meaningful to say, "The system has a probability of 10E-04 of failing after 1000 hours of operation," than to say, "This system has a factor of safety of 2.3."

3) Rational comparisons can be made between two or more competing designs for a proposed system. In the absence of other considerations, the engineer chooses the design having the lowest probability of failure, or as a basis for developing economic strategies.

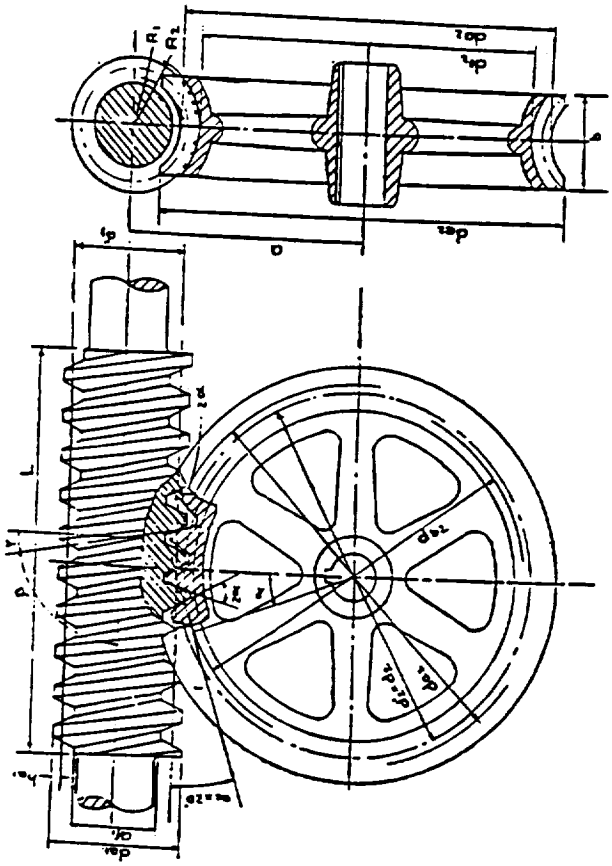
4) By treating each nonstatistical uncertainty as a random variable, its effect on the final design can be quantified. A manager can balance the cost of conducting a research program to remove this uncertainty with the payoff associated with removing the uncertainty and improving the risk.

6.1 Recommendations

1. In order to achieve effective and reliable results, a few things should be taken into consideration. The

distributions for the design parameters should be attained before using PDM. Distributions can be attained from manufaturer's handbooks. The actual deviations that occur should be recorded to get accurate results.

2. The Probabilistic finite element method can be used to compute the maximum stress intensity of the gear tooth and the results can be compared with the values obtained from Cosmos finite element package.



Terminology

Z_2—number of teeth on worm wheel
Z_1—number of starts on the worm
m—axial module, mm
d_1—pitch circle diameter of worm, mm
d_2—pitch circle diameter of worm wheel $= mZ_2$ mm
q—diameter factor $= d_1/m$
a—centre distance $= \frac{1}{2}m(q+Z_2)$
γ—helix angle, lead angle

m_n—normal module $= m \cos \gamma$
L—length of the worm, mm
b—face width of the worm wheel, mm
p_x—axial pitch of worm = circular pitch of worm wheel $= \pi m$
l—lead $= Z_1 \pi m$

$$\tan \gamma = \frac{\text{lead}}{\pi d_1} = \frac{Z_1 \pi m}{\pi q m} = \frac{Z_1}{q}$$

$$\cos \gamma = \frac{q}{\sqrt{Z_1^2 + q^2}}$$

i—gear ratio.

Worm Gear Sketch [23]

Appendix - B

Steps for Running Nessus (Individual Failure mode)

1. Create a **data file** with an extension .dat
2. **Copy the .dat file to for000.dat.** You can do this by typing copy <filename.dat> space for000.dat
3. To input the failure functions **modify** the subroutine **respon.for**
4. To edit the file respon.for, type **edt <respon.for>**. You get an ' * '. Type ' c ' at the ' * ' to get into the full screen mode.
5. Make changes and exit the file by holding **cntrl key** and pressing ' z '. You get ' * '. Type exit to save and close the file.
6. Once the subroutine is modified, it has to be **compiled** and **linked** to the library. To compile type fortran <filename.for>
7. Link the compiled file to the library by typing **link filename** (omit extension), **nes/lib**
8. Do the Probabilistic Analysis by typing **run nessus**.
9. When program asks you to input the data file, give the filename **without** the **extension.dat.**
10. Once you get the output, change the name of for000.dat to <input filename.out>, by typing **ren for000.dat space input filename.out .**
11. To see the **sensitivity analysis** type < **input file name. mov** >.

Appendix - C

Steps for Running Nessus (System Reliability)

1. Create a **data file** with an extension .dat
2. **Copy the .dat file to for000.dat.** You can do this by typing copy <filename.dat> space for000.dat
3. Do the Probabilistic Analysis by typing **run nessus**.
4. When program asks you to input the data file, give the filename **without** the **extension.dat.**
5. Once you get the output, change the name of for000.dat to <input filename.out>, by typing **ren for000.dat space input filename.out .**
6. To see the **sensitivity analysis** type < **input file name. mov** >.

REFERENCES

1. Cruse T.A. at al.,"*An Overview of the NASA (LeRC)-SWRI Probabilistic Structural Analysis (PSAM) Program.*" Structural Safety and Reliability Proceedings of ICOSSAR '89/5th Int'l.Conf. San Francisco, pp2267-2274.

2. Southwest Research Institute, "*4th Annual Short Course on Computational Methods for Probabilistic Analysis.*" SWRI, San Antonio, Texas; September 13-17,1993.

3. Chamis C.C and Hopkins D.A., "*Probabilistic Structural Analysis methods of Hot Engine Structures.*" NASA Technical Memorandum 102091, June 1989.

4. Safie F.M.,"*Use of Probabilistic Design Methods for NASA Applications.*" AD-vol.28, Reliability Technology ASME 1992, pp 17-24.

5. Melchers R.E.*Structural Reliability, Analysis and Prediction.* John Wiley & Sons, New York, 1987

6. Onyebueke L.C. and Onwubiko C. "*Probabilistic Design Methodology and Application to Machine Element Design*". Presented at the third Int'l conf. on stochastic structural dynamics, San Juan, Puerto Rico, Jan.15-18, 1995.

7. Shiao M.C and Chamis C.C., " *A methodology for Evaluating the Reliability and Risk of Structures Under Complex Service Environments.*" NASA Technical Memorandum 103244, April 1990.

8. Shantaram et al. "*Probabilistic Assessment of Space Trusses Subjected to Combined Mechanical and Thermal Loads.*" NASA Technical Memorandum 105429, April 1992.

9. Alfred H.S Ang and Wilson H.Tang, *Probability Concepts in Engineering Planning and Design.* John Wiley & Sons, New York 1984.

10. T.Torng and B.Thacker, "*Confidence Bounds Assessment for Probabilistic Structural Reliability analysis,*" 33rd AIAA/ASME/AHS/ASC Structures, Structural Dynamics and Materials Conference.

11. Shigley, Joseph B., *Mechanical Engineering Design,* New York:McGraw-Hill, Inc., 1989.

12. T.Torng and B.Thacker, "*An Efficient Probabilistic scheme for Constructing Structural Reliability Confidence Bounds,*" 34 the AIAA/ASME/ASCE/AHS/ASC Structures, Structural Dynamics and Materials Conference. April 19-22 1993, La Jolla, CA.

13. Landon C. Onyebueke and Chinyere Onwubiko., "*Overview of Probabilistic Design Methodology with NESSUS as the computer code.*"

14. H.R. Millwater, Y.T. Wu, T.torng, B.Thacker, D.Riha and C.P Leung,"*Recent Developements of the NESSUS Probabilistic Structural Analysis Computer Program,*" AIAA-92-2411, 33rd AIAA/ASME/AHS/ASC Structures, Structural Dynamics and Materials Conference, April 13-15,1992, Dallas Texas.

15. Y.T. Wu, "*Computational Methods for Efficient Structural Reliability and Reliability Sensitivity Analysis,*" AIAA-93- 1626, 34th AIAA/ASME/ASCE/AHS/ASC Structures, Structural Dynamics and Materials Conference, April 19-22, 1993, LA Jolla, CA.

16. Y.T. Wu and Burnside,O.H., "*Efficient Probabilistic Structural Analysis Using an Advanced Mean Value* Method,"Proceedings of the 5th ASCE Specialty Conference on Probabilistic Methods in Civil Engineering, ASCE May 1988.

17. Wu, Y.T. "*Demonstration of a New Fast Probability Integeration Method for Reliability Analysis,*" Journal of Industry, ASME, Feb 1987, pp.24-26.

18. Wu, Y.T., T.Y Torng, "*A Fast Convolution Procedure for Probabilistic Engineering Analysis,*" Proceedings of the

First International Symposium on Uncertainty Modelling and Analysis, IEEE December, 1990.

19. Y.T. Wu, T.Y Torng and M.R Khalessi, "*A New Iteration Procedure for Efficient Structural Reliability Analysis,*" Proceedings of the First International Symposium on Uncertainty Modelling and Analysis, IEEE, December, 1990.

20. Y.T. Wu, H.R. Millwater and T.A. Cruse,"*Advanced Probabilistic Structural Analysis Method for Implicit Performance Functions.*" AIAA Journal Vol.28, No.9, pp.1663-1669, 1990.

21. A.R Shah, M.C. Shiao, V.K. Nagpal and C.C Chamis, "*Probabilistic Evaluation of Uncertainties and risks in Aerospace Components.*" *NASA Technical Memorandum 105603, March 1992.*

22. Southwest Research Institute. "*NESSUS/FPI theoretical Manual,NASA Contract NAS3-24389.*" December 1989.

23. T.V Sundararaja Moorthy, N.Shanmugam, *Machine Design*, Khanna Publishers, India, 1984.

24. S.Domkundwar, *Heat and Mass Transfer*, B.P Publications, India, 1987.

25. Aaron D.Deutschman, Walter J. Michels, Charles E.Wilson, *Machine Design Theory and Practice*, John Wiley & Sons New York, 1987.

26. L.C. Onyebueke, C. Onwubiko and F.C Chen, "*Probabilistic Design Methodology and the Application of Fault Tree Analysis to Machine Design.*" Proceedings of the 11th Biennial Conference on Reliability Stress Analysis and Failure Prevention, Vol2, pp 125-133, Boston Massachussets; September, 1995.

27. Southwest Research Institute. "*NESSUS Release Notes 6.0, NASA Contract NAS3-24389,*" June 1992.

28. T.Y. Torng, Y.T. Wu and H.R. Millwater, "*Structural System Reliability Calculation using a Probabilistic Fault Tree Analysis Method,*" Proceedings of the 33rd

Structures, Structural Dynamics, and Materials Conference, pp.625-639, 1992.

29. H.R. Millwater and Y.T. Wu, "*Computational Structural Reliability Analysis of a Turbine Blade,*" Structural Engineering Department, Presented at the 1993 International Gas Turbine Conference.

30. H.R. Millwater, A.J. Smalley, Y.T. Wu and B.F. Evans, "*Computational Techniques for Probabilistic Analysis of Turbo machinery,*" Southwest Research Institute, San Antonio, Texas, Presented at the International Gas Turbine and Aeroengine Congress and Exposition, Cologne, Germany, June 1-4, 1992.

BIOGRAPHICAL SKETCH

MUTHUSWAMY ETHIRAJAN
4411, Tenn Avenue, Apt # 6,
Nashville, TN-37209.
TEL: (615) 385-7832

OBJECTIVE To obtain a challenging position as a **Mechanical Engineer** with emphasis in **Design , Solid modelling.**

EDUCATION

B.E in **Mechanical Engineering,** **G.P.A 3.5/4.0**
Bharathiyar University, India (08/89 - 05/93)

M.E in **Mechanical Engineering ,** **G.P.A 3.6/4.0**
Tennessee State University (01/94 - 05/96)

PROFESSIONAL EXPERIENCE

MECHANICAL ENGINEER
IGCAR, India. **05/93-12/93**

- Designed **Steam Pipes** on Velocity and Pressure drop basis and thickness on IBR Strength Calculation basis.
- Created a Shell and Tube **Heat Exchanger design** for **Indira Gandhi Center for Atomic Research.**

GRADUATE RESEARCH ASSISTANT **01/94-05/96**
Tennessee State University, TN - 37209

- Designed Worm Gears using **Probabilistic Design Methodolody** with **N.E.S.S.U.S** as the computer code.
- Analyzed the effect of the **critical design parameters** in the Design of worm gears and studied the variation in the **probability of failure.**
- Analyzed the **stress distribution** and **strain displacement** of the tooth of worm gear by applying **Finite Element Methodology** and by using **Cosmos/M**.
- Extensively used **Pro-E /14** solid modelling Package to design **3-D** models.

- Created a solid model of **crank ,shaft, flywheel, bracket, spring, bushing, draft using Pro-E /14.**

COMPUTER SKILL

Languages	Fortran, Quick-basic, Pascal.
Packages	**PRO-E /15, COSMOS/M, Auto Cad,** NESSUS, Matlab,Mc-Draw, Ms Word, Ms Windows
Systems	VAX/VMS, SUN (UNIX), SGI, IBM, PC(DOS), Macintosh.

AFFILIATIONS Member of American society of Mechanical Engineers (**ASME**)
Member of Society of Manufacturing Engineers (**SME**)

ACTIVITIES Tennis, Racquet ball, Travelling.

REFERENCES Available upon request.

COMPARATIVE STUDY OF THE USE OF AGMA GEOMETRY FACTORS AND PROBABILISTIC DESIGN METHODOLOGY IN THE DESIGN OF COMPACT SPUR GEAR SET

A Project

Submitted to the College

of

Engineering and Technology

in

Partial Fulfullment of the requirements

for the Degree of

Master of Engineering

with option in

Mechanical Engineering

By

Shiva M. Gangadharan

December 1996

College of Engineering and Technology

Tennessee State University

ACKNOWLEDGEMENTS

I would like to express my appreciation to Dr. Landon Onyebueke and Dr. F.C. Chen for serving on my committee and for their time in reviewing and critiquing this project. I would like to thank Dr. Chinyere Onwubiko for his help with the technical aspects of this work. His expertise in the area of design optimization proved to be invaluable to me during the course of this study. More importantly, I would like to express my gratitude to Dr. C. Onwubiko for his patience, encouragement, and support. These factors were essential to the completion of this work. This work was supported by NASA, Lewis Research Center under Grant # NAG3-1479 and is gratefully acknowledged.

Shiva M. G.

TABLE OF CONTENTS

Page

LIST OF FIGURES ix

NOMENCLATURE x

Chapter

I. INTRODUCTION 1

Thesis Overview 3

II. INVOLUTE SPUR GEAR MESH GEOMETRY 6

Involute Curve Geometry 6

Spur Gear Mesh Geometry 8

Contact Ratio Development 11

Critical Point Roll Angle Equations 14

III. FAILURE MODES AND DESIGN CONSTRAINTS 19

Tooth Breakage 19

Pitting 23

Scoring 24

Contact Stress Equation 25

Undercut/Involute Interference 29

IV. DETERMINATION OF OPTIMUM GEAR DESIGN USING AGMA J FACTOR AND APPROXIMATE J FACTOR 34

Design Parameters 34
Formulation of Design Model 37
Deterministic Optimization 41
Satisfaction of Gear Ratio Requirement 43
Discussion 47

V. DETERMINATION OF OPTIMUM DESIGN USING PROBABILISTIC DESIGN METHODOLOGY 49

Uncertainty Associated with Design 49
Development of PDO model 51
Limit State Function 56
Safety Index Determination 60
Probabilistic Design Optimization Format 62
Discussion 64

VI. SUGGESTION FOR FUTURE WORK AND SUMMARY 74

Suggestions for Future Work 74
Summary 75

APPENDIX

I. AGMA GEOMETRY FACTOR FOR PITTING RESISTANCE (*I*) 79

II. AGMA GEOMETRY FACTOR FOR BENDING STRENGTH (*J*) 82

III. APPROXIMATE EQUATIONS FOR THE AGMA J-FACTOR 85

IV. CORRECTION FACTORS IN GEAR DESIGN 87

V. PROGRAM LISTING 92

REFERENCES 108

BIO DATA 112

LIST OF FIGURES

Figure

Page

1-1. Flow Chart to illustrate Design Steps 4

2-1. Generation of an Involute and Involute Action 7

2-2. External Spur Gear Mesh Geometry 10

2-3. Internal Spur Gear Mesh Geometry 13

2-4. Critical Points of Contact during a Mesh Cycle 16

3-1. Geometry Used for J Factor Calculation 21

3-2. Interference In the Action of Gear Teeth 30

5-1. Assumption of Gear Tooth in Determination of Lewis Factor 53

5-2. Safe and Unsafe Regions of a Design Space and Definition of Safety Index 57

5-3. Chart showing Values of Center Distance Obtained Using Deterministic and Probabilistic Methods 69

5-4. Chart showing Contact Stress Values Obtained Using Deterministic and Probabilistic Methods 70

5-5. Chart showing Bending Stress Values Obtained Using Deterministic and Probabilistic Methods 71

NOMENCLATURE

Symbol	Definition
$a_{P,G}$	addendum, in
$b_{P,G}$	dedendum, in
C	center distance, in
C_a, K_a	application factors
C_D,K_D	derating factors, $C_D=C_aC_m/C_v$
C_H	hardness ratio factor
C_L,K_L	life factor
C_m,K_m	load distribution factor
C_p	elastic coefficient, $\sqrt{psi}$
C_R,K_R	reliability factor
C_t	bending stress design factor
C_T,K_T	temperature factor
C_v,K_v	velocity factor
d_P	pinion pitch diameter, in
$E_{P,G}$	modulus of elasticity, psi
F	face width, in
HP	power transmitted, horsepower
I	contact stress geometry factor
J	bending stress geometry factor
m_G	gear ratio
m_P	contact ratio
$N_{P,G}$	number of teeth
$n_{P,G}$	speed, rpm
$*p_f$	probability of failure

P	diametral pitch, 1/in
P_b	base pitch, in
P_c	circular pitch, in
r	pinion pitch circle radius
$R_{1,2}$	pitch circle radius, in
r_T	edge radius of cutting tool, in
S_{ac}	AGMA adjusted contact stress, psi
S_{at}	AGMA adjusted bending stress factor
S_c	contact stress number, psi
S_t	bending stress number, psi
v_t	pitch line velocity, ft/min
W_n	normal tooth load
W_t	transmitted tangential load, lb
y	Lewis form factor
Y	tooth form factor
Z	length of action, in
$\alpha,\beta,\gamma,\Delta$	angles used in determining contact ratio, and roll angles to critical positions on the tooth profile
δ	angular tooth spacing
η	load sharing factor
θ	involute roll angle
λ	face width to diameter ratio
$\mu_{P,G}$	Poisson's ratio
π	Pi, 3.1415926...
$\rho_{P,G}$	radius of curvature of tooth surface, in
ϕ	involute pressure angle
$*\beta$	safety index

$*\sigma_z$	standard deviation of transformed variable
$*\gamma$	coefficient of variation
$*\mu_z$	mean value of transformed variable
$*\zeta$	reliability value
*R	resistance offered by machine element
*S	applied stress
*G(.)	limit state function
$*p_f$	probability of failure

* denotes symbols defined in Probabilistic Design approach.

Acronyms

COV	coefficient of variation
FPC	final point of contact
HPSTC	highest point of single tooth contact
IPC	initial point of contact
LPSTC	lowest point of single tooth contact
PDM	probabilistic design methodology
PDO	probabilistic design optimization
PP	pitch point

CHAPTER I

INTRODUCTION

Pliny the Elder in his Historia Naturalis said that "the only thing certain is that nothing is certain." As engineers with creative design work, we are always faced with various uncertainties. Designing a product includes modeling the behavior of materials which we do not know completely. There may also be environmental hazards which we cannot predict precisely. The idealized computational models which we use, often have modeling uncertainties and limited accuracy over a certain range of parameters.

To counteract the uncertainties effects we have introduced the safety factors to prove that our design is safe. However, safety factors do not reflect necessarily the safety of a design. It is known that two products designed using the same safety factors may have very different safety levels depending on their sensitivity to the parameter variabilities in a given lifetime environment. Catastrophic incidents have proved that our engineering judgements were sometimes incomplete and the safety level we decided were sometimes lower than was expected in some cases. This has led to the designs being made very conservative, thereby spending more money without any substantial technical reason. When we use deterministic approach we do not know how safe is our design. This is true especially for new designs for which no past experience and data exist. In the same way, deterministic approach cannot satisfactorily answer questions related to issues on cost and safety. Only partially can we

obtain answers for these questions with no possibility for failure risk quantification.

Tremendous research activities are done on probabilistic methods to enable us to model the uncertainties and random variabilities. Using probabilistic methods we can see if the design is robust or not. By "robustness of the design", we mean the safety of the design that will enable the part designed to perform its intended function without failing at a desired level of reliability. The sensitivity of the failure risk to different uncertainties in design parameters can be analyzed. In the probabilistic approach the decision is taken based on estimated risks and their consequences so that an optimized cost-reliability design solution can be determined. Thus probabilistic design turns out to be cost-effective, especially for new designs for which there is limited engineering experience.

The same concept of improving design holds true in the design of compact gear sets, which is the basis of this project. While arriving at an optimum design of the spur gear set, the emphasis is on minimum weight, compact design, accuracy of the design and running time of the design problem. Willis [1] states that "Weight reduction usually means volume reduction, which in turn lowers cost of materials, handling and shipping." In this project, gear design to minimize the size of the gear set has been studied using deterministic and probabilistic design methods.

The objective of this project is to make a comparative study of the use of AGMA geometry factors and probabilisitc design methodology in the design of a compact spur gear set. The gear design problem is first posed as an optimization problem, then solved using the conventional deterministic techniques suggested by AGMA and other researches [2], [3], [4] and finally solved using the new approach of Probabilistic Design Methodology. The

methodology employed in this thesis is given in the form of a flow chart, see Figure 1-1.

The deterministic formulation followed in this thesis is similar to the one in [2]. However, while considering the probabilistic formulation, the uncertainties are quantified by eliminating the correction factors in the design equations. A special purpose optimization algorithm [2] has been used to solve the design problem. The results include the design parameters like diametral pitch, number of pinion teeth, center distance, face width, stress values, computer time and the reliability level. A brief overview of the remainder of the thesis is presented below.

Thesis Overview

In Chapter II, some of the important aspects of involute gear mesh geometry are presented. The concept of involute "roll angle" and its application in locating points of interest on the tooth profile are explained along with some of the other basic gearing terms such as pressure angle, contact ratio, base pitch, circular pitch, and diametral pitch. The relationship between roll angle and tooth surface radius of curvature is also given.

The various failure modes and design constraints are given in Chapter III. The equations developed in Chapter II are incorporated into the constraint equations. Constraint equations are given for bending fatigue, surface contact fatigue at both the initial point of contact and the lowest point of single tooth contact, and undercut. Justification for the use of these constraints is also given in this chapter.

Chapter IV explains the deterministic approach in gear design. The design parameters are explained in this chapter. Formulation of the optimization model and the optimization algorithm used to tackle the problem are also included. An example problem

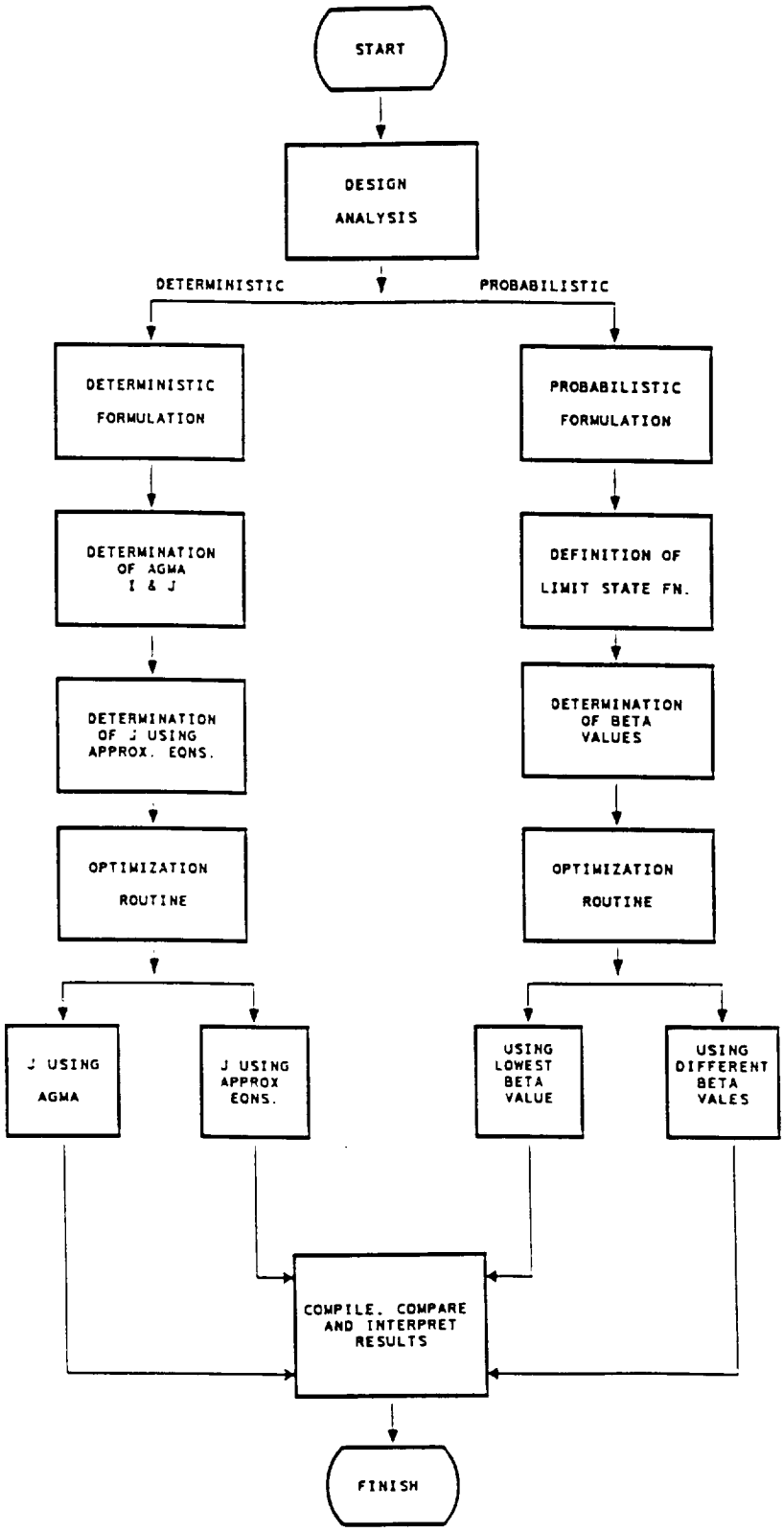


FIGURE 1-1 : CHART TO ILLUSTRATE DESIGN STEPS

is taken from [4] and solved deterministically using AGMA J and Approximate equations for J. The comparison between the two methods is discussed.

Chapter V is the most important chapter in this thesis. This chapter introduces the concept of Probabilistic design methodology and its applicability in gear design. This chapter includes the development of the Probabilistic model, Limit state functions, Calculation of safety indices and the Probabilistic Design Optimization format. An example problem from [5] is used to arrive at optimum results using Deterministic and Probabilistic methods. The results are shown as Tables and to aid comparison charts are also included.

Chapter VI includes suggestions for further work in the area of gear design and some conclusions about this work. Appendix I and Appendix II describe the geometry factors I and J as given by AGMA. The Approximate equations for calculating *J* factor is explained in Appendix III. Appendix IV gives a brief definition of all the correction factors that are incorporated in the deterministic model of the gear design problem. Finally the computer program for the problem is listed in Appendix V.

CHAPTER II

INVOLUTE SPUR GEAR MESH GEOMETRY

Involute gears are by far the most widely used gears in the world today. Gears whose active tooth profiles are portions of an involute curve have the following properties which make them attractive for use. First, they satisfy the requirement of transmitting rotary motion from one gear to another at a constant angular velocity ratio (i.e. conjugate action) at any center distance for which the teeth can be continuously in mesh. Earlier tooth forms (like the cycloidal tooth) satisfied the conjugate action requirement at only one specific center distance. Secondly, involute gears can be easily and accurately machined using "generating" processes such as hobbing and shaping.

There are several basic relationships involving involute geometry which prove useful in both the kinematic and strength design of gears. Those characteristics of the involute curve which are used in design model development will be presented in this chapter.

Involute Curve Geometry

An involute of a circle is defined as the path traced out by a point fixed on a tangent line of the circle as the line rolls without slipping around the circle. An involute curve may be generated as shown in Figure 2-1 (a). A partial flange B is attached to the cylinder A, around which is wrapped a cord *def* which is held tightly. Point *b* on the cord represents the tracing point, and as the cord is wrapped and unwrapped about the cylinder, point *b* will trace

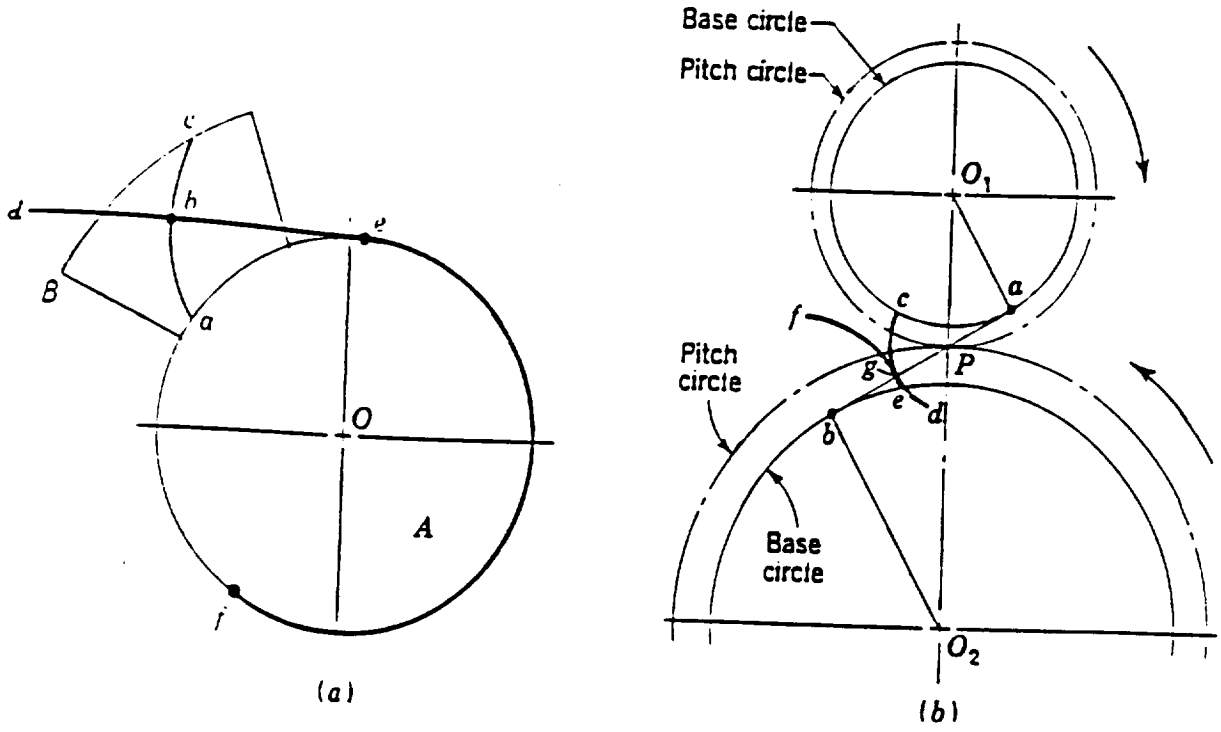


Figure 2-1: (a) Generation Of An Involute (b) Involute Action

(Source: Mechanical Engineering Design, Shigley and Mischke, Fifth Edition)

out the involute curve *ac*. The radius of curvature of the involute varies continuously, being zero at point *a* and a maximum at point *c*. At point *b* the radius is equal to the distance *be*, since point *b* is instantaneously rotating about point *e*. Thus the generating line *de* is normal to the involute at all points of intersection and, at the same time, is always tangent to the cylinder A. The circle on which the involute is generated is the *base circle*.

Figure 2-1 (b) explains how the involute profile satisfies the requirement for the transmission of uniform motion. Two gear blanks with fixed centers at O_1 and O_2 are shown having base circles whose respective radii are O_1a and O_2b. An imaginary cord is wound clockwise around the base circle of gear 1, pulled tightly between points *a* and *b*, and wound counterclockwise around the base circle of gear 2. If, now, the base circles are rotated in different directions so as to keep the cord tight, a point *g* on the cord will trace out the involutes *cd* on gear 1 and *ef* on gear 2. The involutes are thus generated simultaneously by the tracing point. The tracing point, therefore, represents the point of contact, while the portion of the cord *ab* is the generating line. The point of contact moves along the generating line, the generating line does not change position because it is always tangent to the base circles, and since the generating line is always normal to the involutes at the point of contact, the requirement for uniform motion is satisfied.

Spur Gear Mesh Geometry

When two spur gears are brought into mesh they become equivalent to two cylinders rolling without slipping on one another. The surfaces of these cylinders are called pitch surfaces and their profiles are called pitch circles. The point of tangency of the pitch circles is called the pitch point. The smaller of two gears in mesh is called the pinion while the

larger is usually called the gear. Wheel or gear wheel are other terms sometimes encountered for the larger gear. Reference [6] explains most of these terms and their origin.

For a given gear, the pitch circle is always larger than its base circle. A line that goes between and is tangent to the base circles of the pinion and gear intersects the line of centers at the pitch point as shown in Figure 2-2. This line is called the line of action. It is along this line that contact takes place for true involute gearing. The angle that the line of action makes with a perpendicular to the line of centers is called the pressure angle, ϕ. From Figure 2-2 it is seen that the base circle radius is related to the pitch circle radius by relation $r \cos\phi = r_b$.

The base pitch, p_b, is defined as the arc length between similar sides of two adjacent teeth along the base circle. By letting the angular spacing between teeth (equal to $2\pi/N_p$) be called δ, then $p_b = \delta\, r_b$. Due to the properties of the involute curve, the distance between teeth along the line of action is also p_b as shown in Figure 2-2.

The circular pitch, p_c, is defined as the arc length between adjacent teeth along the pitch circle. Therefore, $p_c = \delta r$ or $p_b/\cos\phi$. Since p_c is a factor of π, it is generally an irrational number. For convenience, a third pitch called the diametral pitch, P, is in common use. The diametral pitch is defined as $P = \pi/p_c$. From relationships presented above, it can be shown that gear size (diameter) can be given in terms of the number of teeth and the diametral pitch. The relationship between the pitch diameter, number of teeth and gear diameter is $d = Np/P$.

Contact Ratio Development

The total length of action, Z, is the distance along the line of action from the initial point of contact to the final point of contact for a single tooth. This distance corresponds to

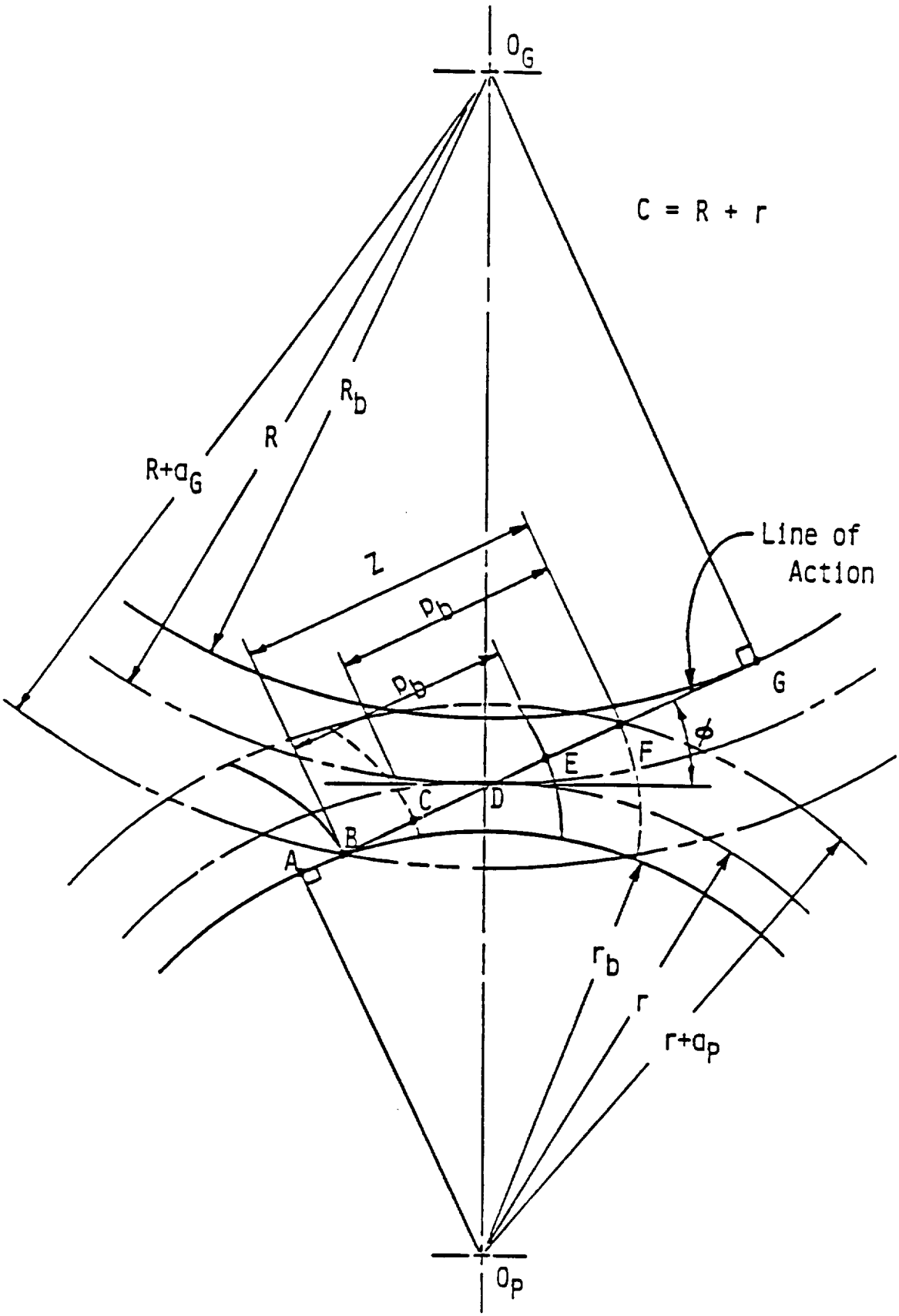


Figure 2-2: External Spur Gear Mesh Geometry

(Source: Design Data, PSG College of Technology)

the distance between the intersections of the line of action with the gear and pinion addendum circles (see Figure 2-2).

The length of action must be greater than the base pitch or there will be times during which no teeth are in contact. The ratio of the length of action to the base pitch is called the contact ratio, m_p. The value of the contact ratio is an indicator of the amount of load sharing between adjacent teeth. Higher contact ratios generally mean smoother operation and less noise.

To derive an expression for contact ratio, the length of action must be determined and then divided by the base pitch. From Figure 2-2 the following equations can be understood:

$$AG = (r+R) \sin \phi = C \sin \phi \tag{2.1}$$

$$AF = [(r+a_P)^2 - r_b^2]^{1/2} \tag{2.2}$$

$$BG = [(R+a_G)^2 - R_b^2]^{1/2} \tag{2.3}$$

and,

$$Z = BF = AF - (AG-BG) = AF + BG - AG \tag{2.4}$$

Therefore,

$$Z = [(r+a_P)^2 - r_b^2]^{1/2} + [(R+a_G)^2 - R_b^2]^{1/2} - C \sin \phi \tag{2.5}$$

An equivalent form of the above equation is:

$$\begin{aligned} Z = {} & [(N_P / (2P) + a_P / P)^2 - (N_P / (2P))^2 \cos^2 \phi]^{1/2} \\ & + [(m_G N_P / (2P) + a_G / P)^2 - (m_G N_P / (2P))^2 \cos^2 \phi]^{1/2} \\ & - (m_G + 1) N_P \sin \phi / (2P) \end{aligned} \tag{2.6}$$

The terms a_P and a_G are constants which when divided by the diametral pitch give the pinion

and gear addendums. Dividing the above equation by the base pitch and factoring out the term $N_P/2$ gives:

$$m_P = N_P / (2\pi) \{[(1+2\, a_P / N_P)^2 - \cos^2\phi]^{1/2} / \cos\phi + [(m_G + 2\, a_G / N_P)^2 - m_G^2 \cos^2\phi]^{1/2} / \cos\phi - (m_G + 1) \tan\phi\} \quad (2.7)$$

The three terms in the braces in the above equation correspond to angles subtended by arcs on the base circle of the pinion of lengths equal to AF, BG, and AG respectively. By letting

$$\alpha = [(1+2\, a_P/N_P)^2 - \cos^2\phi]^{1/2} / \cos\phi \quad (2.8)$$

$$\beta = [(m_G+2\, a_G / N_P)^2 - m_G^2 \cos^2\phi]^{1/2} / \cos\phi \quad (2.9)$$

$$\gamma = (m_G + 1) \tan\phi \quad (2.10)$$

and, as defined earlier,

$$\delta = 2\pi/N_P \quad (2.11)$$

the contact ratio can be written compactly as:

$$m_P = (\alpha + \beta - \gamma) / \delta \quad (2.12)$$

Using the same steps for the internal mesh of Figure 2-3, it is found that the equations for the angles α, β, and γ and the contact ratio are similar to those for the external mesh with the differences being only in changes of sign. A more general set of equations applicable to external or internal meshes is:

$$\alpha = [(1 + 2\, a_P / N_P)^2 - \cos^2\phi]^{1/2} / \cos\phi \quad (2.13)$$

$$\beta = [(mG \pm 2\, a_G / N_P)^2 - m_G^2 \cos^2\phi]^{1/2} / \cos\phi \quad (2.14)$$

$$\gamma = (1 \pm m_G) \tan\phi \quad (2.15)$$

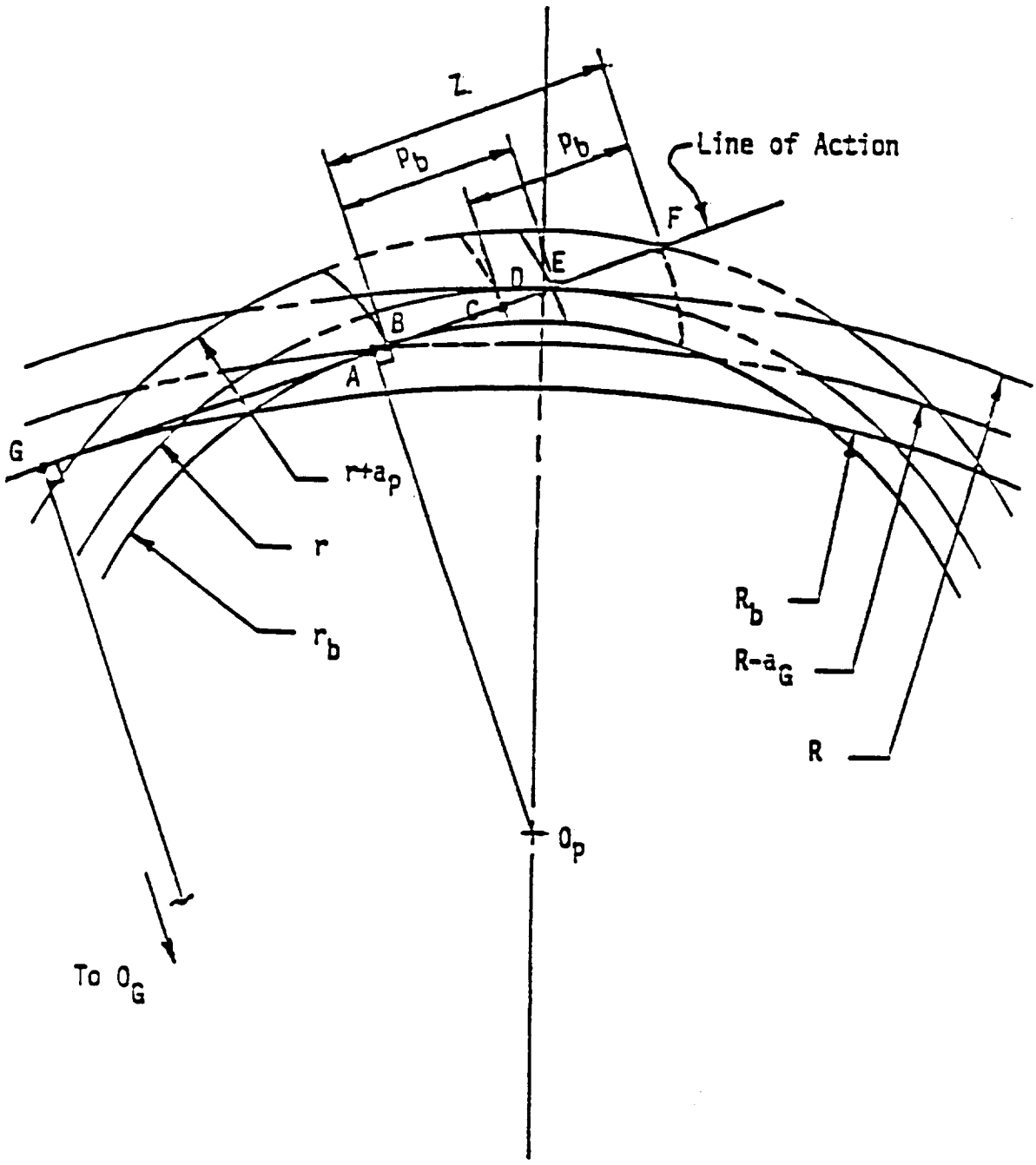


Figure 2-3: Internal Spur Gear Mesh Geometry

(Source: Design Data, PSG College of Technology)

$$m_p = (\alpha \pm \beta - \gamma) / \delta \tag{2.16}$$

where in the case of dual signs, the top signs is for an external mesh and the bottom sign is for an internal mesh.

The above set of equations is valid for standard as well as non-standard teeth as long as the addendum ratios give the correct addenda for the effective diametral pitch. The utility of the above mentioned equations extends beyond a convenient way to express the contact ratio equations. In the next section, it will be shown how critical points of contact can be located by giving the pinion roll angle to that point. The equations for the roll angle to the critical contact points can all be given in terms of the four angles, α, β, γ, and δ, as will be shown.

Critical Point Roll Angle Equations

A gear mesh cycle begins when the flank of the driving tooth contacts the tip of the driven tooth. This point is called the initial point of contact (IPC). The preceding tooth is already in contact and is exactly one base pitch ahead along the line of action. As the gears continue to rotate, the contact point moves upward along the line of action. At a certain point, the preceding tooth loses contact and the entire load is carried by only one tooth. The point is called the lowest point of single tooth contact (LPSTC). From here the contact point proceeds through the pitch point (PP) to a point one base pitch ahead of the inital point of contact called the highest point of single tooth contact (HPSTC). When this point is reached, the succeeding tooth is just making contact and beginning to share the load. The contact point continues to move along the line of action, sharing the load with the succeeding tooth, until the tip of the pinion tooth loses contact with the flank of the gear tooth at the final point

of contact (FPC). This completes one mesh cycle.

It is important to be able to locate these critical points on the tooth surface during the mesh cycle. The inital point of contact is important since the factor $(1/\rho_P + 1/\rho_G)$, which is used in calculating the Hertz contact stress, is most critical for standard equal addendum pinion and gear. Also, high sliding velocities which contribute to heat generation at the contact point, in turn lead to lubricant breakdown and scoring, and occur at the IPC. The lowest point of single tooth contact is critical since the full load is carried there, and consequently, it is usually the point during the mesh cycle with the largest Hertz contact stress.

The highest point of single tooth contact usually corresponds to the most critical load application point in determining the bending stress. In some cases when the accuracy of the gears is not adequate, it is possible for the full load to be carried almost up to the final point of contact. The FPC is also critical because of high sliding velocities.

Using the equations presented earlier in this chapter, equations for the pinion roll angle to these critical points can now be derived. Figure 2-4 shows the locations of the critical contact points along the line of action along with the roll angles to those points. Since the contact ratio and the base pitch are known, from Figure 2-4 it is seen that if the distance from either point A or point G to any of the critical points can be found then the locations of the other points can be found relative to that point using the contact ratio and base pitch.

The roll angle to the final point of contact is the angle subtended by an arc of the base circle of length AF. This angle has already been given as the angle α. Therefore,

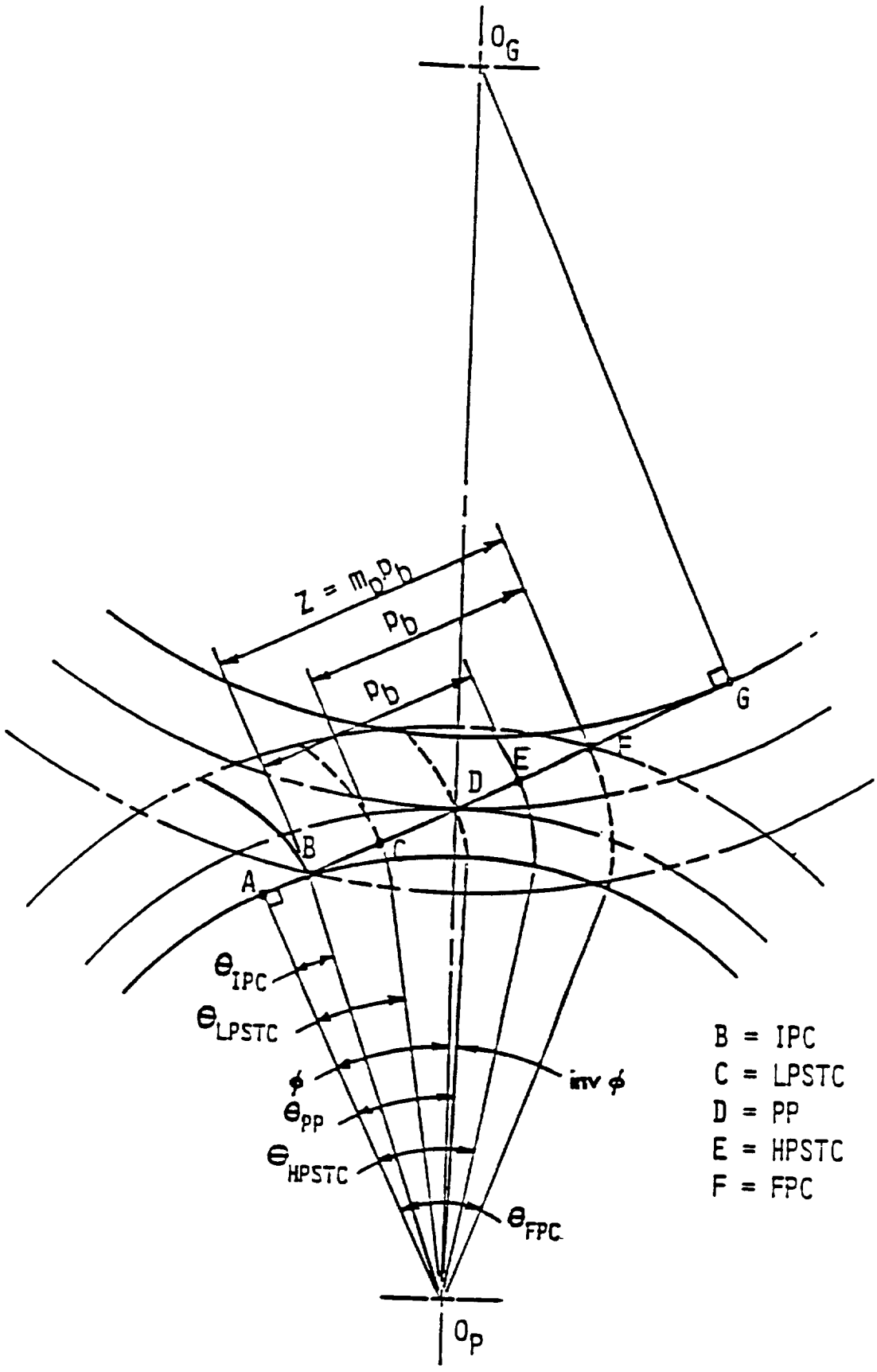


Figure 2-4: Critical Points of Contact During a Mesh Cycle

(Source: Design Data, PSG College of Technology)

$$\theta_F = \alpha$$

$AF = \alpha r_b$ and from Figure 2-4, $AB = AF - m_P p_b$, therefore the roll angle to the initial point of contact is:

$$\theta_i = AB/ r_b = [\alpha r_b - (\alpha \pm \beta - \gamma)\, \delta r_b / \delta]\, r_b \qquad (2.17)$$

which when simplified becomes:

$$\theta_i = \gamma \mp \beta \qquad (2.18)$$

$AC = AF - P_b$ which gives the roll angle to the lowest point of single tooth contact as:

$$\theta_L = AC/rb = (\alpha r_b - \delta rb) / r_b \qquad (2.19)$$

or $\theta_L = \alpha - \delta$

Similarly, $AE = AB + p_b$, giving the roll angle to the highest point of single tooth contact as:

$$\theta_H = AE / r_b = [(\gamma \mp \beta)\, r_b + \delta\, r_b] / r_b \qquad (2.20)$$

or $\theta_H = \gamma \mp \beta + \delta$

The roll angle to the pitch point as seen from Figure 2-4 is given by:

$$\theta_{PP} = \phi + \text{inv}\, \phi = \tan \phi \qquad (2.21)$$

The roll angle equations will prove to be convenient and useful in the design model constraint equations to be presented in Chapter III. By presenting the constraint equations in forms that allow the point of contact to be located by the roll angle, the equations can be generalized to any point of contact in the mesh cycle instead of just one point. This provides a view of the problem which gives the designer insight to help him choose the best design.

CHAPTER III

FAILURE MODES AND DESIGN CONSTRAINTS

In designing spur gears for minimum size, there are several types of failure modes and undesirable characteristics that must be prevented in order to insure satisfactory life and performance of the gears. In this chapter, the most common failure modes are presented. The equations used as constraints on the design to prevent these types of failures are also given, along with some justification for their use.

Tooth Breakage

The most critical type of gear failure is tooth breakage. This type of failure generally leaves the gear unit inoperative. It also happens suddenly without warning. Tooth breakage usually occurs as a fatigue failure resulting from repeated bending. The cyclic bending causes cracks to appear and grow in the root area of the tooth. The cracks eventually weaken the tooth to the point that breakage occurs. A tooth or teeth can also be broken off or "stripped" by a sudden impact or application of a very heavy load.

The gear tooth bending stress equation is based on the mechanics of materials with the stress concentration accounted for empirically. The gear tooth is modeled as a cantilever beam subjected to a bending load and an axial compressive load. The critical stress is evaluated at the tensile side of the tooth because tensile stresses contribute more to fatigue than compressive stresses. The critical point for calculation of the stress is taken as the point

of tangency of an inscribed parabola with the tooth root fillet [7] as shown in Figure 3-1. The vertex of the parabola is located on the tooth centerline where the line of action crosses it. Notice that the tooth centerline rotates with the gear while the line of action is fixed. This means that the location of the critical point varies with the point of load application. The highest bending stress a tooth experience during a single mesh cycle usually occurs at the highest point of single tooth contact (HPSTC). This is the highest point at which the full load is carried. A more conservative evaluation of the critical bending stress is often made by assuming full loading all the way to the final point of contact (FPC). The bending stress equation as given by AGMA in [7] is equivalent to:

$$W_t P K_D / (FJ) \leq S_t \tag{3.1}$$

where $K_D = K_a K_m / K_v$

The K-factors are intended to account for effective increase in load due to momentary overload (K_a), uneven load distribution across the tooth face (K_m), and dynamic load effects (K_v). K_D is called the bending stress derating factor. In general, it is a function of the type of application of the gear set, the accuracy of manufacture and alignment, the speed of rotation, and the size of the gears.

The other factors in the bending stress equation are transmitted tangential load, W_t, the effective face width, F, the diametral pitch, P, the bending stress geometry factor, J, and the modified bending endurance strength, S_t, given by:

$$S_t = S_{at} K_L / (K_T K_R) \tag{3.2}$$

Here, S_{at} is the bending endurance strength for a gear rated at 10^7 cycles of operation with a reliability of 99% under normal operating temperatures. The K-factors are included

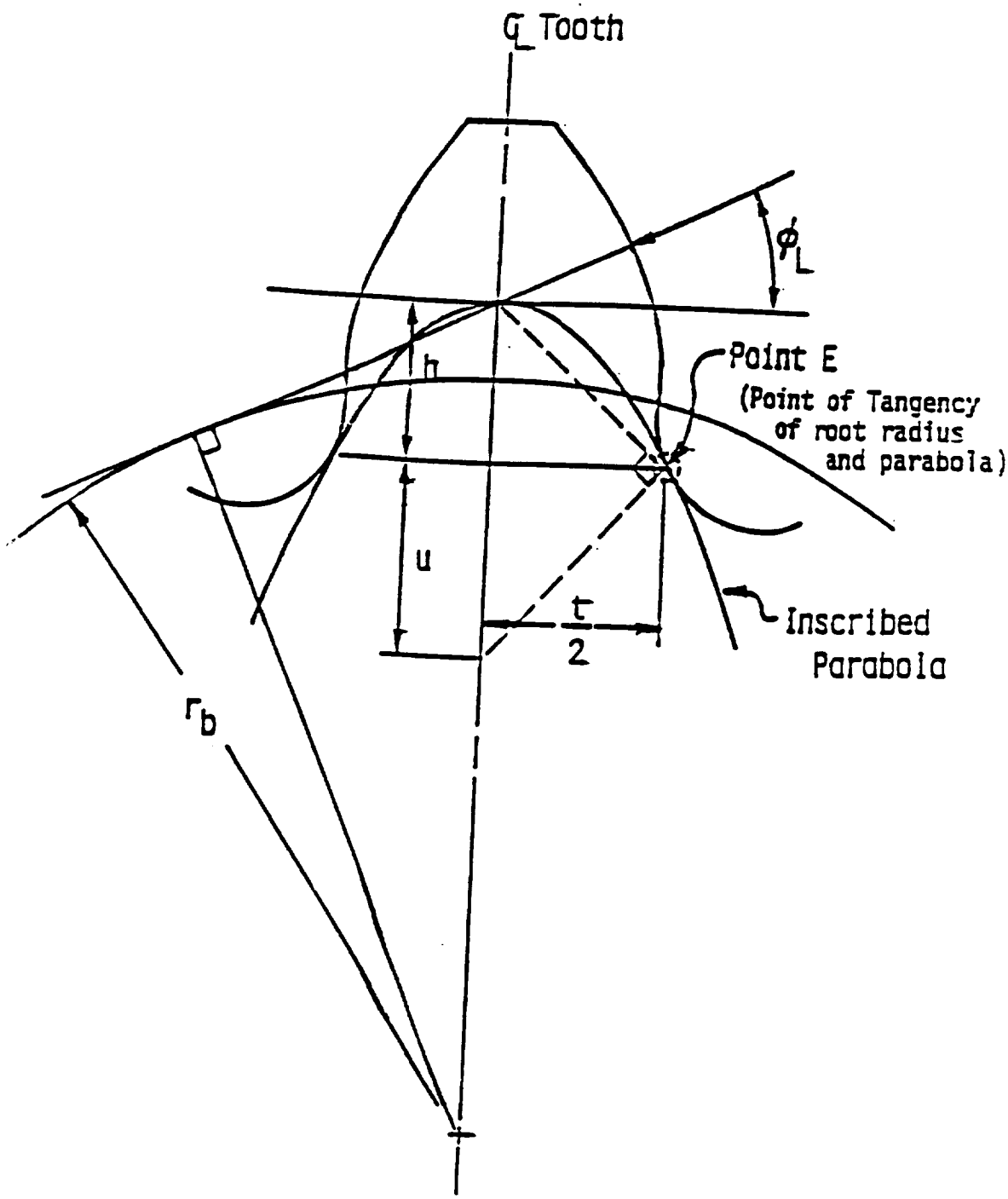


Figure 3-1: Geometry Used for J Factor Calculation

(Source: Design Data, PSG College of Technology)

to account for lives, reliabilities, and temperatures different from the values that S_{at} is based on. Reference [7] gives values for S_{at} as a function of hardness and values for the life (K_L), reliability (K_R), and temperature (K_T) factors.

As the name implies, the bending stress geometry factor, J, takes into account the tooth geometrical parameters: pressure angle, addendum, dedendum, hop tip radius, and location on the tooth of the load application. The J-factor used to be determined graphically from an accurate layout of the tooth. Two iterative numerical techniques for calculation of the J-factor on a computer or programmable calculator have been made available, see [8], [9]. Appendix II explains the J factor as described by AGMA. The Approximate equations for calculation of J as derived by [10] is explained in Appendix III.

The AGMA bending stress equation is based on work done by Wilfred H. Lewis a century ago. The accuracy of the equation has been questioned in recent years, especially since finite element methods have begun to be widely used. Finite element analysis is generally considered to be very accurate if a suitable grid is used. However, it is not suited for design as much as it is for detailed, time-consuming analysis. The bending stress equation, on the other hand, is convenient for design use, especially now that empirical equations can be used for the J-factors. The derating factors, which are based on years of experience, also tend to offset some of the inaccuracies in the basic equation. Until very extensive finite element studies (which over a broad range of tooth forms) are done and the results are made available in empirical form, the basic bending stress equation will continue to be the most convenient available method for obtaining designs quickly.

Pitting

While tooth breakage due to bending fatigue is the most critical type of gear failure, by far the most common type of failure is pitting. Pitting is a surface fatigue failure due to many cycles of contact. As the name implies, pitting is characterized by deterioration of the surface in the form of rough shallow holes or pits [11]. Pitting usually starts slightly below the pitch point on the tooth surface. This is in the region of the lowest point of single tooth contact (LPSTC).

Once pitting begins, the gear unit can continue to operate. However, the noise and vibration level of the unit increases as the pitting progresses. Also, a crack can initiate in the pitted area of the surface, leading to tooth breakage.

Pitting is thought by many to begin as a small crack below the surface. The crack then propagates and eventually makes its way to the surface causing a small amount of material to break away, leaving a pit. This sub-surface crack assumption is based on Hertzian contact stress theory which predicts a maximum shearing stress at a point below the surface of contact.

There is evidence [12], [13] that pitting most often begins as a small surface crack, probably initiated at a machining mark, which is propagated by the hydraulic wedge action of the lubricant being forced into the crack by the contact pressure. In [12], Bowen estimates that more than 80% of pitting failures shows good correlation with the maximum Hertz contact stress. Therefore, Hertzian theory can be used to accurately predict pitting failure even if the maximum sub-surface shear stress is not the major cause.

The AGMA gives a recommended equation for determining the contact stress which leads to pitting. This equation is presented later. A generalized contact stress equation that

can be used as a constraint equation for both of these types of surface failures is presented.

Scoring

The third mode of failure most often encountered is scoring, a type of surface failure resulting from metal to metal contact of the gear teeth due to lubricant breakdown [11]. The breakdown of the lubricant is caused by excessive heat generation at the point of contact. Once metal to metal contact occurs, the two surfaces are instantaneously welded together then torn apart by the rolling and sliding action at the contact point. This type of failure is characterized by radial scratch and tear marks in the direction of sliding, hence the name scoring. Scoring is a major problem for gears used in the aerospace industry. This is because aerospace gears must be as light weight as possible, yet they are subjected to heavy loads and very high speeds.

There are several factors which are known to influence scoring. These include contact pressure, relative sliding, lubricant properties, surface finish, and bulk operating temperature. In this thesis only those factors related to the gear tooth geometry, namely the contact pressure and the relative sliding between surfaces, are considered. It can be shown that reducing the contact pressure through a change in tooth geometry also has the effect of reducing the relative sliding. Therefore, both of these factors which contribute to scoring can be limited by controlling the contact pressure at the initial point of contact (IPC). The most critical combination of contact pressure and relative sliding occurs at this point. However, since scoring is affected to a large degree by other factors, (lubricant, surface finish, etc.), the IPC contact stress equation cannot be considered as an accurate predictor for scoring . Instead, it simply allows the designer to keep those factors which are related to the gear mesh

geometry within some specified limits. Nevertheless, the IPC contact stress equation provides a simple strategy for limiting scoring in the gear design process. For this reason, throughout the remainder of this thesis, the pitting and scoring constraints will be called the LPSTC contact stress constraint and the IPC contact stress constraint, respectively, with the understanding that both are individually important constraints for achieving a good design.

Now, a general stress equation will be developed that can be used to calculate the contact stress for any point of contact through the mesh cycle.

Contact Stress Equation

The contact stress equation is based on Hertzian theory for two cylinders with line contact. For the gear teeth, the maximum contact stress as defined by Hertz equation is given by:

$$\sigma_H^2 = \frac{\eta W_t}{\pi F \cos\phi} \frac{1}{\frac{(1-\mu_P^2)}{E_P} + \frac{(1-\mu_G^2)}{E_G}} \left(\frac{1}{\rho_P} + \frac{1}{\rho_G}\right) \qquad (3\text{-}3)$$

where, σ_H is the value of the surface compressive stress (Hertzian stress). The factor, η, is called the load sharing coefficient and is equal to the fraction of the total load being carried at the particular point of contact. The variation of η depends on the tooth deflection, profile modifications and tooth accuracy. A simple and conservative way to specify η is to assume one-half of the load is carried by one tooth during the period of single tooth contact. This is equivalent to assuming rigid teeth which, of course, do not exist in practice.

From relationships given in Chapter II, it is easy to show that the pinion tooth radius

of curvature is:

$$\rho_P = r_b \theta = (d/2) (\cos \phi) \theta \tag{3-4}$$

and the gear tooth radius of curvature is:

$$\rho_G = r_b (\gamma - \theta) = (d/2) (\cos \phi) (\gamma - \theta) \tag{3-5}$$

Using the above relationships for the radii of curvature, the last term in the contact stress equation can be written as:

$$1/\rho_P + 1/\rho_G = 2 / [d\theta (\cos \phi) (1 - \theta/\gamma)] \tag{3-6}$$

The AGMA [7] defines the elastic coefficient, C_P, as:

$$C_P = \sqrt{\frac{1}{\pi \left(\frac{(1-\mu_P^2)}{E_P} + \frac{(1-\mu_G^2)}{E_G} \right)}} \tag{3-7}$$

Using these relationships, the Hertz contact stress equation becomes:

$$\sigma_H = C_P \sqrt{\frac{2 \eta W_t}{F d \theta \cos^2 \phi \left(1 - \frac{\theta}{\gamma}\right)}} \tag{3-8}$$

This equation is a general form of the Hertz contact stress equation for any point of contact on the tooth surface with the contact point located by the pinion roll angle to that point. Actually, the Hertz equation is derived for the case of pure rolling which exists at the pitch point only. However, it will be assumed that the Hertz contact stress contributes much more to the total surface stress than the frictional shear effects due to sliding. Therefore, the

equation will be used to predict severe surface stress conditions for both cases of pure rolling and combination rolling and sliding.

The AGMA pitting resistance rating formula is based on the Hertz stress at the lowest point of single tooth contact [7]. The AGMA equation is equivalent to:

$$C_P \sqrt{\frac{W_t C_D}{d F I}} \leq S_c \tag{3-9}$$

Here the contact stress derating factor, C_D, is equivalent to the bending stress derating factor. The factor, I, is a function the gear mesh geometry and is therefore called the contact stress geometry factor.

The value S_c is the upper limit of contact stress. It is determined from the equation:

$$S_c = S_{ac} C_L C_H / (C_T C_R) \tag{3-10}$$

In this equation, S_{ac} is the surface endurance strength of the material based on a life of 10^7 cycles, a reliability of 99% and normal operating temperatures, analogous to S_{at} for the bending endurance limit. Similarly, C_L, C_T, and C_R account for variations from the base values of life, temperature, and reliability. The hardness ratio factor, C_H, is used as a multiplier on S_{ac} for the softer of two gears in mesh to account for the desirable work hardening effect on the softer gear.

Equating the general Hertz contact stress equation to the AGMA pitting equation, we see that for equivalence, I must be given by:

$$I = \theta \cos^2 \phi \, (1 - \theta/\gamma) / (2\eta) \tag{3-11}$$

This formula for the I-factor is different from the one given in [7], but it is shown below that

the two equations are equivalent.

The AGMA equation for I for spur gears is:

$$I = \frac{\cos\phi \sin\phi}{2} \frac{m_G}{m_G \pm 1} \frac{\rho_1 \rho_2}{\rho_P \rho_G} \tag{3-12}$$

Here, ρ_1 is the radius of curvature of the pinion at the point of contact and ρ_2 is the radius of curvature of the gear at that point. ρ_P and ρ_G are the radii of curvature of the pinion and gear respectively at the pitch point. Using relationships given in Chapter II, these radii of curvature are given as:

$$\rho_1 = r_b \theta$$

$$\rho_2 = r_b (\gamma - \theta)$$

$$\rho_P = r_b \tan \phi$$

$$\rho_G = \pm r_b m_G \tan \phi$$

Therefore,

$$\frac{\rho_1 \rho_2}{\rho_P \rho_G} = \frac{\theta (\gamma - \theta)}{\pm m_G \tan^2 \phi} \tag{3-13}$$

Substitution of the equation (3-13) into equation (3-12), simplifying, and including the load sharing coefficient, results in equation (3-11) for I.

Undercut / Involute Interference

Another possible undesirable characteristic of a gear mesh is the presence of undercut or involute interference. Undercut occurs during machining of gear teeth when the cutter removes a portion of the involute profile. This in itself is not a type of failure but it

creates problems which could lead to failure. An undercut tooth can be considerably weakened in bending if the degree of undercut is pronounced. Also, the length of action is reduced. This causes a reduction in contact ratio which generally leads to less smooth operation. Both of these effects are undesirable; consequently, undercutting should be avoided if possible.

Involute interference is similar to undercut. In fact, undercut is a result of involute interference between the cutting tool and the gear. Involute interference occurs when the tip of one gear makes contact with the noninvolute portion of the mating gear. This causes non-conjugate action between teeth which leads to vibration and noise. Consider Figure 3-2. Two gears are shown with centers O_2 and O_3. Gear 2 is the driving gear and Gear 3 is the driven gear. Driving gear turns clockwise. The initial and final points of contact are designated A and B, respectively, and located on the pressure line. It can be noted that the points of tangency of the pressure line with the base circles C and D are located inside the points A and B. This tells that interference is present.

Interference is explained as follows. Contact begins when the tip of the driven tooth contacts the flank of the driving tooth. In this case the flank of the driving tooth first makes contact with the driven tooth at point A, and this occurs before the involute portion of the driving tooth comes within range. In other words, contact is occurring below the base circle of gear 2 on the noninvolute portion of the flank. The actual effect is that the involute tip or face of the driven gear tends to dig out the noninvolute flank of the driver. The same effect occurs again as the teeth leaves contact. Contact should end at point D or before. Since it does not end until point B, the effect is for the tip of the driving tooth to dig out, or interfere

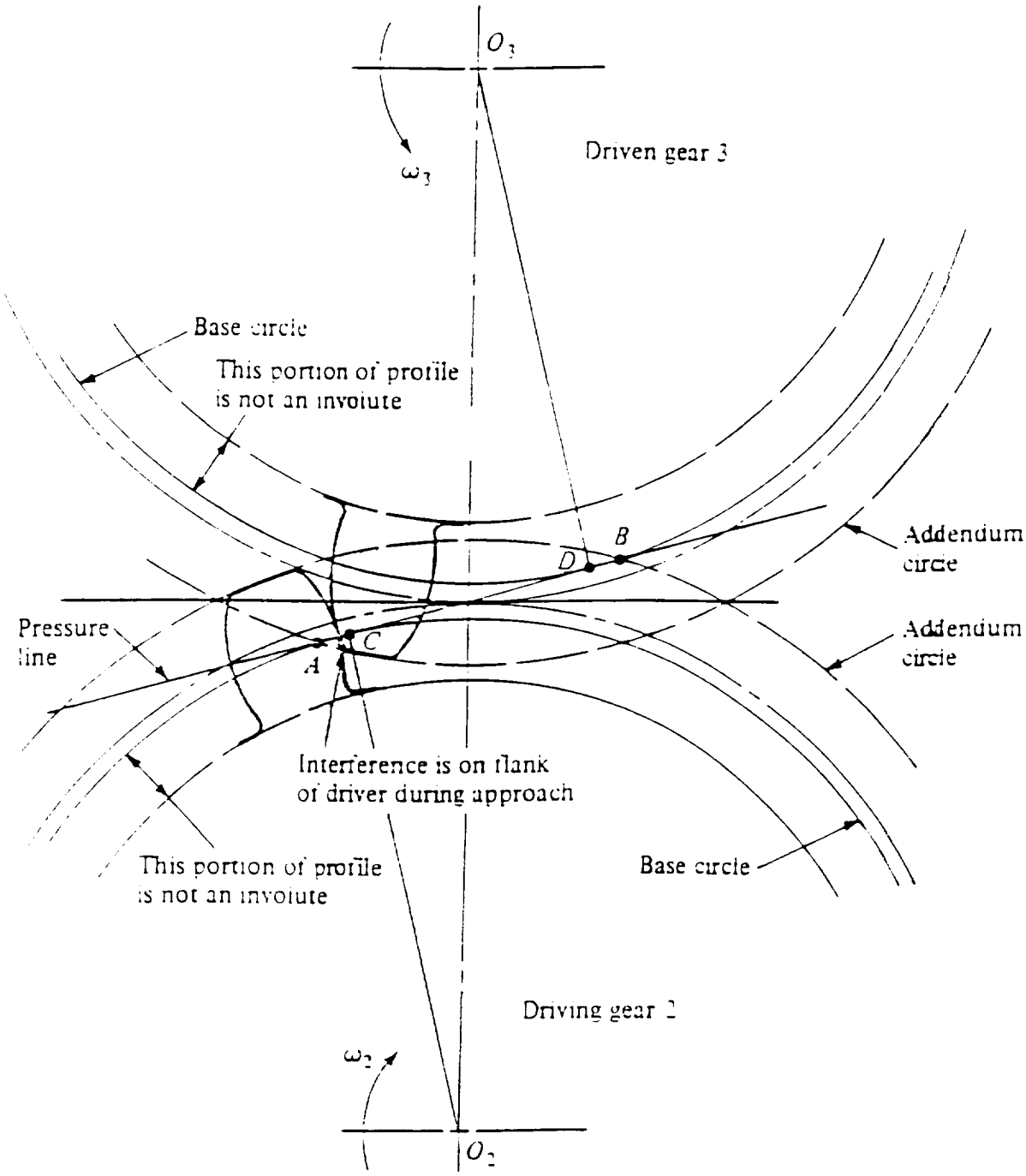


Figure 3-2: Interference In The Action of Gear Teeth

(Source: Mechanical Engineering Design Shigley and Mischke, Fifth Edition)

with, the flank of the driven tooth. Involute interference and undercut can be avoided if the number of teeth is greater than a certain minimum. In general, if the number of teeth is large enough so that undercut does not occur during machining, then involute interference will not occur during operation either. This is because the involute interference limit increases with gear ratio and becomes maximum for mesh with a rack.

The equations for determining the undercut and involute interference limits are given below. The involute interference equation is solved in [2] and is given as:

$$(N_P)_{\min} = \frac{\pm 2 a_G P}{[m_G{}^2 + (1 \pm 2m_G) \sin^2\phi]^{1/2} - m_G} \tag{3-14}$$

In the above equation as m_G approaches infinity (mesh with a rack), the equation becomes:

$$(N_P)_{\min} = \frac{2 a_G P}{\sin^2\phi} \tag{3-15}$$

The equation for determining the undercut limit for hobbed gears is derived in [14] and is given as:

$$(N_P)_{\min} = \frac{2 [b_P P - r_T (1 - \sin\phi)]}{\sin^2\phi} \tag{3-16}$$

Interference can be eliminated by using more teeth on the gears. However, if the gears are to transmit a given amount of power, more teeth can be used only by increasing the pitch diameter. This makes the gears larger, which is seldom desirable, and it also increases the

pitch-line velocity. This increased pitch-line velocity makes the gears noisier and reduces the power transmission to some extent. Another way of reducing interference is by using a larger pressure angle. This results in a smaller base circle, so that more of the tooth profile becomes involute.

In general, the involute interference or undercut limits will not be active constraints at the optimum. However, it is important to have these equations formulated in the design model from a computational perspective.

In summary, equations which define a feasible design space have been presented in this chapter. Constraints were given for bending fatigue, Hertz contact stress at both LPSTC and IPC, and undercut/involute interference. In Chapter IV and V, these constraint equations and their interactions will be studied in order to determine optimal gear designs using the AGMA method and Probabilistic Design Methodology respectively.

CHAPTER IV

DETERMINATION OF OPTIMUM GEAR DESIGN USING AGMA J FACTOR AND APPROXIMATE J FACTOR

In this chapter, the focus is on determining the optimal design for a compact spur gear set in mesh, using the geometry factors I and J as given by AGMA in [15] and using the J as given by [10]. A comparative study would be made on these two, based on the design values and running time of the computer program written on the above mentioned methods.

Design Parameters

It is important to define a criterion by which we can compare different designs. One that comes to mind is cost. Tucker [16] says that maximizing load capacity for a given material and size generally results in lowest cost per horsepower transmitted.

In specifying the material and its properties, the designer should realize that the strongest (hardest) material will yield the smallest design. Gears of very hard materials are expensive to produce because they require special heat treating processes and almost always require grinding to eliminate distortion caused by heat treating. However, the size reduction obtainable by using very hard materials usually offsets the increased production cost because the other components in the gear box (bearings, shafts, seals, housings) are also reduced in size. An added bonus is that smaller gears run more smoothly than larger gears and, therefore, have lower derating factors. Dudley [17] points out that a ten to one reduction in

weight can be obtained by using fully hardened gears as opposed to low hardness gears.

In designing a minimum size spur gear set, there are many parameters to consider. These include those related to the application of the gear set (power transmitted, input and output speeds, derating factors) and those related to the mesh geometry (number of teeth, diametral pitch, pressure angle, addenda and dedenda, face width). In this project it will be assumed that the parameters related to the application of the gear set will be known or will be available through a functional relationship and the geometrical parameters (ϕ, a, b, r_T, λ) will be chosen by the designer.

The design model is solved by assigning values to the geometrical parameters and then treating the remaining two parameters (N_P, P) as design variables. Also, the materials to be used is assumed to be known. This is the approach used in reference [4], [18] . This approach is well founded for the following reasons. First, reducing the number of design variables to two enables this problem to be tackled as an optimization problem. Second, the pressure angle, addenda, dedenda, and hob tip radius are all standardized variables; therefore, the designer can choose values for these variables from a small number of commonly used standard data.

Based on information in references [4], [7], [16], [17], [18], it seems that, it is a common practice among designers to specify the face width as a proportion of the pinion diameter. It is known that a wider face width can carry a greater load, however, it is also more sensitive to alignment errors which can cause uneven load bearing instances.

Tucker [16] recommends the formula, $\lambda = m_G / (m_G + 1)$, for obtaining an initial estimate for λ. Dudley [19] recommends a value of 0.25 for λ when alignment between

gears is a serious problem, 0.5 for good alignment and 1.0 for extremely good alignment. In Reference [20], Juvinall suggests lower limit on face width as 9/P and upper limit as 14/P, or in terms of module as $9m < F < 14m$.

In some sources, as in [21], it is recommended that the face width be between three and five times the circular pitch. This was an adequate rule of thumb earlier when low hardness gears were being used more often. This rule for determining the face width penalizes the finer pitch gears, which are more common in use today, to an excessive degree. Therefore for gears with finer pitch ($P \geq 20$), the face width to diameter approach is a more logical approach to use in specifying the face width.

The problem, therefore, has been reduced to one of only two variables, the number of pinion teeth, N_P, and the diametral pitch, P. Designing a compact spur gear set involves minimizing the center to center distance, C, as in [4], [18], which is given as; $C = N_P (1 + m_G) / 2P$. It is shown in [2] that the optimum is clearly constraint bound since d is monotonically increasing in N_P and decreasing in P. It is shown that the optimum occurs at an intersection of two constraints, usually the LPSTC contact stress constraint and the bending stress constraint. Furthermore, the constraint intersection depends only on N_P, so even though the design space is two-dimensional, the optimum is obtained by solving a one-dimensional problem.

Formulation of Design model

Our design objective is to minimize the size of the gear. This can be interpreted in many ways: reduction in the volume of the pinion, reduction in the center distance between

pinion and gear, or reduction in the pinion pitch diameter. As will be seen, all these are equivalent. The volume of a pinion can be expressed as;

$$\text{Volume} = F(\pi d_P^2) / 4 \tag{4.1}$$

This is not exact, as the tooth addendum region will not exactly fill the root space between teeth, but is close enough to be relevant. The problem is then to minimize volume. As discussed earlier, face width can be expressed as a fraction of pinion diameter, i.e.,

$$\lambda = F/d_P. \tag{4.2}$$

If we now combine equations (4.1) and (4.2) we have;

$$\text{Volume} = (\pi/4)\ \lambda\ d_P^3 \tag{4.3}$$

In a general design problem, the facewidth to diameter ratio λ is specified by the designer and hence can be treated as a constant in equation (4.3). It can now be seen that minimizing the volume and minimizing the pinion pitch diameter are equivalent. The equation for the distance between pinion and gear centers (center distance) can be expressed as:

$$C = \tfrac{1}{2}\ (d_P + d_G) \tag{4.4}$$

The pitch diameter of the gear, d_G, is related to that of the pinion by the gear ratio m_G:

$$d_G = m_G * d_P \tag{4.5}$$

The gear ratio is always given in a gear design problem, with a certain maximum margin for error. Then, the center distance can be expressed as:

$$C = d_P\ (m_G + 1)/2 \tag{4.6}$$

Expressing d_P in terms of the design variables N_P and P, we have:

$$C = (N_P/P)\ (m_G + 1)/2 \tag{4.7}$$

From equation (4-6), we see that minimizing the center distance is equivalent to minimizing the pinion pitch diameter d_p. In this project, however, the objective function is taken as minimizing the center distance, as the center distance is expressed in terms of the gear ratio and the design variables N_P and P. This is the method followed in [4] and [18].

The optimization problem can thus be summarized as:

$$\text{MINIMIZE } C = N_P (1 + m_G) / (2P) \tag{4.8a}$$

such that

$$N_P \geq 2 [bP - r_T (1 - \sin \phi)] / \sin^2 \phi \tag{4.8b}$$

$$s_c \geq C_P [W_t C_D / (dFI)]^{1/2} \tag{4.8c}$$

$$s_t \geq W_t P K_D / (FJ) \tag{4.8d}$$

with known parameters:

$H, n_p, m_G, \phi, a, b, r_T, \lambda, s_c, s_t$.

In most practical application, the undercut constraint (equation (4.8b)) will not be active at the solution. Equation (4.8c) safeguards against pitting and scoring failures of the teeth. In chapter II it was stated that, the LPSTC contact stress constraint can be taken as the Pitting constraint and that the IPC contact stress constraint can be taken as the Scoring constraint. Equation (4.8c) is a general form of contact stress equation that can be used to calculate the contact stress for any point of contact through the mesh cycle. Equation (4.8d) is the bending fatigue constraint which accounts for the failure due to bending fatigue. Both the constraints (4.8c) and (4.8d) include AGMA geometry factors I and J, that are discussed further in Appendix I and II.

In [10], a simple, analytical method to accurately estimate the AGMA bending stress geometry factor J has been presented. This is a non-iterative method and yields results with good accuracy. The optimization model has been solved using the Approximate equation for J factor and a comparison was made with the use of AGMA J factor. The results are discussed later in this chapter.

The formulation of the constraints for the optimization problem has been discussed in [2]. Equation (4.8b) gives the lower bound on N_p. Although limiting the contact stress at the initial point of contact will eliminate the possibility of involute interference, from a computational perspective it is prudent to include equation (4.8b) in the formulation. It can be noted that the terms on the right side of equation (4.8b) are all constants in a given design context and so this lower bound on N_p is determined only once in the design algorithm.

In [17], the Hertzian contact stress is evaluated at the initial point of contact and at the lowest point of single tooth contact. The classical Hertz contact stress equation as applied to spur gearing is given as:

$$\sigma_H = C_p \left[(W_t / F\cos\phi) \, (1/\rho_1 + 1/\rho_2) \right]^{1/2} \qquad (4.9)$$

The pinion radius of curvature as given in [2] is simply: $\rho_1 = \theta R_1 \cos\phi$ (4.10)

It is shown that the sum of the gear and pinion radii of curvature is always a constant and given by: $\rho_1 + \rho_2 = \pm C \sin\phi$ (4.11)

This requires the radius of curvature of an internal tooth to be negative. Realizing that $C = R_1(m_G \pm 1)$ and solving equation (4.11) for ρ_2, we get:

$$\rho_2 = R_1 \left[(1 \pm m_G) \sin\phi - \theta \cos\phi \right] \qquad (4.12)$$

Therefore the term $(1/\rho_1 + 1/\rho_2)$ from equation (4.9) can be written as:

$$(1/\rho_1 + 1/\rho_2) = [1/(R_1\theta\cos\phi)]\,[(1 \pm m_G)\sin\phi$$

$$/\,[(1 \pm m_G)\sin\phi - \theta\cos\phi]] \qquad (4.13)$$

If the expression for the roll angle to the pitch point is substituted into equation (4.13) it becomes:

$$(1/\rho_1 + 1/\rho_2)_{PP} = [1/(R_1\sin\phi)]\,[m_G \pm 1)/m_G]$$

$$= [2/(d_1\sin\phi)]\,[m_G \pm 1)/m_G] \qquad (4.14)$$

Substitution of this expression into equation (4.9) gives the standard AGMA surface durability equation; $\sigma_{HPP} = C_P[W_t / (Fd_pI)]^{1/2}$ (4.15)

where I is the AGMA durability geometry factor.

$$I = [\sin\phi\cos\phi / 2][(m_G \pm 1)/m_G] \qquad (4.16)$$

The actual AGMA equation contains a dynamic factor, C_v, to account for dynamic load effects. The generalized form of equation (45c) which would compute the Hertz contact stress at any point of contact through the mesh cycle is given as;

$$\sigma_H = C_p\,\{[\delta C_a C_m W_t C_f C_s/(C_v d_p F)]\,[1/[\theta\cos^2\phi\,(1-\theta\cos\phi)/(\sin\phi\,(1\pm m_G))]]\}^{1/2} \qquad (4.17)$$

where, $C_v = 1/\,[1 + (1/A)\,(v_t)^{1/2}]^B$

A and B are constants given by AGMA 218.01 ref [7]. A and B are calculated as:

$$B = (1/4)\,(12 - Q)^{2/3} \quad \text{and} \quad A = 50 + 56(1-B)$$

where Q being the AGMA Quality Number.

Equation (4.17) is valid at any point during the contact cycle and σ_H can be computed for values of δ and θ. At the initial point of contact, $\delta = 1$ and $\theta = \theta_{IPC}$. At the lowest point of single tooth contact, $\delta = 2$ and $\theta = \theta_{LPSTC}$.

As the expression for σ_H at the initial point of contact and at the lowest point of single

tooth contact are readily available, the surface stress constraints are simply stated as inequalities that require these two critical values of σ_H to be less than the surface strength of the softer material. The surface strength in the inequalities must be appropriately modified for overload, face misalignment, life, temperature, reliability, size, and surface finish.

Similarly, the AGMA bending stress equation is developed from the Lewis Equation, which considers the gear tooth as a cantilever beam. This is further discussed in the next chapter. The AGMA bending stress equation is given as [7]:

$$\sigma_B = \frac{K_a K_s K_m W_t P}{K_v F J} \qquad (4\text{-}18)$$

Deterministic Optimization

The optimization problem on hand is summarized as:

MINIMIZE $C = N_P (1 + m_G) / (2P)$

such that

$N_P \geq 2 [bP - r_T (1 - \sin \phi)] / \sin^2 \phi$

$s_c \geq C_P [W_t C_D / (dFI)]^{1/2}$

$s_t \geq W_t P K_D / (FJ)$

The formulation mentioned above can be called as Deterministic formulation, as all the design variables are deterministic in nature. The correction factors and geometry factors introduced by AGMA makes the problem more deterministic. The next chapter focusses on formulating the optimization model without any AGMA correction factors, thereby including

randomness in the problem.

Several attempts have been made to solve the optimization problem stated above [4]. Carroll and Johnson, see [2], came up with the most efficient optimization algorithm which could solve for the design values. This algorithm is a special purpose algorithm that is applicable only to this gear design problem, rather than to the broad class of general nonlinear programs. The operation of the algorithm is described below.

First, a feasible starting value for N_P is chosen. Once this is established, the bracketing phase of the algorithm begins. An initial step of magnitude $\Delta N_P = 2^{q1}$, where q1 is a specified non-negative integer, and is taken in the direction of decreasing N_P. The pinion diameter and constraints are evaluated at the new point. If the new point is infeasible (i.e., violates any of the constraints), then d_P for that point is artificially set to a large value (10^6 in the current work). If the new d_P is less than the previous one, the step size exponent, q1, is increased by one and another step is taken. The process is repeated until the new d_P is greater than the previous one. An upper bound on the step size is set at $\Delta N_{max} = 2^{qmax}$ where q_{max} is a specified non-negative integer greater than or equal to q1. In general the step size of the *i*th step is given by $(\Delta N_P)_i = 2^{q_i}$ where $q_i = \min \{(q1 + i - 1), q_{max}\}$.

Now a bracket on the minimum having a width of $\Delta N_P = 2^{q1}$ (the last step size of the bracketing phase) has been established. Since the bracket width is a power of two, the minimum is found in exactly q_i additional function evaluations by halving the bracket q_i times and discarding the half not containing the minimum each time until ΔN_P is the minimum while the other is infeasible.

Satisfaction of Gear Ratio Requirement

An additional problem that must be considered involves the integer tooth number requirement for the gear, [2]. So far, only the pinion has been considered in the design process. However, even if the number of pinion teeth is an integer, it may be impossible to have an integer number of gear teeth for some values of the gear ratio, like the one cosidered in this thesis, where $m_G = 3.78$. The only sensible solution to this problem is to allow the gear ratio to vary to some acceptable amount about the desired value. In most gear applications where load must be transmitted, the actual gear ratio can vary a limited amount from the specified value without adversely affecting the desired performance.

To determine an acceptable value for N_G the following steps could be taken. First, find the minimum feasible integer value of N_P. Next, calculate the product of m_G and N_P. If the fractional part of this product exists (nonzero) then N_G should be set equal to the integer portion of the product plus one. The actual gear ratio should then be calculated and compared to the desired gear ratio. If the absolute difference is less than the acceptable deviation, then those values of N_P and N_G are taken as the design values pending their satisfaction of other constraints (feasibility). If the gear ratio tolerance is exceeded, the only alternative is to increase N_P until a suitable combination of N_P and N_G can be found.

The minimum value of N_P using the desired value of m_G is obtained so that none of the design constraints are violated; however, if the gear ratio has to be varied to satisfy the integer tooth number requirement on N_G, the locations of the constraints in the design space will change. It is then possible that an infeasible design could result due to the gear ratio variation. Therefore, the final design must be checked for feasibility when the actual gear ratio is different from the value used to obtain the minimum N_P.

To illustrate the design technique, an example cited in [4] is considered below:

Example Problem :

A gear set is to be designed to transmit 20 hp at a speed of 1260.5 rpm. The gear ratio is 5, pressure angle is 20 degrees, face width to diameter ratio is 0.25, surface strength is 200 ksi, bending strength is 60 ksi, elastic modulus is 3E7 psi, poisson's ratio is 0.25, external mesh and standard teeth. The dynamic factor is considered as unity.

This problem was solved in two ways using the model defined in [2]: One using the AGMA geometry factor, J, and the other using the J calculated using Approximate equations, see [10]. The results are shown in Table 4-1 and Table 4-2.

Discussion :

Referring to Table 4-1, note that using the J given by AGMA, for a diametral pitch of 16, the minimum feasible number of pinion teeth was found to be 33, and the minimum center distance of 6.188 in. For the same diametral pitch of 16, using the Approximate equations for J value, see Table 4-2, the feasible number of pinion teeth was found to be 36 (rather than 33), and the value of center distance is 6.75 inches. However, the minimum value of center distance obtained using the J from Approximate equations is 6.50 inches for a diametral pitch of 12. Also note the computer time taken for both the methods. As explained in Appendix III, determination of J using the approximate equations is much faster. The computer time taken by the AGMA method is considerably higher than the time taken by J using approximate equations.

Table 4-1

DESIGN OF SPUR GEAR SET USING DETERMINISTIC METHODS

Data Input :-

Gear ratio = 5
Pr. angle = 20 deg.
q1 = 1 qmax = 3
rpm = 1260.5
add. a = 1.000/p ded. d = 1.250/p hobtip radius = .300/p
velocity factor kv = 1
Horse power = 20 hp
Allowable bending stress : 60 ksi
Allowable contact stress : 200 ksi
Face width f = 0.25 * d_p
Mod. of elasticity = 3E+7 psi
Poisson's ratio = 0.25

DETERMINISTIC SOLUTION USING J OBTAINED BY AGMA METHOD

P (in)	NP	NG	C (in)	F (in)	SB (KSI)	SLPSTC (KSI)	SIPC (KSI)	TIME (secs.)
2.000	16.000	80.000	24.000	2.000	0.548	27.798	128.336	≈ 0
2.250	16.000	80.000	21.333	1.778	0.780	33.169	153.136	0.049
2.500	16.000	80.000	19.200	1.600	1.070	38.848	179.354	0.049
3.000	17.000	85.000	17.000	1.417	1.606	45.983	100.992	0.049
4.000	17.000	85.000	12.750	1.063	3.807	70.796	155.488	0.109
6.000	19.000	95.000	9.500	0.792	9.958	107.729	159.599	0.109
8.000	21.000	105.000	7.875	0.656	18.827	140.505	175.681	0.160
10.000	23.000	115.000	6.900	0.575	30.011	169.276	191.423	0.160
12.000	26.000	130.000	6.500	0.542	39.577	182.701	187.994	0.160
16.000	33.000	165.000	6.188	0.516	56.038	193.062	177.005	0.221
20.000	44.000	220.000	6.600	0.550	59.725	172.763	145.945	0.221

Note: ≈ 0 indicates value too close to zero.

Table 4-2

DESIGN OF SPUR GEAR SET USING DETERMINISTIC METHODS

Data Input :-

Gear ratio = 5
Pr. angle = 20 deg.
q1 = 1 qmax = 3
rpm = 1260.5
add. a = 1.000/p ded. d = 1.250/p hobtip radius = .300/p
velocity factor kv = 1
Horse power = 20 hp
Allowable bending stress : 60 ksi
Allowable contact stress : 200 ksi
Face width f = 0.25 * d_p
Mod. of elasticity = 3E+7 psi
Poisson's ratio = 0.25

DETERMINISTIC SOLUTION USING J OBTAINED BY APPROXIMATE EQUATIONS

P (in)	NP	NG	C (in)	F (in)	SB (KSI)	SLPSTC (KSI)	SIPC (KSI)	TIME (secs.)
2.000	16.000	80.000	24.000	2.000	0.733	27.798	128.336	≈ 0
2.250	16.000	80.000	21.333	1.778	1.044	33.169	153.136	≈ 0
2.500	16.000	80.000	19.200	1.600	1.432	38.848	179.354	≈ 0
3.000	17.000	85.000	17.000	1.417	2.140	45.983	100.992	≈ 0
4.000	17.000	85.000	12.750	1.063	5.073	70.796	155.488	≈ 0
6.000	19.000	95.000	9.500	0.792	13.152	107.729	159.599	0.059
8.000	21.000	105.000	7.875	0.656	24.649	140.505	175.681	0.059
10.000	23.000	115.000	6.900	0.575	38.964	169.276	191.423	0.059
12.000	26.000	130.000	6.500	0.542	50.770	182.701	187.994	0.059
16.000	36.000	180.000	6.750	0.563	57.721	168.577	150.083	0.059
20.000	48.000	240.000	7.200	0.600	59.807	151.157	125.426	0.059

Note: ≈ 0 indicates value too close to zero.

It is concluded that a smaller feasible design is obtained using the AGMA method. The smallest value of center distance using AGMA method is 6.188 inches for a pitch of 16 and a pinion teeth number of 33. The smallest value of center distance using J from Approximate equations is obtained as 6.5 inches for a diametral pitch of 12 and a pinion teeth number of 26. The solutions shown in Table 4-1 and Table 4-2 are both deterministic. The features of the method and code are; (i) Determination of the best design for each candidate diametral pitch, (ii) Designs which provide a tight satisfaction of the specified gear ratio are obtained, (iii) A complete analysis of each design is obtained with output including contact stresses, bending stress, face width, center distance and the computer time for each design. Since the smallest feasible gear set is obtained for each candidate diametral pitch, the designer can survey the results and choose the final design based on practical trade-offs between size and other design aspects.

However, the design suffers a serious set back in not being able to define the safety of the design in terms of reliability. There is no safety level associated with the design. In the next chapter, it is shown how Probabilsitic Design methodology, when incorporated in gear design can define the safety level of the design, apart from the above mentioned features of the deterministic method. Probabilistic design methodology thereby gives added flexibility to the designer to consider the aspect of safety in the design. This is discussed in the next chapter.

CHAPTER V

DETERMINATION OF OPTIMUM GEAR DESIGN USING PROBABILISTIC DESIGN METHODOLOGY

Several methods have been proposed in the past for optimum design of spur gears. These methods have utilized deterministic design optimization techniques to obtain what could be considered satisfactory design parameters. There are at least two problems that arise with the results of deterministic approach; the inability to deal with uncertainties in material properties and over conservative design. Moreover, in an optimally designed structure based on deterministic considerations, this drawback can be more troublesome, because optimized structures tend to be more sensitive to fabrication defects and improper definition of the loading environment, see [22], [23], [24]. This has given rise to research in the areas of Probabiiistic Design Methodologies applicable to structural and machine component design. This method seeks to account for the uncertainties in material properties, loading conditions and disparate failure models. In this chapter, the applicability of probabilistic design methodology in compact spur gear design is discussed.

Uncertainty associated with design

Engineering uncertainty is not limited to the variability observed in the basic variables. First, the estimated values of a given variable (such as the mean), based on observational data, will not be error-free. Second, mathematical or simulation models often

have modeling uncertainties and limited accuracy at least over certain range of parameters. For example, formulae, equations, algorithms, and laboratory models, that are often used in engineering analysis and design are idealized representations of reality. Consequently, predictions and calculations made on the basis of these models may be inaccurate and thus also contain uncertainty. Human error can result from errors made by engineers and technicians during the design or operation phases. It can be reduced by improving the quality of control program, but it cannot be avoided entirely. In general, human error is very difficult to define. It is common practice to treat human error as modeling error, see [25]. In some cases, the uncertainties associated with such predictions or model errors may be much more significant than those associated with the inherent variabilities. All uncertainties, whether they are associated with inherent variability or with prediction error, may be precisely assessed in statistical terms and the evaluation of their significance on the design can be accomplished by the concepts and the methods of probability.

If there are uncertainties in the design, the next step is, to ask how should designs be formulated or decisions affecting a design be resolved? Presumably, we may assume the worst conditions and develop conservative design on this basis. From the system performance and safety point of view, this approach may be suitable. However, the resulting design would be too costly as a result of over-conservatism. On the other hand, an inexpensive design may not ensure the desired level of performance and safety. Therefore, the decisions should be made considering cost and safety of the design. The most desirable solution is one that is optimal, in the sense of minimum cost and maximum benefits. If the available information and the models to be evaluated contain uncertainties, the analysis

should include the effects of such uncertainties.

Thus, probabilistic design is concerned with the probability of failure or preferably reliability. This methodology is most useful when uncertainties in material properties and loading conditions are considered. To apply probabilistic methodologies in design, the design parameters are modeled as random variables, with selected distribution types, means, and standard deviations, see [26]. The primitive (random) variables that affect the structural behavior have to be identified.

Development of PDO Model

The probabilistic model of the same design problem cited in the previous chapters would be different from the deterministic model that has been described in chapter IV. The difference is that the AGMA correction factors and geometry factors that have been incorporated in the design model are neglected. This enables the problem to be treated as completely non-deterministic, or in other words, probabilistic. The design variables are treated as random variables with some known distribution. The uncertainties in the design equations are thereby quantified.

Accordingly, our next step is to restate the design constraints defined in Chapter III, to be modeled using the probabilistic methodologies. This is done by eliminating the correction factors and defining the possible uncertainties in the design variables.

Wilfred Lewis [27] was the first to present a formula for computing the bending stress in gear teeth in which the tooth form entered into the equation. The formula was announced in 1892, and it still remains the basis for most gear design today. This formula is used to define the failure surface due to bending fatigue, in this project.

A gear tooth is essentially a stubby cantilever beam. At the base of the beam, there is tensile stress on the loaded side and compressive stress on the opposite side. When gear teeth break, they usually fail by a crack at the base of the tooth on the tensile-stress side. The ability of gear teeth to resist tooth breakage is referred to as *beam strength* or *flexural strength* in [19].

The flexural strength of gear teeth was first calculated to a close degree of accuracy by Wilfred Lewis. This was achieved by inscribing a parabola of uniform strength inside a gear tooth, see Figure 5-1. When this parabola is made into a cantilever beam, the stress is constant along the surface of the parabola. By inscribing the largest parabola that will fit into a gear tooth shape, one can locate the most critically stressed position on the gear tooth. This position is at the point at which the parabola of uniform strength becomes tangent to the surface of the gear tooth. The gear tooth is modeled as a cantilever beam of cross-sectional dimensions F and t, having a length l and a load W_t uniformly distributed across the distance F. The length l is same as the sum of the addendum and dedendum. The thickness of the tooth is half the circular pitch, since circular pitch is equal to the sum of the tooth thickness and width of space between teeth. The section modulus is $I/c = Ft^2/6$, and therefore the bending stress is:

$$\sigma_B = \frac{M}{I/c} = \frac{6W_t l}{Ft^2} \tag{5.1}$$

Equation (5.1) has further been developed to define more accurately the bending strength in a gear tooth under load. This was achieved by incorporating the correction factors

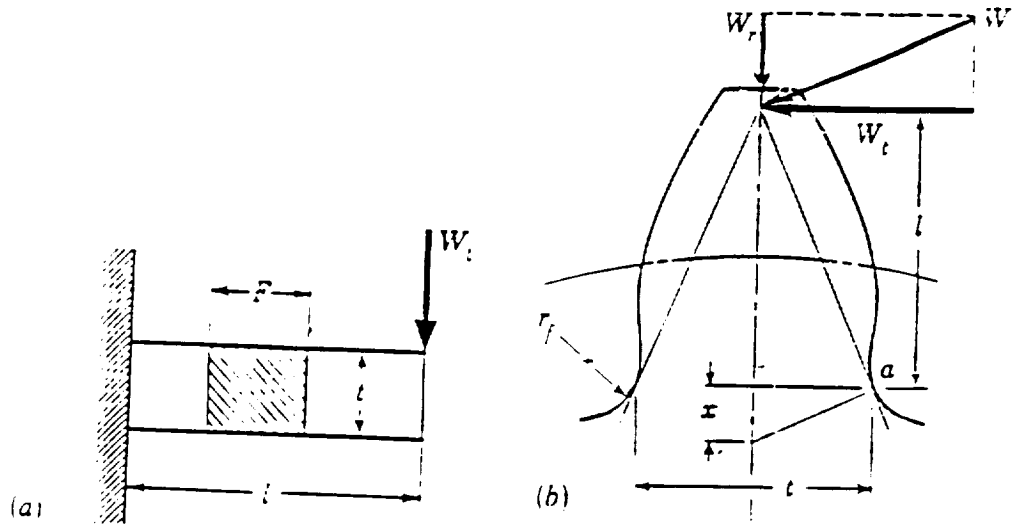


Figure 5-1: Assumption of Gear Tooth in Determination of Lewis Factor

(Source: Mechanical Engineering Design
Shigley and Mischke, Fifth Edition)

and geometry factors J. The corrected equation for bending strength was stated in Chapter IV to define the bending failure in deterministic method. As the idea of this work is to arrive at the optimum design of a gear set without involving any correction factors, equation (5.1) would be used to define the bending strength failure equation in this chapter. By modeling the gear tooth as a beam all the uncertainties in the design variables can be treated.

The contact stresses on the gear tooth can be determined by the formulas derived from the work of Hertz. It is easy to visualize that any contact point on a set of spur gears can be simulated by a pair of cylinders of the appropriate radii. The applied load P is the normal tooth load W_N per inch of face width F; thus,

$$P = W_N / F \tag{5.2}$$

The normal tooth load on a set of spur gears is given as:

$$W_N = W_t / \cos(\phi) \tag{5.3}$$

where W_T is the tangential tooth load and ϕ is the pressure angle; thus,

$$P = W_t / (F \cos\phi) \tag{5.4}$$

In the late nineteenth century, H. Hertz developed a mathematical theory for the surface stresses and deformations produced when two curved bodies are pressed together. For cylinders with parallel axes, Hertz's equations become:

$$S_c = 0.564 \sqrt{\frac{P[(\rho_P + \rho_G)/(\rho_P \rho_G)]}{[(1-\mu_P^2/E_P] + [(1-\mu_G^2)/E_G]}} \tag{5.5}$$

Substituting equation (5.4) into equation (5.5):

$$S_c = C_P \sqrt{\frac{W_T}{F \cos\phi} \left(\frac{\rho_P + \rho_G}{\rho_P \rho_G}\right)} \tag{5.6}$$

The AGMA geometry factor I is defined as:

$$I = \frac{\cos\phi}{d_P} \left(\frac{\rho_P \rho_G}{\rho_P + \rho_G}\right) \tag{5.7}$$

Equation (5.6) may simply be written as:

$$S_c = C_P \sqrt{\frac{W_t}{F d_P I}} \tag{5.8}$$

Equations (5.1) and (5.8) represent the bending and contact stress equations. These were the expressions that were used to define the limit state functions in probabilistic analysis, as can be seen in the following sections. These equations are in their primitive form without any correction factors. This enables the problem to be treated as a probabilistic model.

Limit State Function

Probabilistic analysis is mainly concerned with the probability of failure of a designed part or rather the reliability of the machine part or structure. By reliability it is meant the probability that designed part will perform its intended function without failing. This assumes that the part is used within the condition for which it is designed. Two factors are considered in this methodology. The first is the limit strength of a material and the other

is an acceptable level of safety. Because of this we define what is known as limit state function or equation and safety index. The concept of limit state function can be expressed as:

$$G(\mathbf{x}) = g(\mathbf{x}) - S_l \tag{5.9}$$

where

$\mathbf{x}$ = a vector of random design variables

S_l = a strength limit

The function $G(\mathbf{x})$ is called a limit state function. It divides the design space into safe and unsafe regions, see Figure 5-2a.

The major concern in probabilistic analysis is the computation of the probability of failure of a structure or machine element. Therefore, the question arises as to how to define a measure of the reliability of a designed structural member or machine element. In general we are concerned that the applied stress, S, should not exceed the resistance, R, offered by the designed structure. Hence, the failure surface is given by:

$$G(R, S) = 0 \tag{5.10}$$

The minimum distance from the origin to a point on the failure surface is defined as the safety index, β, see Figure 5-2b. In [28], Hasofer and Lind (1974) calls this value the "Reliability Coefficient". The failure surface or "limit state" is defined by the equation (5.10) which can also be written as $g = 0$, as in [29]. The feasible or safe region is defined by the inequality $g > 0$ while the infeasible (unsafe) region is defined by $g < 0$.

In dealing with failure of a structure or machine component, it is desirable to determine the probability of R being less than or equal to S. Hence the probability of failure,

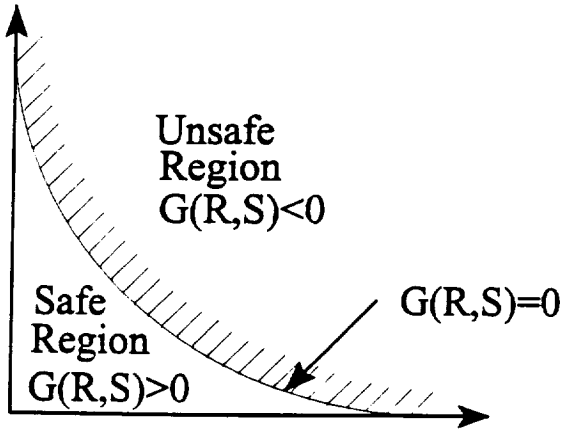


Figure 5-2 (a): Safe and Unsafe regions of a design space

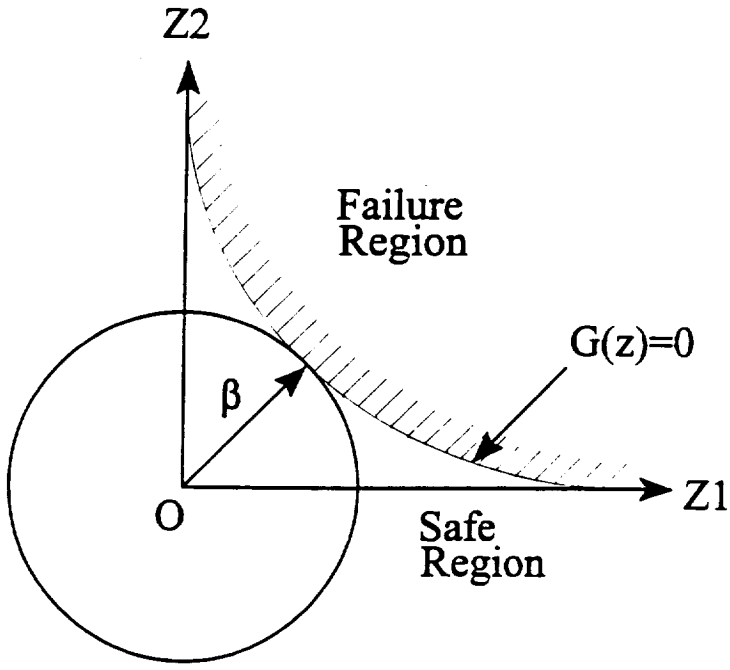


Figure 5-2(b): Definition of Safety Index

p_f, is:

$$p_f = P\ (R \leq S) \tag{5.11}$$

or in general

$$p_f = P[G(R, S) \leq 0] \tag{5.12}$$

where G() is the limit state function and P[.] denotes the probability of event [.]. From basic statistics

$$p_f = P\ (R - S \leq 0) = \int \Omega \int f_{RS}\ (r, s)\ dr\ ds \tag{5.13}$$

where

Ω = failure domain

f_{RS} = joint density function.

If R and S are independent, equation (5.13) becomes:

$$p_f = P(R-S \leq 0) = \int_{-\infty}^{\infty} \int_{-\infty}^{s \geq r} f_R(r) f_S(s)\ dr ds \tag{5.14}$$

where

f_R = density function for R

f_S = density function for S.

It is known that the cumulative distribution function, F_Z (z), of any random variable Z is given by:

$$F_Z(z) = P(Z \leq z) = \int_{-\infty}^{z} f_z(x)\, dx \tag{5.15}$$

provided $z \geq x$. Consequently equation (5.14) may be written as:

$$p_f = P(R_S \leq 0) = \int_{-\infty}^{\infty} F_R(z) f_s(z)\, dz \tag{5.16}$$

The design constraints defined in chapter III, have to restated as limit state functions, in order to be treated as probabilistic. Consider the bending stress equation defined by equation (5.1). As mentioned earlier in this chapter, the gear tooth is considered as a cantilever beam and the bending strength on the gear tooth is considered as same as the bending strength equation of a beam. To prevent failure in bending, the calculated bending stress can be compared to the adjusted bending strength of the material:

$$\frac{6 W_t l}{F t^2} \leq S_t \tag{5.17}$$

Expressing as a limit state function, equation (5.17) can be written as:

$$\frac{6 W_t l}{F t^2} - S_t \leq 0 \tag{5.18}$$

Similarly, expressing equation (5.8) which is the Hertz contact stress equation as a limit state function, we get:

$$C_P \sqrt{\frac{W_t}{F d_P I}} - S_c \leq 0 \tag{5.19}$$

Equations (5.18) and (5.19) define the corresponding failure surface when the design variables are transformed in a two dimensional space. Next topic deals with determining the

minimum distance of these failure surfaces from the origin, β.

Safety Index Determination

The evaluation of equation (5.16) is not always easy especially since the distribution of R and S are not always known. However, for the case when it is known that R and S are random normal variables the probability of failure is determined very rapidly. If the safety margin is defined by;

$$Z = R - S \tag{5.20}$$

then

$$p_f = P(R-S \le 0) = P(Z \le 0) = \Phi(\frac{0-\mu_z}{\sigma_z}) \tag{5.21}$$

where

$\Phi(\,)$ = the standard normal distribution function

$\mu_Z = \mu_R - \mu_S$

$\sigma_Z = (\sigma_R^2 + \sigma_S^2)^{1/2}$

Hence,

$$p_f = \Phi(-\beta) \tag{5.22}$$

where

$$\beta = \mu_Z / \sigma_Z \tag{5.23}$$

The safety index, β, defined by equation (5.23) is due to Cornell, see [30], and it is said to be based on the first two moments, that is mean and standard deviation. It is possible

that various values of safety index may be obtained for the same limit state condition, depending on how the safety index is defined, see [31]. When this is the case we say that safety index lacks invariance, [32]. To insure that β is invariant Hasofer and Lind in [28] suggested the transformation of the variables into their standard form where the mean is zero and the variance has a value of unity, using the expression

$$\mathbf{z} = (X - \mu_x) / \sigma_x \tag{5.24}$$

Similarly the limit state function is also transformed to give

$$G(\mathbf{z}) = 0 \tag{5.25}$$

In probabilistic analysis, the failure surfaces have to be defined as limit state functions in the form mentioned in equation (5.25). This will define the surface that divides the safe and unsafe regions in the transformed design space.

The safety index, being the minimum distance to the surface, as in [33], is determined as

$$\beta = \min (\mathbf{z}^T\mathbf{z})^{1/2} \tag{5.26}$$

subject to (5.25).

To determine the safety index, β, for the failure modes defined earlier, certain assumptions were made. The material properties were assumed to be at their mean value. The coefficient of variation γ was assumed to be 0.05. An example problem taken from Motts (1992) [5] was considered. The values of safety indices were determined using a program, that is based on General Reduced Gradient algorithm. The results will be shown later in this chapter, along with the problem statement.

Probabilistic Design Optimization Format

The format of the probabilistic design optimization is very similar to that of the

deterministic. Generally, the problem should be modeled first deterministically as:

$$\text{Minimize } F(\mathbf{x}) \tag{5.27a}$$

$$\text{Subject to } G_i(\mathbf{x}) \le 0, \quad i = 1,.....,m \tag{5.27b}$$

$$\mathbf{x}_l \le \mathbf{x} \le \mathbf{x}_u \tag{5.27c}$$

where $\mathbf{x}$ is a column vector with n rows and the subscripts l and u represent the lower and upper bounds on $\mathbf{x}$ respectively. In the design of either a machine element or structure, the constraint is generally related to the limit imposed by either stress or deformation or any other criteria that must be satisfied for a safe design.

Because probabilistic design is concerned with probability of failure or the reliability of a system the probabilistic equivalent formulation of (5.27) is:

$$\text{Minimize } F(\mathbf{x}) \tag{5.28a}$$

$$\text{Subject to } P[G_i(\mathbf{x}) \le 0] \ge \zeta_i, \quad i = 1,.....,m \tag{5.28b}$$

where $\mathbf{x}$ is a vector of n random variables and ζ_i is the specified reliability level of the system. However, after the determination of safety index as demonstrated above, the constraint (5.28b) is expressed as:

$$G_i(\mathbf{x}) = \beta_i - \Phi^{-1}(\zeta_i) \qquad i = 1,.....,m \tag{5.28c}$$

where $\Phi^{-1}(.)$ is the inverse of the standard normal distribution function.

The probabilistic formulation of (5.28) can be restated in terms of design variables as:

$$\text{Minimize } C = N_P (1 + m_G) / (2P) \tag{5.29a}$$

subject to

$$2 [bP - r_T (1 - \sin \phi)] / \sin^2 \phi - N_P \le 0 \tag{5.29b}$$

$$C_P [W_t / (d_P FI)]^{1/2} - S_c \leq \beta_H - \Phi^{-1}(\zeta) \quad (5.29c)$$

$$6 W_t l / (Ft^2) - S_t \leq \beta_B - \Phi^{-1}(\zeta) \quad (5.29d)$$

where β_H is the safety index determined for the pitting failure surface and β_B is the safety index determined for the bending failure surface. As mentioned earlier, equation (5.29b) is to check on the lower limit on the number of teeth on pinion, in order to avoid involute interference. Limiting the contact stress at the initial point of contact will eliminate the possibility of involute interference. Note that in equation (5.29b), all the terms except N_P, which is a design variable, are constants in a given design context and so the lower bound on N_P is determined only once in the design algorithm. Yet, Equation (5.29b) was incorporated in the design algorithm only from a computational perspective.

From the formulation defined by (5.29), it can be seen that two different values of safety index are used for the bending and pitting constraints. This is to account for the correlation between the failure modes. However, Hasofer and Lind [28] have suggested that, for multiple failure modes, the least of all the β values need to be used to define the constraints in the formulation.

In this thesis, both the ways of incorporating safety indices were considered and the results are shown for an example problem taken from Motts, [5].

Example Problem : Design a pair of spur gears with 20 degrees full-depth teeth. The pinion operates at 1750 rpm. The gear ratio is 3.78. The set must transmit 3 hp. The material to be used is AISI OQT 1300. The yield stress is 61 ksi, tensile stress is 88 ksi. Poisson's ratio of 0.25, modulus of elasticity 30×10^6 psi, facewidth to diameter ratio is 0.25.

The AGMA allowable stresses are calculated as; contact = 85.841 ksi, bending = 25.197 ksi.

In executing the same problem using probabilistic techniques, the data given are assumed to be at their respective mean values. The coefficient of variation (COV) for the distribution is taken as 0.05. The distribution type is taken as *normal distribution.*

Discussion :

Since the objective of this project is to make a comparative study of the use of AGMA geometry factors and Probabilistic design methodology in gear design, the problem is first solved deterministically. Solutions are presented in Table 5-1 and Table 5-2. As mentioned in Chapter IV, deterministic approach in gear design can be achieved in two ways: One utilizing geometry factor *J* defined by AGMA and other using *J* from Approximate Equations. The optimum design achieved using these two methods are shown in Table 5-1 and Table 5-2. To aid easy comparison of these methods with probabilistic method the results obtained using probabilistic methods are also shown in the same table. This is further explained below.

The first step in solving the problem using probabilistic methods is to identify the design variables. In this case, the design variables are diametral pitch P and number of pinion teeth N_P. The next step is to calculate the values of safety indices for the pitting failure and bending failure limit functions. While doing this, all the variables are treated as stochastic. The material properties are assumed to be at their mean value. All the variables are transformed into a reduced space. On transformation, the variables P and N_P, will have a mean value zero and standard deviation one. The mean value of all other variables are given as input or treated as standard data which are readily available. The coefficient of

Table 5-1

OPTIMAL DESIGN OF SPUR GEAR SETS USING DETERMINISTIC AND PROBABILISTIC METHODS

Data Input :-

Gear ratio = 3.78
q1 = 1 qmax = 3
add. a = 1.000/p
hobtip radius = .300/p
Allowable bending stress : 25.841 ksi
Face width f = 0.25 * d_P
Poisson's ratio = 0.25

Pr. angle = 20 deg.
rpm = 1750
ded. d = 1.25/p
Horse power = 3 hp
Allowable contact stress : 85.841 ksi
Mod. of elasticity = 3E+7 psi
Distribution type: *Normal* COV = 0.05

RESULTS FOR EXAMPLE PROBLEM:
Formulation incorporates different values of safety indices for their corresponding Pitting and Bending constraints.
Safety Index for Pitting stress constraint = 2.432314
Safety Index for Bending stress constraint = 2.196645

REL.	P (in)	NP	C (in)	F (in)	S_t (ksi)	S_c (ksi)	TIME(sec)
@	8.0000	20.0000	6.0000	1.2500	4.5326	80.1924	0.0625
*	8.0000	20.0000	6.0000	1.2500	3.4531	80.1924	0.1094
50.0000	9.0000	21.0000	5.5556	1.1667	5.7057	92.3944	0.0586
70.5000	9.0000	21.0000	5.5556	1.1667	5.7057	92.3944	0.0508
81.3270	8.0000	20.0000	6.0000	1.2500	4.5345	80.0757	0.0586
85.3140	8.0000	20.0000	6.0000	1.2500	4.5345	80.0757	0.0508
90.3200	8.0000	20.0000	6.0000	1.2500	4.5345	80.0757	0.0625
95.0530	8.0000	20.0000	6.0000	1.2500	4.5345	80.0757	≈ 0
98.0300	8.0000	20.0000	6.0000	1.2500	4.5345	80.0757	0.0469
99.0610	7.0000	19.0000	6.4286	1.3571	3.4672	78.0643	0.0625
99.8650	5.0000	21.0000	9.9000	2.1000	1.0683	35.6087	0.0469
99.9720	-	-	-	-	-	-	-

Note: @ indicates deterministic solution obtained using Approximate J value
* indicates deterministic solution obtained using AGMA method for J factor
\- indicates no feasible solution
≈ 0 indicates value too close to zero.

Table 5-2

OPTIMAL DESIGN OF SPUR GEAR SETS USING DETERMINISTIC AND PROBABILISTIC METHODS

Data Input :-

Gear ratio = 3.78
q1 = 1 qmax = 3
add. a = 1.000/p
hobtip radius = .300/p
Allowable bending stress : 25.841 ksi
Face width f = 0.25 * d_p
Poisson's ratio = 0.25

Pr. angle = 20 deg.
rpm = 1750
ded. d = 1.25/p
Horse power = 3 hp
Allowable contact stress : 85.841 ksi
Mod. of elasticity = 3E+7 psi
Distribution type: *Normal* COV = 0.05

RESULTS FOR THE EXAMPLE PROBLEM:
Formulation incorporates the same lowest value of the two safety indices for both the Pitting and Bending constraints.
Safety Index = 2.196645

REL.	P (in)	NP	C (in)	F (in)	S_t (ksi)	S_c (ksi)	TIME(sec)
@	8.0000	20.0000	6.0000	1.2500	4.5326	80.1924	0.0625
*	8.0000	20.0000	6.0000	1.2500	3.4531	80.1924	0.1094
50.0000	9.0000	21.0000	5.5556	1.1667	5.7057	92.3944	0.0508
70.5000	9.0000	21.0000	5.5556	1.1667	5.7057	92.3944	0.0586
81.3270	8.0000	20.0000	6.0000	1.2500	4.5345	80.0757	0.0508
85.3140	8.0000	20.0000	6.0000	1.2500	4.5345	80.0757	≈0
90.3200	8.0000	20.0000	6.0000	1.2500	4.5345	80.0757	0.0586
95.0530	8.0000	20.0000	6.0000	1.2500	4.5345	80.0757	0.0508
98.0300	8.0000	20.0000	6.0000	1.2500	4.5345	80.0757	0.0625
99.0610	7.0000	20.0000	6.7857	1.4286	3.0940	66.1451	0.0469
99.8650	5.0000	30.0000	14.2000	3.0000	0.5023	17.4085	0.0508
99.9720	-	-	-	-	-	-	-

Note: @ indicates deterministic solution obtained using Approximate J value
* indicates deterministic solution obtained using AGMA method for J factor
- indicates no feasible solution
≈ 0 indicates value too close to zero.

variation of these values are given in the problem statement.

The values of safety indices found are; for bending failure $\beta = 2.196645$ and for pitting failure $\beta = 2.432314$. These values are also shown in Table 5-1. The next step was to use the probabilistic formulation given in (5.29) and run the optimization routine to arrive at the optimal design. Since the constraints are the same in both deterministic and probabilistic methods, the same optimization routine [2], is used for probabilistic analysis, with some modification. At this point, it must be realized that in obtaining the results using probabilistic methods, all the correction factors including the geometry factor *J* have been ignored. The results are presented in Table 5.1 and Table 5.2.

From the results shown, it can be seen that, the values of center distance obtained using the AGMA J and J using Approximate equations, are the same for this problem. The bending stress value obtained using the AGMA J is noticeably lower than the one using the Approximate equations for J. Of course, the computer time taken by the optimization problem running on AGMA J is higher than the one running on Approximate equations for J. This is shown later in this discussion.

In running the probabilistic analysis, two different situations were considered. It is to be remembered that both these situations are devoid of the Correction factor for Bending Strength, *J*, and all other AGMA correction factors utilized in Chapter IV. Table 5.1 shows the results obtained by incorporating the corresponding values of safety indices in the bending and pitting constraints. Table 5-2 shows the results obtained by incorporating the lowest value of both the safety indices, in the bending and pitting constraints, as suggested in [28]. The values of center distance obtained using deterministic and probabilistic methods

are plotted in Figure 5.3. In Table 5.1, a design point of (N_P = 19, P = 7) may be selected for a reliability of 99.061%. The corresponding value of center distance is 6.4286 inches. For the same reliability level of 99.061% in Table 5.2, the value of center distance is 6.7857 inches and design point is (N_p = 20, P = 7). For higher values of diametral pitch the difference in values of center distance is more significant. This indicates that by using the corresponding values of safety indices in the failure constraint equation, a smaller value of center distance is attained than using the lowest safety index value. To aid comparison of the results, actual contact and bending stresses on the pinion tooth are shown in Figures 5.4 and Figure 5.5.

It can also be noted that, using deterministic methods in design, there is only one design attainable for one value of diametral pitch, without any mention about safety level. In probabilistic design methodology, however, the designer can select a design with a particular safety level in mind. Deterministic method gives a center distance of 6.0 inches, for a design point of N_P = 20, P = 8. The result reveals that deterministic approach provides a reliability of 81.327% to 98.03%. However, probabilistic design method allows the designer to select a different design point that gives a higher reliability than the deterministic result. For example, from Table 5.1, a design point (N_P = 19, P_d = 7) may be selected for a higher reliability of 99.061%.

One other basis of comparison between the deterministic and probabilistic methodologies is in the computer time taken. In Table 5.1 and Table 5.2, the time taken for each run is shown. It can be seen that among the deterministic methods, the one employing *J* given by AGMA takes a higher CPU time of 0.1094 secs. to arrive at the optimum. The

VALUES OF CENTER DISTANCE OBTAINED USING DETERMINISTIC AND PROBABILISTIC METHODS

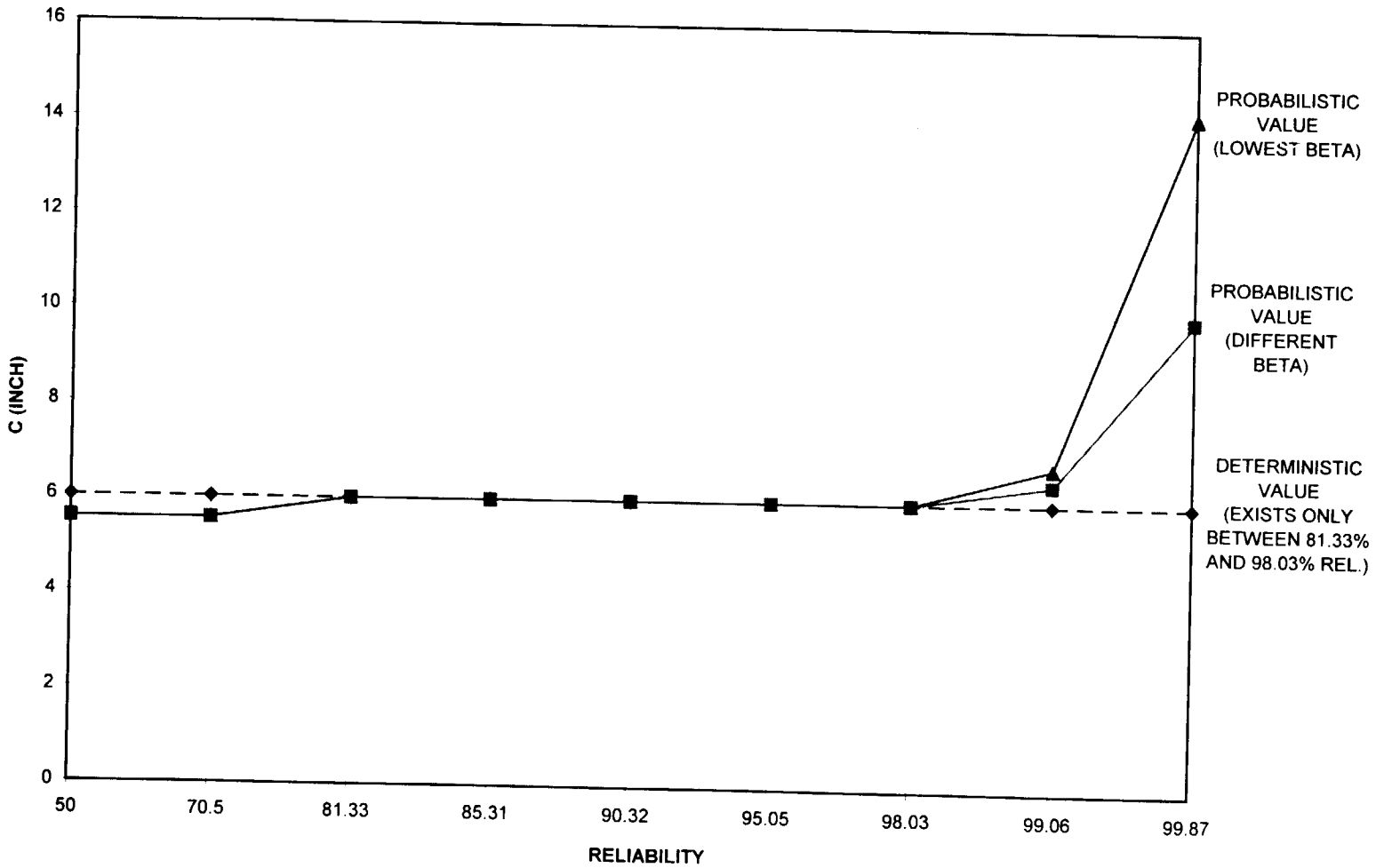


Figure 5-3

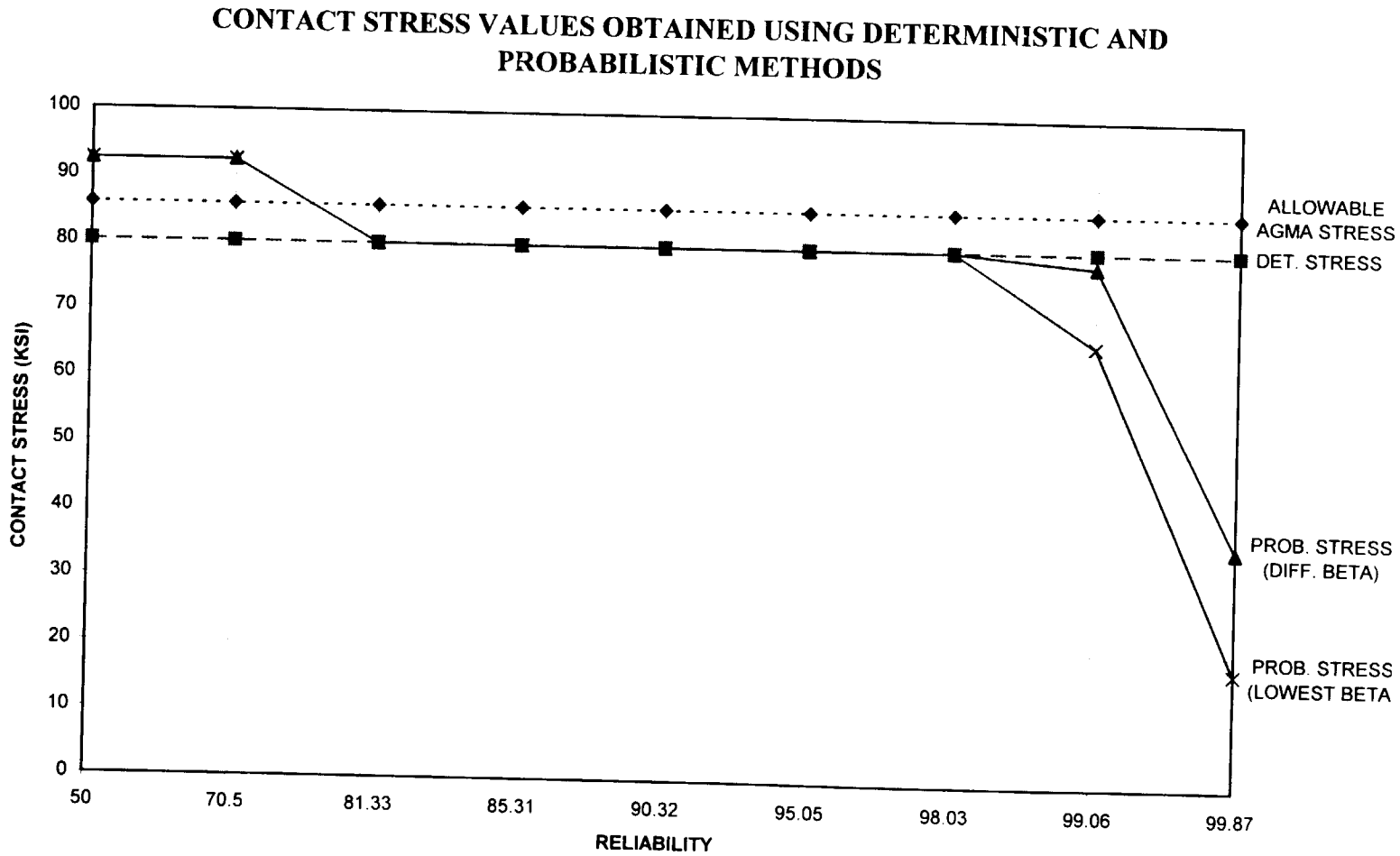

CONTACT STRESS VALUES OBTAINED USING DETERMINISTIC AND PROBABILISTIC METHODS
CONTACT STRESS (KSI)
100
90
80
70
60
50
40
30
20
10
0
50
70.5
81.33
85.31
90.32
95.05
98.03
99.06
99.87
RELIABILITY
ALLOWABLE AGMA STRESS
DET. STRESS
PROB. STRESS (DIFF. BETA)
PROB. STRESS (LOWEST BETA

Figure 5-4

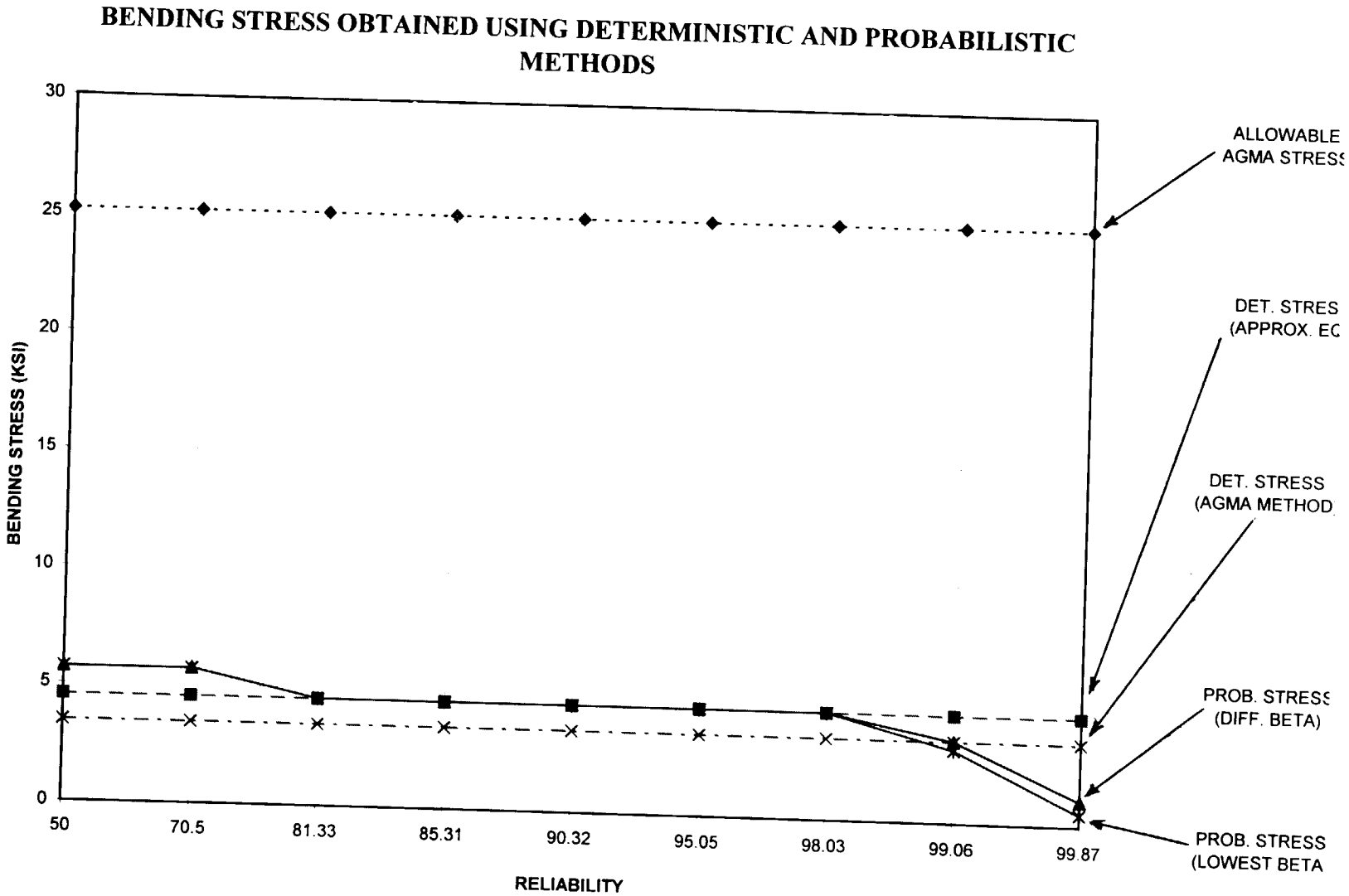

BENDING STRESS OBTAINED USING DETERMINISTIC AND PROBABILISTIC METHODS
30
25
20
15
10
5
0
BENDING STRESS (KSI)
50
70.5
81.33
85.31
90.32
95.05
98.03
99.06
99.87
RELIABILITY
ALLOWABLE AGMA STRESS
DET. STRES (APPROX. EC
DET. STRESS (AGMA METHOD
PROB. STRESS (DIFF. BETA)
PROB. STRESS (LOWEST BETA

Figure 5-5

deterministic run utilizing J from Approximate equations takes a lower CPU time of 0.0625 secs. However, the probabilistic run takes a much lower time than both the deterministic methods. This is because in probabilistic method there is no need to compute the value of Geometry factor J. Calculation of J value is an optimization problem by itself, which is necessary to be calculated only in the deterministic techniques.

For various design points in the probabilistic run the time taken is different but they are all either equal to or lower than the time taken by deterministic run using Approximate value for J, which by itself is lower than the deterministic run using AGMA J factor. It can be noted that some instances in probabilistic run take very low computer time that has almost zero value. This is because, it happens that the design point is close to the optimum and hence the optimization routine requires only fewer evaluations to reach the optimum point. The programs were written in Quick Basic Version 4.50 and the computer time shown is the time taken for the run in a 100 MHz Pentium Processor.

Another factor that may be considered during this design may be the acceptable risk level. It may be that a higher level of reliability is required and in that case one may opt for a slightly heavier gear set. If one can suffice with a lower reliability level, a much smaller design is obtained which could be sometimes smaller than the one obtained using deterministic methods. In addition, the probabilistic method indicates that for the given design condition, the most achievable level of reliability is 99.865%. Perhaps, the most useful and important advantage is that since the results obtained are based on the uncertainties in the materials, if any manufacturing inaccuracies are introduced we have the confidence that the reliability obtained is still applicable.

CHAPTER VI

SUGGESTIONS FOR FUTURE WORK AND SUMMARY

Suggestions for Future Work

A direct extension of the work presented in this thesis should be its application to gear types other than spur gears. Helical, bevel, and spiral bevel gears are widely used and design of these types of gears is dictated by the same failure modes that apply to spur gears with difference in the mathematical formulations of the resulting design constraints. The analysis considered in this project can be applied directly to helical gears with known helix angles. However, if the helix angle is treated as a design variable, the problem may become more complex.

A second important additional area of study in gear design optimization should be in the area of tooth proportion modifications. Deviation from standard proportions can increase the bending strength of the pinion tooth and also reduce the tendency for scoring. The overall size of the gear set cannot be improved a great deal by deviating from standard proportions because the constraint which usually limits the design, the LPSTC contact stress constraint, is less sensitive to tooth proportion modifications than the IPC contact stress and bending stress constraints, see [2].

In reference [34] Estrin used a nonlinear programming algorithm to optimize the gear tooth proportions for a given pinion diameter and number of teeth. He also introduced some

additional design constraints that are necessary when standard proportions are not used. His work provides a good starting point for a more detailed analysis of the problem with deviations in tooth proportions.

Even though the probabilistic analysis attempts to quantify the many uncertainties that may be encountered during gear design, efforts should be directed in trying to minimize uncertainties in computer and simulation models. This step calls for more improved computer and simulation models.

Some specific areas that attracts research are development of an accurate scoring predictor, development of a more accurate stress concentration factor for the bending stress equation, and development of a more accurate velocity (dynamic effects) factor which considers more factors than just the accuracy of manufacture and pitch line velocity.

As the supremacy of probabilistic design methodology in gear design, has been clearly established through this work, this new area must be further research and ventured in the design of other machine elements. Spur gear was chosen in this study because of the fact that it is one of simplest, oldest machine part that humans knew and has lot of significance in terms of cost of manufacture, stresses induced, failure modes etc.

Summary

In this thesis, the objective has been to clearly substantiate the supremacy of Probabilistic design methodology in design of compact spur gear sets over the conventional deterministic methods. The idea was also to establish Probabilistic Design Methodology as the new way to design. This has been achieved by way of a comparative study between the two design methodologies.

The idea of minimizing the size of the gear set was suggested in [4]. In [7] a more logical treatment to the problem which is relatively easier to apply has been presented. This incorporates the AGMA geometry factor J in computing the bending stress equation. In spite of several other improvements, the approach to gear design has remained rather deterministic. This ignored the uncertainties that could arise in gear design process. In this project, the model development included all the uncertainties by omitting the correction factors.

This project is the first attempt to explicitly compare the probabilistic and deterministic methods applicable in spur gear design, in terms of design parameters, computer time and reliability of design. Gear design process has been fully analyzed using both methods. In Deterministic Optimization a comparison is made in the use of AGMA J factor and J from Approximate equations. Both these techniques have their own advantages. While the deterministic model incorporating J from AGMA method is more accurate in defining the bending strength, the one using Approximate equations for J is much faster in terms of running time. If the criterion is running time then the use of Approximate equations for J would be a better choice and if the emphasis is on higher accuracy then the AGMA equation for J would be ideal. However, it should be noted that in either of these two methods there is no mention about safety or reliability of the design. Probabilistic design methodology has proven to fill this void.

This work comprises a detailed analysis of the gear design problem using Probabilistic design methodology. All the uncertainties in the system were quantified by

ignoring the correction factors suggested by AGMA and others. The design variables were treated as stochastic with some distribution. Limit functions for pitting and bending failure surfaces were defined and their corresponding values for safety indices were determined. The probabilistic analysis was then conducted in two ways: One using the corresponding safety indices for both the pitting and bending failures and other using the lowest of the two safety indices for both the failure surfaces, as suggested by Hasofer and Lind, [28]. It has been observed that a smaller value for center distance can be achieved by applying corresponding values of safety indices for the failure constraints, at higher values for diametral pitch. There is no significant difference in the running time among these methods.

When compared with the deterministic results the probabilistic methods seem to be a more favorable design tool for the designer. The probabilistic method of designing is faster than the deterministic method using Approximate value for *J*, which by itself is faster than the one using AGMA *J*. Probabilistic design technique offers the designer more flexibility in selecting a design. While the deterministic method gives one design for a particular factor of safety, the probabilistic design offers several design points for different levels of reliability. If the application calls for a higher reliability, then the designer can go for a slightly heavier set. If one can suffice with a lower reliability level, a smaller design can be achieved, which sometimes can be smaller than the one achieved by deterministic methods.

Another useful advantage of the approach used in this thesis is that, since the results obtained using probabilistic methods are based on the uncertainties in the materials, if any manufacturing inaccuracies are introduced the designer can have the confidence that the reliability obtained is still applicable. Hence it is concluded that probabilistic design

methodology is a more comprehensive tool for a designer than the deterministic methodology.

Probabilistic design methodology is becoming an important design method in industries. It is a method that can be applied in every field of engineering where uncertainties in design parameters exist. It is used only in limited areas at present due to the fact that many are unaware of this powerful design tool. The growing interest in this design method can be attributed to the fact that it takes into consideration reliability, dependability, optimization, and cost parameters which are the factors that influence the rating of the design.

APPENDIX I

AGMA Geometry Factor for Pitting Resistance *(I)*

The pitting resistance geometry factor, *I*, is a dimensionless number. It takes into account the effects of;

i. radii of curvature

ii. load sharing

iii. normal component of the transmitted load

The AGMA pitting resistance formula is based on the Hertz contact stress equation for cylinders with parallel axes. The original formula for the calculation of Pitting Resistance Geometry Factor, *I*, is given in [35]. The final formula is given as:

$$I = \frac{\cos\phi_r \, C_\psi^2}{\left[\frac{1}{\rho_1} \pm \frac{1}{\rho_2}\right] d \, m_N} \tag{I.1}$$

For spur gears, the helical overlap factor is given as $C_\psi = 1.0$ and the pinion operating pitch diameter is given as; $d = (2\ C_r)/(m_G \pm 1)$. Another simpler way of calculating the pitting resistance factor has been given in [2], which involves the determination of the pinion roll angles. This method is particularly useful when the value of I factor is to be determined at the Initial Point of Contact (IPC) and at the Lowest Point of Single Tooth Contact

(LPSTC). The method is outlined below:

$$I = \frac{\theta \cos^2\phi}{2\eta}\left[1 - \frac{\theta}{\gamma}\right] \tag{I.2}$$

In equation (I.2), when $\eta = 0.5$ and $\theta = \theta_{IPC}$, then the value of I is at the IPC of the teeth. Similarly, when $\eta = 1$ and $\theta = \theta_{LPSTC}$, then the value of I is at LPSTC. The values of θ_I and θ_L can be determined as follows:

$$\alpha = \frac{\sqrt{(1 + a_P/R_1)^2 - \cos^2\phi}}{\cos\phi} \tag{I.3}$$

$$\beta = \frac{\sqrt{m_G \pm (a_G/R_1)^2 - m_G^2 \cos^2\phi}}{\cos\phi} \tag{I.4}$$

$$\gamma = (1 \pm m_G)\tan\phi \tag{I.5}$$

$$\Delta = 2\pi/N_P \tag{I.6}$$

Using these relationships (I.3) through (I.6), the values of θ_{IPC} and θ_{LPSTC} can be found using

$$\theta_{IPC} = \gamma \mp \beta \tag{I.7}$$

$$\theta_{LPSTC} = \alpha - (2\pi/N_P) \tag{I.8}$$

The Hertz Contact stress as applied to spur gear design is given as:

$$\sigma_H = C_P\sqrt{\frac{C_a C_m W_t C_S C_F}{F d_P I}} \tag{I.9}$$

In order to maintain feasibility of the design,

$$\sigma_H \leq S_c \tag{I.10}$$

AGMA has defined a term, adjusted contact stress S_c, which is given by the relation;

$$S_c = S_{ac}\frac{C_L C_H}{C_T C_R} \tag{I.11}$$

It can be seen that, the geometry factor I, is very significant in determining the contact stress equations at any point in the mesh cycle. Equation (I.11) defines the contact stress constraint in the AGMA approach of the gear design problem.

APPENDIX II

AGMA Geometry Factor for Bending Strength *(J)*

The bending strength geometry factor, *J*, is a dimensionless number like the *I* factor. It takes into account the effects of:

i. shape of the tooth

ii. worst load position, i.e., the combined effects of radial and tangential load components.

iii. stress concentration at tooth root fillet

iv. load sharing between oblique lines of contact

While the *I* factor is applicable for both internal and external spur gears, the *J* factor analysis applies only to external gears. In [35] the original derivation for the Bending Strength factor is given. The formula given by AGMA in [35] is;

$$J = \frac{YC_{\psi}}{K_f m_N} \tag{II.1}$$

The helical overlap factor in (II.1), $C_{\psi} = 1$ for spur gears. The factor K_f is the stress correction factor introduced by AGMA (see Appendix IV for more on these AGMA correction factors). m_N is the load sharing ratio which has a value of one for spur gears. Y is the tooth form factor. The complex formula for the calculation of Y can be seen in [35].

The value of Y can be obtained from a generated layout of the tooth profile in the normal plane and is based on the highest point of single tooth contact.

Failure due to bending has been considered as critical, due to catastrophic consequences preventing further operation of the gear set. The bending stress was traditionally calculated using the Lewis bending equation:

$$\sigma_B = \frac{W_t P}{F Y} \tag{II.2}$$

The Y factor or Lewis form factor was derived from an approximation of the gear tooth to a cantilever beam. This equation is not used directly now-a-days except for crude or low precision, low speed gears. The Lewis bending equation has been refined through the years, improving its accuracy. The result is the AGMA geometry factor J which is given in equation (II.1). With the inclusion of J given in (II.1), the improved bending stress equation is given as;

$$\sigma_B = \frac{K_a K_s K_m W_t P}{K_v F J} \tag{II.3}$$

K_a, K_s, K_m, K_v are the correction factors introduced by AGMA, which would be explained in Appendix IV. To prevent failure in bending, the calculated stress can be compared to the adjusted bending strength of the material, which is introduced by AGMA in [7]:

$$\sigma_B \geq S_t \tag{II.4}$$

The adjusted bending strength is calculated as in AGMA 218:01 (ref [7]):

$$S_t = \frac{S_{at} K_L}{K_R K_T} \qquad \text{(II.5)}$$

Here, S_{at} is the allowable bending stress value for the material chosen, for a life of 10^7 cycles. This can be found in Table 6 in reference [7] or calculated from the endurance limit for the material. K_L, K_R, K_T are AGMA correction factors.

APPENDIX III

APPROXIMATE EQUATIONS FOR THE AGMA *J*-FACTOR

The J factor is a fundamental quantity in calculating the design parameters when gears are designed to meet the American Gear Manufacturers Association (AGMA) requirements against bending failure. However, the J factor defined in [7] is not easy to determine exactly. It used to be obtained by making an accurate graphical layout of the gear tooth, see [36]. The next improvement is the development of iterative techniques for calculating the J factor numerically [8], [9].

The methods in [8] and [9] provided excellent results. However, it is difficult to use these iterative techniques. The calculations are often lengthy, cumbersome and time consuming. A very simple, accurate, approximate equation for the J factor was introduced in 1988, [10]. Using this approximate equation it has become very easy to calculate the J factor.

$$1/J = A + (B + C/m_G)/N_P \qquad \text{(III.1)}$$

A, B, C are constants which depend on the standard tooth proportions. The coefficients A, B, and C were determined by two variable linear regression on the inverses of J factors calculated for every combination of the standard tooth numbers, for a total of 324 J factors. The correlation coefficient, for each of the sets, is greater than 0.99 and the

maximum percentage error at any point is slightly greater than 2%. The values of coefficients A, B, and C are shown in Table 1 of reference [10], along with the correlation coefficient values.

APPENDIX IV

CORRECTION FACTORS IN GEAR DESIGN

AGMA has introduced many correction factors in the pitting resistance and bending stength equations, see reference [35]. These correction factors account for many different cases that a designer may encounter while trying to arrive at a optimal design for spur gear sets. In [7], AGMA has defined expressions for adjusted contact and adjusted bending stresses which incorporates some more correction factors in them.

In this Appendix, the various correction factors are explained briefly. The expressions for the stresses with correction factors embedded in them are given below (from [37] and [38]). The actual Hertz contact stress given by AGMA is;

$$\sigma_H = C_P \sqrt{\frac{W_t C_a}{C_v} \frac{C_s}{d_P F} \frac{C_m C_f}{I}} \qquad \text{(IV.1)}$$

For feasibility;

$$\sigma_H \leq S_c \qquad \text{(IV.2)}$$

where S_c the adjusted contact stress is given;

$$S_c = S_{ac} \frac{C_L C_H}{C_T C_R} \qquad \text{(IV.3)}$$

Similarly in deriving the Bending stress equations, it has been shown that the actual bending stress is;

$$\sigma_B = \frac{K_a K_s K_m W_t P}{K_v F J} \qquad \text{(IV.4)}$$

Again for feasibility of the design;

$$\sigma_B \leq S_t \qquad \text{(IV.5)}$$

where, the S_t is the adjusted Bending Strength and given by;

$$S_t = \frac{S_{at} K_L}{K_R K_T} \qquad \text{(IV.6)}$$

On reviewing equations (IV.1) through (IV.6) one can understand how vital it is to consider the correction factors in the design equations, if the gear has to be designed to satisfy the AGMA requirements. However, use of these correction factors preserves the deterministic nature of the problem. By ignoring these correction factors in the design equations, the problem can be treated in a probabilistic perspective.

1. DYNAMIC FACTORS C_v AND K_v :

Dynamic factors are used to account for inaccuracies in the manufacture and meshing of gear teeth in action. In other words, they account for "Transmission error". This can be defined as the departure from uniform angular velocity of the gear pair. Some of the effects which produce transmission error are; 1) Inaccuracies produced in the generation of the tooth profile like errors in tooth spacing, profile lead, and runout 2) vibration of the tooth during meshing due to tooth stiffness 3) magnitude of the pitch-line velocity 4) dynamic unbalance of the rotating members 5) wear and permanent deformation of contacting portion of the teeth 6) gearshaft misalignment and deflections of shaft 7) tooth friction. In an attempt to control these effects, AGMA has defined a set of quality-control numbers Q_v, which can be taken as 8 (as in this work) for precision quality.

2. APPLICATION FACTORS C_a AND K_a :

The purpose of the application factor is to compensate for the fact that situations arise where the actual load exceeds the nominal tangential load W_t.

3. SURFACE CONDITION FACTOR C_f :

AGMA suggests values greater than unity to be used for C_f, when obvious surface defects are present.

4. SIZE FACTORS C_s AND K_s :

The AGMA recommendation is to use a size factor of unity for most gears provided a proper choice of steel is made for the size of the part and the heat treatment and hardening process. The original intent of the size factor is to account for any nonuniformity of the material properties. When there are any effects due to the nonuniformity then a size factor

value greater than unity should be used.

5. LOAD DISTRIBUTION FACTORS C_m AND K_m :

The load-distribution factor is used to account for; 1) misalignment of rotational axes for any reason 2) deviation of lead 3) load-caused elastic deflections of shafts, bearings and/or housings. In [8], AGMA presents two methods, one empirical and other analytical of obtaining values for the load-distribution factor. These values are available in the table in the above mentioned reference.

6. HARDNESS RATIO FACTOR C_H :

The pinion generally has a smaller number of teeth than the gear and consequently is subjected to more cycles of contact stress. If both the pinion and gear are through hardened, then a uniform surface strength can be obtained by making the pinion harder than the gear. A similar effect can be obtained when a surface-hardened pinion is mated with a through-hardened gear. The hardness-ratio factor C_H is used for only the gear. Its purpose is to adjust the surface strength for this effect. The values of C_H can be determined using the method as given in [21].

7. LIFE FACTORS C_L AND K_L :

In [7], AGMA defines the adjusted bending stength value for a life of 10^7 cycles. The purpose of the tooth life factors is to modify the AGMA strengths for lives other than 10^7.

8. RELIABILITY FACTORS C_R AND K_R :

The AGMA standards strengths are based on reliability of R = 0.99 corresponding to 10^7 cycles of life. For other reliabilities, AGMA suggests the use of other values that can be supported by statistical data.

APPENDIX V

PROGRAM LISTING

```
'PROGRAM NAME: DESIGN.BAS

'A program for determining the optimum value of the center
'distance for a spur gear set.  Results include stress values,
'Values of face width, center distance, contact ratio, J
'factor,pinion number of teeth, diametral pitch and relia-
'bility  in case of probabilistic analysis.  This program with
'slight modification can be used for both deterministic
'analysis and probabilistic analysis.

COMMON SHARED n, pi, aa1, tf, th, tphi, hr, j
COMMON SHARED ys, alfa, rt, xs, no2, theta, beta
COMMON SHARED rc, fa, fap, xe, ye
COMMON SHARED ratio, poi, emod, d, nmin, a$, itor, rpm
COMMON SHARED ap, p, mg, ss, bs, dp
COMMON SHARED cphi2, cphi, tphi, sphi
COMMON SHARED a1, b1, a2, b2, c2
COMMON SHARED ka, kl, km, kv, kr
COMMON SHARED aa1, alpha, beta, gamma, delta
COMMON SHARED inum, ti, tl, i

'DECLARATION OF SUB-ROUTINES IN THE PROGRAM

DECLARE SUB agmaj (j!)
DECLARE SUB calcfa (fa!, fap!, alfa!, n!)
DECLARE SUB feasible (n!, d!, mg!)
DECLARE SUB approxj (j!)
DECLARE SUB angles (n!, mg!)
DECLARE SUB ifact (inum!, i!)

'DEFINING THE OUTPUT FILE TO WRITE THE RESULTS

OPEN "result.dat" FOR OUTPUT AS #1

'SETTING INITIAL TIME, IN ORDER TO COMPUTE THE CPU TIME
'TAKEN FOR THE OPTIMIZATION RUN.  THIS TIME GIVEN BY 'TIMER'
'FUNCTION IS THE NUMBER OF SECONDS ELAPSED SINCE MIDNIGHT.
start = TIMER
```

```
CLS

'ENTER DATA FOR THE PROBLEM

INPUT "ENTER VALUE FOR GEAR RATIO :"; mg
INPUT "ENTER VALUE FOR PRESSURE ANGLE IN DEG. :"; phi
INPUT "ENTER THE SPEED IN RPM :"; rpm
INPUT "ENTER THE INPUT TORQUE TO PINION : "; itor
INPUT "ENTER THE FACEWIDTH TO DIAMETER RATIO : "; ratio
INPUT "ENTER THE VALUE OF VELOCITY FACTOR : "; kv
INPUT "ENTER ADDENDUM,DEDENDUM, HOBTIP RADIUS : "; ap, dp, hr
INPUT "ENTER  SURFACE AND BENDING STRENGTH : "; ss, bs
INPUT "ENTER AGMA QUALITY NUMBER : "; qv
INPUT "ENTER YOUNG'S MODULUS, POISSON'S RATIO : "; emod, poi
INPUT "ENTER VALUE FOR FACTORS (Ka,Kr,Kl) : "; ka, kr, kl

ca = ka: cr = kr: cl = kl
q1 = 1: qmax = 3
READ p

'CALCULATE CONSTANT VALUES
'PRESSURE ANGLE AND TRIG FUNCTIONS OF PRESSURE ANGLES

pi = 3.1415926539#
phi = phi * pi / 180
cphi = COS(phi)
sphi = SIN(phi)
tphi = sphi / cphi
cphi2 = cphi ^ 2
sphi2 = sphi ^ 2

'ELASTIC COEFFICIENT

cp2 = 1 / (2 * pi * ((1 - poi ^ 2) / emod))
cp = cp2 ^ .5

'FACTOR BASED ON LOAD REQUIREMENTS USED FOR
'INITIAL GUESS OF Np

wtfact = 396000 * itor / (pi * rpm)

'PITCH POINT I- FACTOR (USED IN INITIAL GUESS FOR Np)

ipp = sphi * cphi * mg / (2 * (mg + 1))

'CALCULATE MINIMUM NUMBER OF TEETH TO PREVENT UNDERCUTTING
```

```
nmin = ABS((2 * ap / mg) / (1 - (cphi2 + ((1 / mg) + 1)
        ^ 2 * sphi2) ^ .5))
nnmin = INT(nmin)
ninc = 1
IF (nmin - nnmin) = 0 THEN ninc = 0
nmin = nnmin + ninc

'FACTORS USED IN J-FACTOR CALCULATION

aa1 = dp - hr
delmax = 2 ^ qmax
aj = 1.763476
bj = 17.3632
cj = 6.676833
j = 1 / (aj + (bj + cj / mg) / nmin)
vt = pi * nmin * rpm / (12 * p)

'OUTPUT HEADER

PRINT #1, "   P          "; "NP         "; "NG          "; "C ";
        "F     "; "SB   "; "SLPSTC     "; "SIPC        "; "TIME"
PRINT #1, "================================================"
        ============================="

DO UNTIL p > 30
i = 0
ap = 1
dp = 1.25
hr = .3
PRINT
READ p

'GENERATE AN INITIAL GUESS FOR Np

na = (cp2 * wtfact * p ^ 3 / (kv * ratio * ss ^ 2 * ipp))
        ^ (1 / 3)
nb = (wtfact * p ^ 3 / (j * kv * ratio * bs)) ^ .5
IF na > nb THEN
        IF na > nmin THEN
                n = na
        ELSE
                n = nmin
        END IF
ELSEIF nb > nmin THEN
        n = nb
ELSE
        n = nmin
```

```
END IF
nn = INT(n)
ninc = 1
IF (n - nn) = 0 THEN ninc = 0
n = nn + ninc

'INSURE STARTING VALUE IS FEASIBLE

DO UNTIL a$ <> "no"
        CALL feasible(n, d, mg)
        IF a$ = "no" THEN n = n + delmax
LOOP

'ESTABLISH A BRACKET ON THE MINIMUM

DO UNTIL d >= lastd
q = q1 + i
i = i + 1
deln = 2 ^ q
deln = deln
IF deln < delmax THEN
        deln = deln
ELSE
        deln = delmax
END IF
lastn = n
lastd = d
n = n - deln
CALL feasible(n, d, mg)
LOOP

'NOW THAT THE MINIMUM HAS BEEN BRACKETED, REDUCE THE
'BRACKET TO A LENGTH OF ONE.

nr = lastn
dr = lastd
nl = n
dl = d
IF (nr - nl) <> 1 THEN
        IF q < qmax THEN
                jmax = q
        ELSE
                jmax = qmax
        END IF
        FOR jj = 1 TO jmax
                deln = nr - nl
                nm = nl + deln / 2
```

```
                n = nm
                d = dm
                CALL feasible(n, d, mg)
                nm = n
                dm = d
                n = nl
                d = dl
                IF dm < dr THEN
                        nr = nm
                        dr = dm
                ELSE
                        nl = nm
                        dl = dm
                END IF
        NEXT
ELSE
END IF

'DETERMINE THE MINIMUM OF THE FINAL TWO DESIGN POINTS

IF dl < dr THEN
        d = dl
ELSE
        d = dr
END IF
IF d = dl THEN
        np = nl
ELSE
        np = nr
END IF

'CALCULATION OF GEAR RATIO AT THE NEW DESIGN POINT

ng = np * mg
nng = INT(ng)
IF (ng - nng) <= .5 THEN
        ng = nng
ELSE
        ng = nng + 1
END IF
mgg = ng / np

'RECALCULATE ALL DESIGN VALUES USING THE FINAL PARAMETERS

n = np
d = dp
mg = mgg
```

```
CALL feasible(n, d, mg)
np = n
dp = d
mgg = mg
npint = INT(np)
ngint = INT(ng)
cr = (np + ng) / (2 * p)
finish = TIMER
cputime = finish - start

'PRINT OUT THE FINAL VALUES

PRINT USING "###.###  "; p; npint; ngint; cr; f;
        sigmab / 1000; slpstc / 1000; sipc / 1000; cputime
PRINT #1, USING "###.###  "; p; npint; ngint; cr; f;
        sigmab / 1000; slpstc / 1000; sipc / 1000; cputime
LOOP

'END OF MAIN PROGRAM

END
```

```
'
'
'
'
'
'
'
'
 SUB agmaj (j)

 'THIS SUB-ROUTINE CALCULATES THE VALUE OF AGMA GEOMETRY
 'FACTOR J USED IN BENDING STRESS CALCULATIONS.  THE
 'METHOD USED HERE IS FROM AGMA STANDARD 218.01

 tbend = th

 'CONSTANT VALUE CALCULATIONS BASED ON Np AND TBEND

 no2 = n / 2
 xs = pi / 4 + aa1 * tphi + hr / cphi
 ys = -aa1
 phil = tbend - tphi + phi - delta / 4
 cphil = COS(phil)
 sphil = SIN(phil)
 tphil = sphil / cphil
 rc = no2 * cphi / cphil

 'ITERATIVE SOLUTION FOR ALFA

 alfa = pi / 4    'initial value for alfa

 DO UNTIL ABS(da) <= .000001
 CALL calcfa(fa, fap, alfa, n)
 da = -fa / fap
 alfa = alfa + da
 LOOP

 'ONCE ALFA HAS BEEN DETERMINED, CALCULATE J

 CALL calcfa(fa, fap, alfa, n)
 xx = xe ^ 2 / (rc - ye)
 y = 1 / (cphil / cphi * (1.5 / xx - tphil / (2 * xe)))
 rr = rt + aa1 ^ 2 / (no2 + aa1)
 ee = .4583662 * phi      'CONSTANT VALUES SUGGESTED BY AGMA
 kf = .34 - ee + ((2 * xe / rr) ^ (.316 - ee)) *
         ((2 * xe / (rc - ye)) ^ (.29 + ee))
 j = y / kf

 'END OF AGMAJ SUB-ROUTINE

 END SUB
```

```
'
'
'
'
'
'
'
'
SUB angles (n, mg)

'SUB-ROUTINE TO CALCULATE ROLL ANGLES

alpha = ((1 + 2 * ap / n) ^ 2 - cphi2) ^ .5 / cphi
beta = ((mg + 2 * ap / n) ^ 2 - mg ^ 2 * cphi2) ^ .5 / cphi
gamma = (1 + mg) * tphi
delta = 2 * pi / n
ti = gamma - beta
tl = alpha - delta
th = ti + delta
tf = alpha

'END OF ROLL ANGLE CALCULATION

END SUB
```

```
'
'
'
'
'
'
'
SUB approxj (j)

'SUB-ROUTINE TO CALCULATE J VALUE FROM APPROXIMATE EQUATIONS

z$ = "Tooth proportions are not AGMA standards !"

IF phi = 20 THEN
        IF ap = 1 THEN
                IF dp = 1.25 THEN
                        IF hr = .3 THEN
                                aa = 1.763476
                                bb = 17.3632
                                cc = 6.676833
                        j = 1 / (aa + bb / n + cc / mg / n)
                        ELSE
                                PRINT z$: STOP
                        END IF
                ELSEIF dp = 1.4 THEN
                        IF hr = .35 THEN
                                aa = 1.791756
                                bb = 20.13339
                                cc = 6.039893
                        j = 1 / (aa + bb / n + cc / mg / n)
                        ELSE
                                PRINT z$: STOP
                        END IF
                ELSEIF dp = 1.157 THEN
                        IF hr = .239 THEN
                                aa = 1.779485
                                bb = 16.06663
                                cc = 7.208083
                        j = 1 / (aa + bb / n + cc / mg / n)
                        ELSE
                                PRINT z$: STOP
                        END IF
                ELSE
                        PRINT z$: STOP
                END IF
        ELSEIF ap = .8 THEN
                IF dp = 1 THEN
                        IF hr = .304 THEN
                                aa = 1.94547
                                bb = 11.57097
                                cc = 5.661053
                        j = 1 / (aa + bb / n + cc / mg / n)
                        ELSE
```

```
                                PRINT z$: STOP
                        END IF
                ELSE
                        PRINT z$: STOP
                END IF
        ELSE
                PRINT z$: STOP
        END IF
ELSEIF phi = 25 THEN
        IF ap = 1 THEN
                IF dp = 1.25 THEN
                        IF hr = .3 THEN
                                aa = 1.534702
                                bb = 13.44529
                                cc = 4.121288
                        j = 1 / (aa + bb / n + cc / mg / n)
                        ELSE
                                PRINT z$: STOP
                        END IF
                ELSEIF dp = 1.35 THEN
                        IF hr = .2447 THEN
                                aa = 1.595463
                                bb = 15.35728
                                cc = 3.807733
                        j = 1 / (aa + bb / n + cc / mg / n)
                        ELSE
                                PRINT z$: STOP
                        END IF
                ELSEIF dp = 1.3154 THEN
                        IF hr = .27 THEN
                                aa = 1.570434
                                bb = 14.64792
                                cc = 3.909965
                        j = 1 / (aa + bb / n + cc / mg / n)
                        ELSE
                                PRINT z$: STOP
```

```
                                END IF
                                ELSE
                                PRINT z$: STOP
                        END IF
                ELSE
                        PRINT z$: STOP
                END IF
        ELSE
                PRINT z$: STOP
        END IF

        'END OF APPROXJ SUB-ROUTINE

        END SUB
```

```
'
'
'
'
'
'
'
'
 SUB calcfa (fa, fap, alfa, n)

 'SUB-ROUTINE USED IN CALCULATION OF J-FACTOR.  THE
 'PARAMETERS CALCULATED IN THIS ROUTINE ARE DEPENDENT
 'ON VALUE OF ALFA FROM THE AGMAJ SUBROUTINE (CALCUL-
 'ATION OF AGMA J FACTOR)

 ks = ys / SIN(alfa)
 ke = ks - rt
 theta = (xs - ks * COS(alfa)) / no2
 beta = alfa - theta
 xe = n * SIN(theta) / 2 + ke * COS(beta)
 ye = n * COS(theta) / 2 + ke * SIN(beta)
 h = rc - ye
 fa = 2 * h * TAN(beta) - xe
 fap = ((2 * h / (COS(beta)) ^ 2) - ke * SIN(beta)) *
         (1 - 2 * ks / (n * SIN(alfa))) + ks * SIN(beta)

 ' END OF CALCFA SUB-ROUTINE

END SUB
```

```
'
'
'
'
'
'
'
'
 SUB feasible (n, d, mg)

 'THIS SUB-ROUTINE ANALYSES A GIVEN SPUR GEAR DESIGN
 'USING EQUATIONS GIVEN IN AGMA STANDARD

 'WRITE OUT THE VALUE OF Np TO SCREEN EACH TIME THE
 'ROUTINE IS ENTERED

 PRINT "Number of teeth: ", n

 'SAVE THE PREVIOUS SET OF DESIGN VALUES IN CASE THIS
 'DESIGN TURNS OUT TO BE INFEASIBLE

 f1 = f
 j1 = j
 mp1 = mp
 sigmab1 = sigmab
 si1 = sipc
 sl1 = slpstc
 a$ = "yes"

 'ABORT THE ANALYSIS IF Np IS LESS THAN Nmin

 IF n < nmin THEN
          'NEW DESIGN WAS INFEASIBLE.
          'RETURN OLD DESIGN VALUES
          a$ = "no"
          d = 1000000
          f = f1
          j = j1
          mp = mp1
          sigmab = sigmab1
          sipc = si1
          slpstc = sl1
          RETURN
ELSE
END IF

'LOAD, SPEED, AND DERATING FACTOR CALCULATIONS
'(CD=Ca*Cm/Cv)

vt = pi * n * rpm / (12 * p)
wt = 33000 * itor / vt
f = ratio * n / p

'FACTORS USED IN STRESS EQUATIONS
```

```
fact1 = wt * p / f / kv
fact2 = fact1 * cp2 / n

'ROLL-ANGLE, CONTACT RATIO, AND I-FACTOR CALCULATION

CALL angles(n, mg)
mp = (alpha + beta - gamma) / delta
inum = 1
CALL ifact(inum, i)
il = i
inum = 2
CALL ifact(inum, i)
ii = i

'CONTACT STRESS CALCULATIONS AT IPC AND LPSTC

slpstc = (fact2 / il) ^ .5
sipc = (fact2 / ii) ^ .5

'ABORT THE ANALYSIS IF EITHER OF CONTACT STRESS CONSTRAINTS
'ARE VIOLATED

IF slpstc > sipc THEN
        IF slpstc > ss THEN
                'NEW DESIGN WAS INFEASIBLE.
                'RETURN OLD DESIGN VALUES
                a$ = "no"
                d = 1000000
                f = f1
                j = j1
                mp = mp1
                sigmab = sigmab1
                sipc = si1
                slpstc = sl1
                RETURN
        ELSE
        END IF
```

```
    ELSEIF sipc > ss THEN
            'NEW DESIGN WAS INFEASIBLE.
            'RETURN OLD DESIGN VALUES
            a$ = "no"
            d = 1000000
            f = f1
            j = j1
            mp = mp1
            sigmab = sigmab1
            sipc = si1
            slpstc = sl1
            RETURN
    ELSE
    END IF

    'J- FACTOR AND BENDING STRESS CALCULATIONS

    CALL approxj(j)
    'CALL agmaj(j)
    sigmab = fact1 / j

    'ABORT ANALYSIS IF BENDING STRESS CONSTRAINT IS VIOLATED

    IF sigmab > bs THEN
            'NEW DESIGN WAS INFEASIBLE.
            'RETURN OLD DESIGN VALUES
            a$ = "no"
            d = 1000000
            f = f1
            j = j1
            mp = mp1
            sigmab = sigmab1
            sipc = si1
            slpstc = sl1
            RETURN

'RETURN WITH NEW DESIGN VALUES

d = n / p

'END OF ANALYSIS ROUTINE

END SUB
```

REFERENCES

1. Willis, R.J., Jr., "New Equations and Charts Pick Off Lightest Weight Gearing," Product Engineering, Jan. 21, 1963.

2. Carrol, R. K. and G. E. Johnson, "Optimal Design of Compact Spur Gear Sets," Journal of Mechanisms, Transmissions, and Automation in Design, Vol. 106, March 1984, pp. 95-101.

3. Onwubiko, C., "Spur Gear Design by Minimizing Teeth Deflection," Proceedings of the 1989 International Power Transmission and Gearing Conference, Vol. 1, April 1989, pp.115-120.

4. Savage, M., J.J. Coy, and D.P. Townsend, "Optimal Tooth Numbers for Compact Standard Spur Gear Sets," ASME Jouurnal of Mechanical Design, Vol. 104, No. 3, Oct. 1982, pp. 749-758.

5. Mott, R. Machine Elements in Mechanical Design, Merrill, an imprint of Macmillan Publishing Company, New York, 1992.

6. AGMA Standard 115.01, "Basic Gear Geometry"

7. AGMA Standard 218.01, "Rating the Pitting Resistance and Bending Strength of Spur and Helical Involute Gear Teeth."

8. AGMA Standard 218.01, "Analytical method for Calculation of Tooth Form Factor, Y, for External Gears, " Appendix E of [3].

9. Mitchiner, R. G. and H. H. Mabie, "The Determination of the Lewis Form Factor and the AGMA Geometry Factor J for External Spur Gear Teeth," ASME Journal of Mechanical Design, Vol. 104, No. 1, Jan. 1982, pp. 148-158.

10. Carrol, R. K. and G. E. Johnson, "Approximate Equations For the AGMA J-Factor, " Mech. Mach. Theory, Vol. 23, No. 6, 1988, pp. 449-450.

11. AGMA Standard 110.04, "Nomenclature of Gear Tooth Failure Modes."

12. Bowen, C. W., "The Practical Significance of Designing to Gear Pitting Fatigue Life Criteria," Tans. J. Mechanical Design, Vol. 100, No. 1, Jan. 1978, pp.

46-53.

13. Burr, A. H., Mechanical Analysis and Design, Elsevier, New York, 1981.

14. Mabie, H. H., Mitchiner, R. G., and Moosavi-Rad, H., "The Undercutting of Hobbed Spur Gear Teeth," Trans. ASME J. Mechanisms, Transmissions, and Automation in Design, Vol. 105, No. 1, March 1983, pp. 122-128.

15. AGMA Standard 2001.B88, "Fundamental Rating Factors and Calculation Methods for Involute Spur and Helical Gear Teeth."

16. Tucker, A.I, "The Gear Design Process," ASME Paper 80-C2/DET-13, Aug.1980.

17. Dudley, D. W., "How Increased Hardness Reduces the Sizes of Gear Sets," Product Engineering, November 9, 1964.

18. Onwubiko, C., L. Onyebueke, and F.C. Chen, "Probabilistic Optimum Design of Compact Spur Gear Sets," Proceedings of the 1995 Design Engineering Technical Conferences, Vol. 2, ASME 1995, pp. 115-124.

19. Dudley, D. W., Handbook of Practical Gear Design, McGraw-Hill, New York, 1984.

20. Robert C. Juvinall, Fundamentals of Machine Component Design, John Wiley & Sons, Inc., 1983.

21. Shigley, J.E., and Mischke C.R., Mechanical Engineering Design, McGraw-Hill, Ed. 5, 1989.

22. Thompson, J.M.T., and Hunt, C.W., "Dangers of Structural Optimization," Engineering Optimization, Vol. 2, 1974, pp. 99-110.

23. Torng, T.Y. and R.J. Yang, "Robust Structural System Design Using A System Reliability-Based Design Optimization Method," Proceedings of the International Union of Theoretical and Applied Mechanics, San Antonio, Texas, June 7-10, 1993.

24. Venkayya, V.B., "Structural Optimization: A Review and Some Recommendations," Intl. J. Numr. Meth. Engr.,Vol.13, 1978, pp. 203-228.

25. Torng, T., and B. Thacker, "Confidence Bounds Assessment for Probabilistic Structural Reliability Analysis," 33rd AIAA/ASME/AHS/ASC Structures, Structural Dynamics and Materials Conference.

26. Torng, T., and B. Thacker, "An Efficient Probabilistic Schem for Constructing Structural Reliability Confidence Bounds," Southwest Research Institute, Texas.

27. Lewis, Wilfred, "Investigation of the Strength of Gear Teeth," Proc. Eng. Club, Philadelphia, 1893.

28. Hasofer, A. M. and N. C. Lind, "Exact and Invariant Second-Moment Code Format," Journal of the Engineering Mechanics Division, ASCE, 100, EM1, pp. 111-121, 1974.

29. Belegundu, A. D., "Probabilistic Optimal Design Using Second Moment Criteria," Journal of Mechanisms, Transmissions, and Automation in Design, Vol. 110., Sept. 1988, pp. 325-329.

30. Cornell, C. A. "A Probability Based Structural Code," J. Amer. Conc. Inst.,66, No. 12, pp.974-985, 1969.

31. Melchers, R. E., Structural Reliability - Analysis and Prediction, John Wiley and Sons, New York, 1987.

32. Nikolaidis, E. and R. Burdisso, "Reliability Based Optimization: A Safety Index Approach," Computer and Structures, Vol. 28, No. 6, 1988, pp. 781-788.

33. Ang A.H.S. and W.H. Tang, Probability Concepts in Engineering Planning and Design. Vol II, pp 333-447, John Wiley, New York (1984).

34. Estrin, M., "Optimization of Tooth Proportions for a Gear Mesh," ASME Paper 80-C2/DET-101, Aug. 1980.

35. AGMA Standard 908.B89, "Geometry factors for Determining the Pitting Resistance and Bending Strength of Spur and Helical Gear Teeth."

36. AGMA Standard 226.01, "Geometry Factors for Determining the Strength of Spur, Helical, Herringbone and Bevel Gear Teeth."

37. AGMA Standard 918.A93, "A Summary of Numerical Examples Demonstrating the Procedures for Calculating Geometry Factors for Spur and Helical Gears."

38. AGMA Standard 220.02, "Rating the Strength of Spur Gear Teeth."

BIO DATA

SHIVA M. GANGADHARAN
4040, SCOTWOOD DRIVE,
NASHVILLE, TN 37211-3520.

PHONE: (615)331-6462
E-MAIL : gangas@harpo.tnstate.edu

PROFESSIONAL OBJECTIVE: **Mechanical Engineer** position requiring design skills.

EDUCATION:

TENNESSEE STATE UNIVERSITY NASHVILLE, TENNESSEE 1994-1996
Master's Degree in **Mechanical Engineering** with specialization in Design.
G.P.A: 3.6/4.0

BHARATHIAR UNIVERSITY TAMILNADU, INDIA 1989-1993
Bachelor's Degree in **Mechanical Engineering**
G.P.A: 3.6/4.0
Gold Medalist, May 1993.

EXPERIENCE:

RESEARCH ASSISTANT Tennessee State University, Nashville, TN Dec. 1994-Aug. 1996

- conducted extensive research on **Probabilistic Design Methodology (PDM)** as a new design tool. The work was supported by **NASA Grant**.
- proved the effectiveness of using PDM over conventional deterministic methods, in the **Design of Compact Spur Gear Set.**
- using **Reliability based Optimization** Techniques, determined ways of attaching different safety levels to design of spur gears.
- trained voice recognition patterns using **Artificial Neural Networks**.
- simulated the displacement of the center of gravity of a car running under various road conditions and speed using **Vibration Analysis Techniques** and MATLAB.
- conducted stress/strain and displacement analysis on a spur gear tooth using COSMOS as **Finite Element Analysis** tool.

TEACHING ASSISTANT Tennessee State University, Nashville, TN Aug. 1994-Dec. 1995

- assisted the faculty in instructing the course on Design of Machine Elements, gave lectures, assignments, problem-solving sessions and led discussions. Supervised 45 undergraduate students in their lab lessons on Computer Aided Design.

ENGINEER Indira Gandhi Center for Atomic Research, India. Jun.1992-Mar.1993

- **Designed Steam Pipes** on velocity and pressure drop basis and thickness on IBR strength calculation basis, using a special purpose French software called INCA.
- Created a **Shell and Tube Heat Exchanger Design** for Indira Gandhi Center for Atomic Research, India. The new design saved Rs. 52,000 per year in terms of

improved efficiency. The design was successfully implemented at Plant B of IGCAR, India.

- **Simulated a real-life model** of Shell and Tube heat exchanger and validated the theoretical conclusions using the experimental set-up.

COMPUTER SKILLS:

LANGUAGES	Fortran, Quick-basic version 4.50, Pascal, Quick-C.
PACKAGES	Pro-E version 15.0, AutoCad, NESSUS, INCA, Matlab, WordPerfect, Mc Draw, Ms Word, Harvard Graphics, Lotus 1-2-3, dBASE, Quattropro, Ms Excel.
SYSTEMS	DOS, UNIX, VAX/VMS, Windows 95, Windows NT 3.51, Sun, HP, SGI.

PUBLICATION:

Shiva Gangadharan, Chinyere Onwubiko, and Landon Onyebueke *"Comparative Study of the Use of AGMA Geometry Factors and PDM in the Design of Compact Spur Gear Sets."* (In Print)

AFFILIATIONS:

Member, The American Society of Mechanical Engineers.
Member, Society of Manufacturing Engineers.

REFERENCES

Available upon request.